

11-8-2015

Phosphorus Sorption Dynamics in Shallow Groundwater, Coastal Everglades, Florida, USA

Hilary Flower

University of South Florida, hflower@mail.usf.edu

Follow this and additional works at: <http://scholarcommons.usf.edu/etd>

 Part of the [Geochemistry Commons](#), [Geology Commons](#), and the [Hydrology Commons](#)

Scholar Commons Citation

Flower, Hilary, "Phosphorus Sorption Dynamics in Shallow Groundwater, Coastal Everglades, Florida, USA" (2015). *Graduate Theses and Dissertations*.

<http://scholarcommons.usf.edu/etd/5946>

This Dissertation is brought to you for free and open access by the Graduate School at Scholar Commons. It has been accepted for inclusion in Graduate Theses and Dissertations by an authorized administrator of Scholar Commons. For more information, please contact scholarcommons@usf.edu.

Phosphorus Sorption Dynamics in Shallow Groundwater, Coastal Everglades, Florida, USA

by

Hilary Dervin Flower

A dissertation submitted in partial fulfillment
of the requirements for the degree of
Doctor of Philosophy
School of Geosciences
College of Arts and Sciences
University of South Florida

Major Professor: Mark C. Rains, Ph.D.
Mark T. Stewart, Ph.D.
Matthew Pasek, Ph.D.
Sarah E. Kruse, Ph.D.
Joseph D. Hughes, Ph.D.

Date of Approval:
October 21, 2015

Keywords: saltwater intrusion, submarine groundwater discharge; mangroves;
adsorption/desorption, bicarbonate, mixing zone

Copyright © 2015, Hilary Dervin Flower

Dedication

I dedicate this work to Dan and Kate Dervin, who have not only been my parents, they have also been my friends, cheerleaders, Everglades companions, and safety net. Little did my father know, when he shared his passion for the mountains with me, including the beauty to be found in individual rocks, that he was shaping a future geologist.

I dedicate this work to Dr. Tanya Furman, who let an unknown English major unload a backpack of semi-identified rocks on her desk, and who took the opportunity to suggest I become a geologist.

I dedicate this work to Cathy Busby, who was the first to take me in as a PhD student years ago, even though I only had a single geology class under my belt.

I dedicate this work to Mark Rains, who made the prospect of a PhD in hydrology seem not only possible but fun, and then made it so.

I dedicate this work to my son Ramsay, who held my hand at my lowest point, and my son Dervin, who made sure that even the longest and latest lab day ended with icecream.

And most of all I dedicate this work to my barefoot swamp-walking girl, Nora Jade. I see my father in her deep connection to the natural world and I marvel at her wealth of scientific knowledge, from birds to chemistry.

My fondest hope for my children is for them to discover a pursuit in life that gives them the contentment, adventure and purpose that science has given me, and that, like me, they are surrounded by generous and interesting people to help them along their way.

Acknowledgements

I won the lottery when it comes to PhD advisors. Actually it was because I knew he'd be a great advisor that I dared to think a PhD just might work. For his part, he was crazy enough to see no problem in taking on a working single mother as a full time student, and he never flinched... even when things got truly out of hand. Bringing problems to him always resulted in my path forward becoming smoother and more clear, one of his many super powers. He modeled and expected scholarship that is both rigorous and efficient. Funny, wise, and kind, Dr. Mark Rains was the best PhD advisor I could have asked for. Thank you, Mark!

One of the great pleasures of graduate school for me has been the wonderful people I got to spend time with. Dr. Mark Stewart, AKA Mark the Elder, indulged me with hours of intellectually stimulating discussions on my own research as well as climate change. It was he who suggested I pursue phosphorus sorption (I like to remind him that he added, "It'll be dead easy."). It was Dr. Matt Pasek who suggested that I do geochemical modeling (for which this dissertation turns out to be an extended prologue). All of my committee members, including Dr. Joe Hughes and Dr. Sarah Kruse, were very kind to take time from their busy schedules to move me through the steps and stages. Even my qualifying exam is a fond memory of intriguing written questions and collegial discussion during the oral portion, which says all you need to know about the spirit of this dream team. Thank you committee!

Dr. Jia-Zhong Zhang of NOAA, whose phosphorus sorption work I had read closely and admired, made all of the difference when he became my mentor and collaborator. Countless times he saved me from dead-ends and erroneous thinking, and kept me moving forward. Even though he was on the other coast of Florida, he was always there for me by email and phone, working diligently to bring out the best in each project. Dr. David Lewis provided the equipment, lab space, and guidance for me to make the hundreds of phosphorus measurements that are the foundation for this dissertation. I was honored that he invited me to be part of his wonderful lab. His student Viviana Penuela Useche trained me in the necessary analytical protocol, and her impeccable lab techniques remain my model.

I would like to acknowledge the help, humor, and encouragement of my lab mates, especially Dr. Mike Callahan, ReNae Nowicke, Hunter Clasen, and Dr. Kai Rains. Paul Bryan was very kind to put in endless orders of equipment and consumables for me, and helped me solve many problems. Mandy Stuck reminded me to breathe and cheerfully navigated me through the bureaucratic labyrinths. My family and friends stepped up to care for my children when I need to travel for field work or conferences: especially my parents (driving down from Virginia), Anne Hirsch, Chelsea Hirsch, Tanya Coovadia, Maureen Corbett, and Joe O'Connor.

Thank you to everyone who made my five years of graduate school at USF so enjoyable.

Table of Contents

List of Tables	iii
List of Figures	iv
Abstract	vii
Chapter 1: Introduction	1
Objectives and organization.....	4
References.....	10
Chapter 2: Control of phosphorus concentration through adsorption and desorption in shallow groundwater of subtropical carbonate estuary	12
Note to reader.....	12
Abstract	12
Introduction.....	13
Methods.....	17
Study area.....	17
Water samples.....	19
Sediment samples.....	20
Sorption isotherm experiments	22
Soluble reactive phosphorus analysis	23
Sorption isotherm parameters	23
Results.....	27
Discussion	30
Conclusion	38
Acknowledgments.....	39
References.....	39
Chapter 3: Saltwater intrusion as potential driver of phosphorus release from limestone bedrock in a coastal aquifer	45
Note to reader.....	45
Abstract	45
Introduction.....	46
Methods.....	51
Study area.....	51
Water samples.....	53
Rock samples	54
Mixing continuum sorption experiments	55

Sorption isotherm experiments	56
Sorption isotherm parameters	56
Results	58
Discussion	61
Conclusion	67
Acknowledgments.....	68
References.....	68
Chapter 4: Rapid and sustained phosphorus desorption with saltwater intrusion in carbonate aquifer.....	72
Note to reader.....	72
Abstract	72
Introduction.....	73
Methods.....	74
Study area.....	74
Rock samples	75
Water samples.....	76
Column experiments	77
Sorption isotherm experiments	80
Sorption isotherm parameters	80
Results.....	81
Discussion	85
Conclusion	90
Acknowledgments.....	90
References.....	91
Chapter 5: Conclusions.....	94

List of Tables

Table 2.1:	Selected characteristics of the three field waters.	20
Table 2.2:	Selected phosphorus analysis of the sediment, in $\mu\text{mol g}^{-1}$	22
Table 2.3:	Phosphorus sorption isotherm parameters of the ecotone sediment	29
Table 3.1:	Selected phosphorus analysis of the rocks, in $\mu\text{mol g}^{-1}$	58
Table 3.2:	Phosphorus sorption characteristics for RB rock and Canepatch rock.	61
Table 4.1:	Lithologic descriptions of the rock samples	79
Table 4.2:	Sorption isotherm parameters... ..	84

List of Figures

Figure 1.1	Illustration of the concept of groundwater mixing zone in aquifer, and groundwater discharge.....	1
Figure 1.2	Schematic illustration of adsorption.....	2
Figure 1.3	Schematic illustration of positive adsorption sites on the mineral surface.....	3
Figure 1.4	Schematic illustration of desorption through anion competition in saltwater.....	4
Figure 1.5	Schematic illustration of a three-water-type mixing system.....	5
Figure 1.6	Illustration of the concept of groundwater discharge varying in salinity along a mixing continuum.....	6
Figure 1.7	Schematic illustration of two alternative ways in which increased phosphorus from desorption may change along a mixing continuum.....	7
Figure 1.8	The location of the ion exchange front, depicted in yellow, at the freshwater edge of a mixing zone.....	8
Figure 1.9	Schematic illustration of two contrasting kinetic reactions to an influx of saltwater.....	9
Figure 2.1	Collection locations for samples: fresh GW (red triangle), ecotone GW and sediment (green circle), and bay SW (blue square).....	18
Figure 2.2:	Selected water composition for fresh GW (red triangle), ecotone GW (green circle), and bay SW (blue square) with SRP concentration in filled shapes, and HCO_3^- concentration in open shapes.....	21
Figure 2.3	a) Schematic of P sorption isotherm; b) Schematic of the y-intercept and P_{max}	25

Figure 2.4	Fresh GW (red triangles), ecotone GW (green circles), and bay SW (blue squares), accompanied by dashes representing the Langmuir two-surface sorption isotherms; a) in standard plot; b) in reciprocal plot from which Langmuir two surface isotherm parameters were determined; and c) the extended two-surface isotherm for fresh GW.....	28
Figure 3.1:	Schematic cross-section of saltwater intrusion with a broad transition zone, loosely based on Kohout.....	48
Figure 3.2:	Schematic comparison of three hypothetical patterns of P sorption response to gradational increases in saltwater content, where the two mixing water types have low SRP concentration: (A) conservative mixing; (B) SRP availability from desorption increasing in direct proportion to saltwater content; (C) non-linear response, here depicted as a logarithmic increase in SRP from desorption at the freshwater end of the mixing continuum.....	50
Figure 3.3:	Map of southern Everglades, showing the two major flow-ways, Shark River Slough and Taylor Slough; sampling sites for rock samples Canepatch (CP; square) and RB (triangle); and sampling location for fresh groundwater (solid star), and saltwater from Florida Bay (open star).....	52
Figure 3.4:	Percent adsorption of added SRP in mixtures of freshwater with varying amounts of saltwater, indicated by added chloride concentration, by RB rock (red triangles) and Canepatch rock (blue squares).....	60
Figure 3.5:	Freundlich sorption isotherms for a) RB rock and b) CP rock, with freshwater (solid marker with solid line), 10% saltwater mixture (solid marker with dashed line) and saltwater (open marker with solid line).....	63
Figure 4.1:	Location map showing well G-3784 (star), fresh groundwater well TSB15 (triangle), and saltwater sampling from Florida Bay (square).....	77
Figure 4.2:	Schematic diagram of column apparatus.....	78
Figure 4.3:	Selected rock composition along the vertical section of well core with geologic formations demarcated; organic $MgCl_2$ -P (red diamonds); inorganic $MgCl_2$ -P (P_{exch}) (open diamonds); total sedimentary P (green triangles), total iron (blue circles); saltwater K_d (open squares); freshwater K_d (solid black squares).....	82

Figure 4.4: Column experiments with rock from the 30 m depth interval showing three column experiments: one (open green squares); two (solid yellow squares); and three (blue crosses)85

Figure 4.5: Column experiments with depth interval 14 m; a) column experiment four, with the sequence: freshwater-saltwater-freshwater; and b) column experiment five, with a single influx of freshwater followed by a sustained flow of saltwater.....86

Abstract

For this dissertation I studied phosphorus (P) sorption dynamics in the shallow groundwater of the southern Everglades. In particular, I examined how the ambient water type governs soluble reactive P (SRP) availability through adsorption/desorption reactions with the aquifer matrix. Chapter 2 investigated how P sorption dynamics of the mangrove root zone sediment are affected by high bicarbonate brackish groundwater compared to both fresh groundwater and saltwater. The results from chapter 2 show that the sediment exhibited exceptionally low sorption efficiency in the high bicarbonate brackish water, which would allow ambient water SRP concentration to be maintained at a higher level. Chapter 3 is a detailed analysis of how P sorption dynamics in two bedrock samples are affected by incremental increases in saltwater content in a freshwater-saltwater transition zone. The results of chapter 3 indicate that a sorption edge occurs at 3 mM Cl^- concentration. In water exceeding this Cl^- concentration, SRP would be expected to desorb from the bedrock due to a sharp decrease in sorption efficiency between the freshwater saltwater. These results suggest that SRP is active in the ion exchange front of saltwater intrusion, with a rapid increase in SRP availability expected at the leading edge of saltwater intrusion. A landward incursion of 3 mM Cl^- concentration water would be expected to raise ambient SRP concentration along the affected aquifer zone, in turn increasing SRP availability in the ecosystem where the transitional waters discharge to the surface. Chapter 4 investigates the kinetics SRP release accompanying saltwater intrusion using a column of carbonate aquifer solids and alternating inflow between fresh groundwater and saltwater. The

results show an immediate and high magnitude increase in SRP concentration when saltwater flows into the column. The combined results of this dissertation show that, in the southern Everglades and possibly other carbonate coastlines as well, water type strongly controls P sorption behavior of the sediment and bedrock, and may have a direct influence on the local ecology through increased P availability. A fundamental understanding of the abiotic exchange mechanisms between SRP and the aquifer solids can aid in the successful management and protection of this unique and important ecosystem.

Chapter 1: Introduction

Coastal estuaries are extraordinarily productive and are critical for maintaining global biodiversity. Many are phosphorus-limited, and phosphorus budgets determines productivity and community structure.¹ One of the important sources of phosphorus to estuaries is the release of phosphorus from mineral surfaces as a result of freshwater and saltwater mixing.² These two endmember waters mix at the mouths of tidally connected rivers, and at depth in the aquifer, where freshwater and saltwater meet in a mixing zone. Because of these reactions, mixing zone groundwater can have an order of magnitude more phosphorus than overlying coastal rivers.³ Phosphorus-enriched mixing zone groundwater is then delivered to overlying ecosystems through groundwater discharge (Figure 1.1).⁴ Saltwater intrusion can trigger new sorption reactions, by mixing saltwater into portions of the aquifer that had been immersed in fresh water.

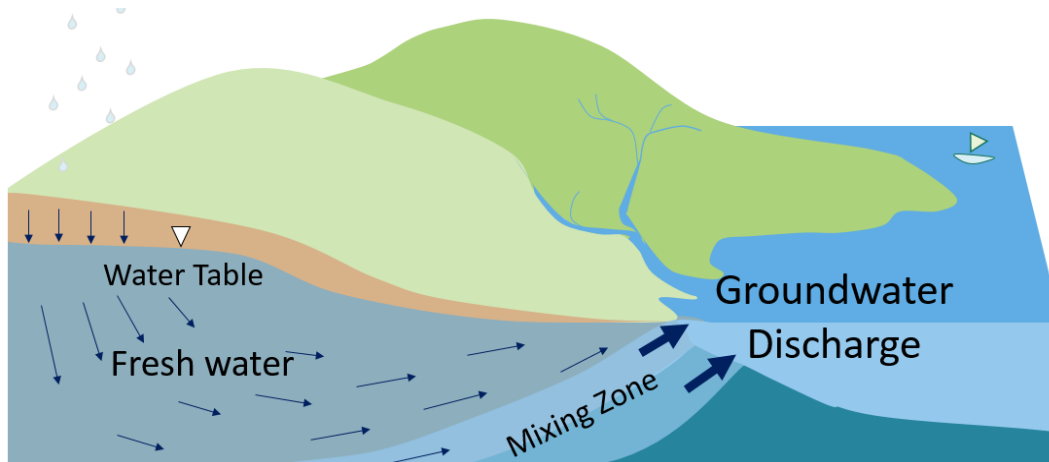


Figure 1.1 Illustration of the concept of groundwater mixing zone in aquifer, and groundwater discharge

Particularly in freshwater, SRP adsorbs to sediment. The bioavailable form of phosphorus is inorganic dissolved ortho-phosphate, which occurs in neutral groundwater as the anion H_2PO_4^- . It is measured as soluble reactive phosphorus (SRP). The phosphorus anion is attracted to positively charged sites on the mineral surface such as the positively charged edges of clay particles made of iron oxides (Figure 1.2 and 1.3). Adsorption is typically not a chemical bond, but a loose electrostatic attraction.⁵

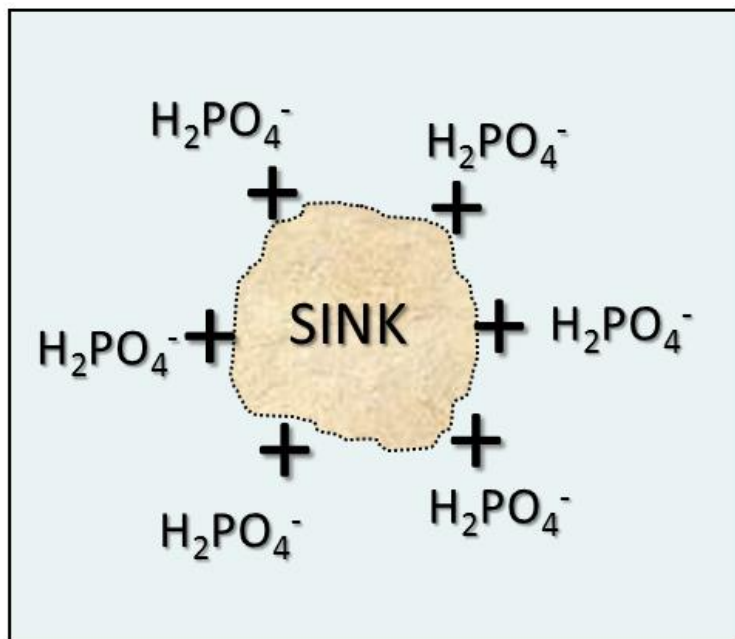


Figure 1.2 Schematic illustration of adsorption

The same mineral grain will behave differently with respect to water SRP depending on the surrounding water. Saltwater causes desorption of SRP from the mineral surface not because of saltwater's high sodium chloride content, but because of its high concentration of bicarbonate and sulfate anions that compete for positive exchange sites.⁶ Switching from a water with high sorption efficiency to one with low sorption efficiency reduces the solid's ability to "hold onto"

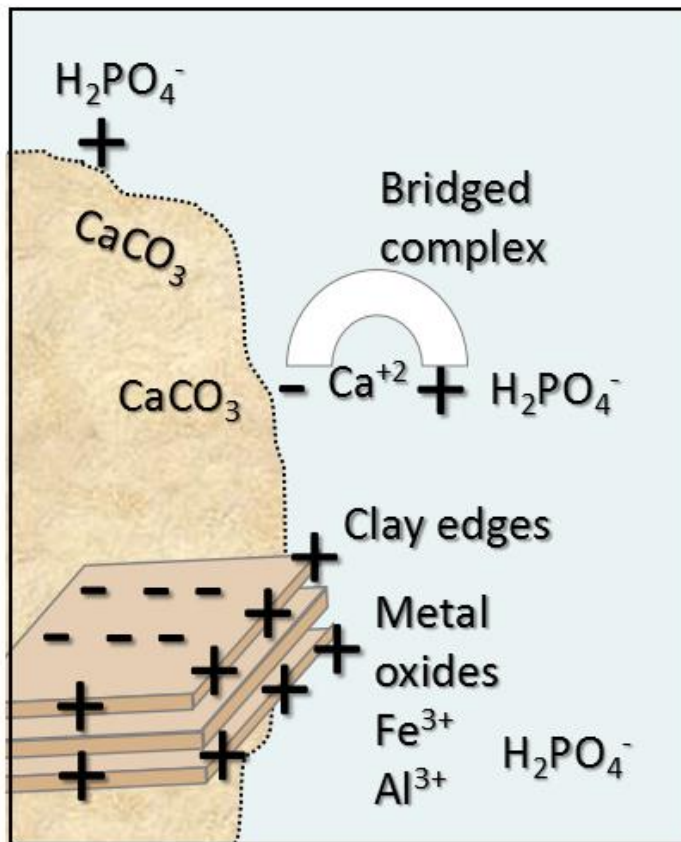


Figure 1.3 Schematic illustration of positive adsorption sites on the mineral surface

the phosphorus, triggering desorption, and raising the phosphate concentration of the ambient water (Figure 1.4). The sediment is an SRP sink in a water that gives it high sorption efficiency and an SRP source in a water that diminishes its sorption efficiency.²When SRP enters the system, the sediment can scavenge if it is in a water that allows it to adsorb efficiently, reducing water SRP concentration. In this way sediment acts as a phosphorus buffer.² When the sediment has weak buffering intensity the ambient water can be maintained at a higher concentration of phosphorus. Any phosphorus that is released at the root zone, or delivered there through groundwater discharge, is immediately available for root uptake.

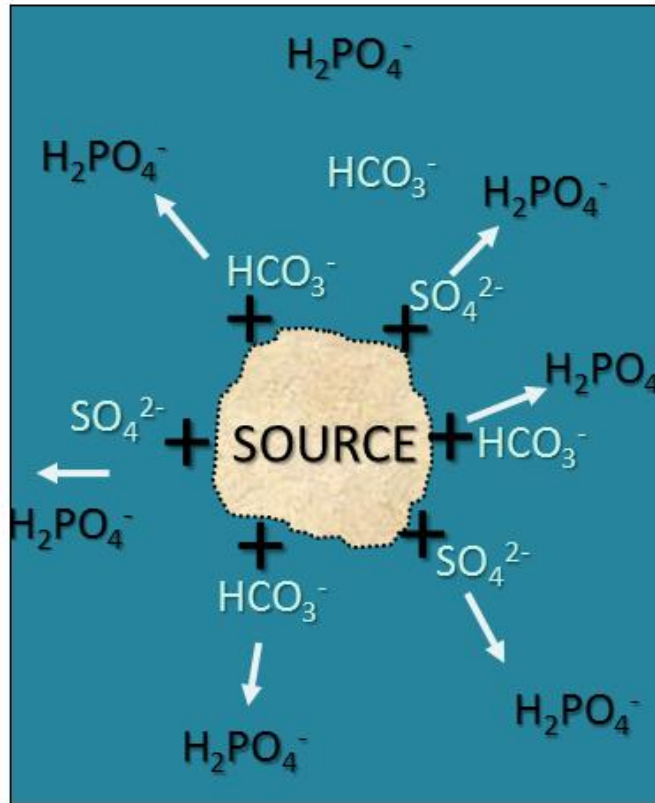


Figure 1.4 Schematic illustration of desorption through anion competition in saltwater

Objectives and organization

The objectives of this dissertation is to investigate three process-based questions related to P sorption as a driver of SRP availability that are not addressed by existing literature. I chose to focus on carbonate lithologies because they have been the subject of fewer phosphorus sorption studies than siliclastic lithologies. They occur on many coastlines globally. Many carbonate coastal zones are undergoing saltwater intrusion, such as the Bahamas, Florida, Apulia Italy, and Majorca Spain.

Some estuaries have groundwater with many times more bicarbonate content than seawater, as a result of microbial activity.⁷ In such mixing zones there are three distinct water types: freshwater, saltwater, and a bicarbonate enriched water (Figure 1.5). Millero et al.⁶ found that calcite crystals in synthetic high bicarbonate water had lower sorption efficiency than synthetic saltwater. They suggested that phosphorus availability would be greater in an estuary with high bicarbonate water than the freshwater upstream and marine water downstream, and an influx of saltwater would cause adsorption. Since 2001 this hypothesis has remained untested for natural mineral solids and waters. Chapter 2 examines the influence of high bicarbonate brackish groundwater on P sorption behavior of mangrove soils, as compared to fresh groundwater and saltwater.

Secondly, with saltwater intrusion, freshwater does not typically change to saltwater abruptly, but mixes gradually across a mixing zone that can be meters to kilometers wide (Figure 1.6).

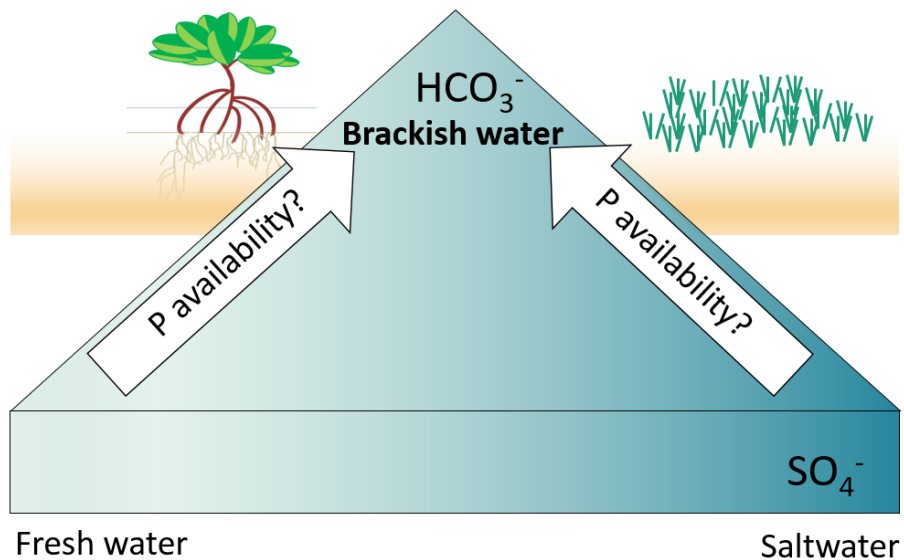


Figure 1.5 Schematic illustration of a three-water-type mixing system

It would be important to know: How does P sorption vary along a gradational mixing continuum? The answer would affect phosphorus availability in the overlying ecosystem that receives mixing zone groundwater discharge. In some regions mixing zone groundwater discharges seaward of the coastline to coral reefs or sea grass in coastal lagoons. In some regions mixing zone groundwater discharges landward of the coastline in wetlands such as salt marshes and mangrove swamps.

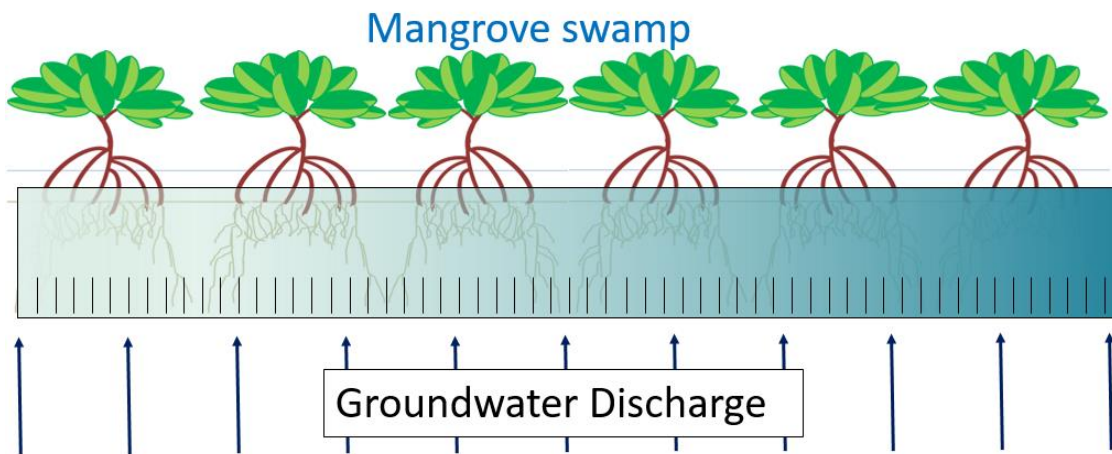


Figure 1.6 Illustration of the concept of groundwater discharge varying in salinity along a mixing continuum

One might expect the availability of SRP from desorption to increase in a linear fashion with increasing salinity, depicted as Curve A of Figure 1.7. Alternatively, SRP could behave like other highly reactive ions, and confine its changes in concentration to the ion exchange front (Figure 1.8). For example, calcium and magnesium undergo cation exchange with the sodium from saltwater almost exclusively at the very low salinity edge of saltwater intrusion, known as the ion exchange front, with little change in concentration of these ions as saltwater content increases because the exchange sites are already saturated. In this scenario phosphorus from

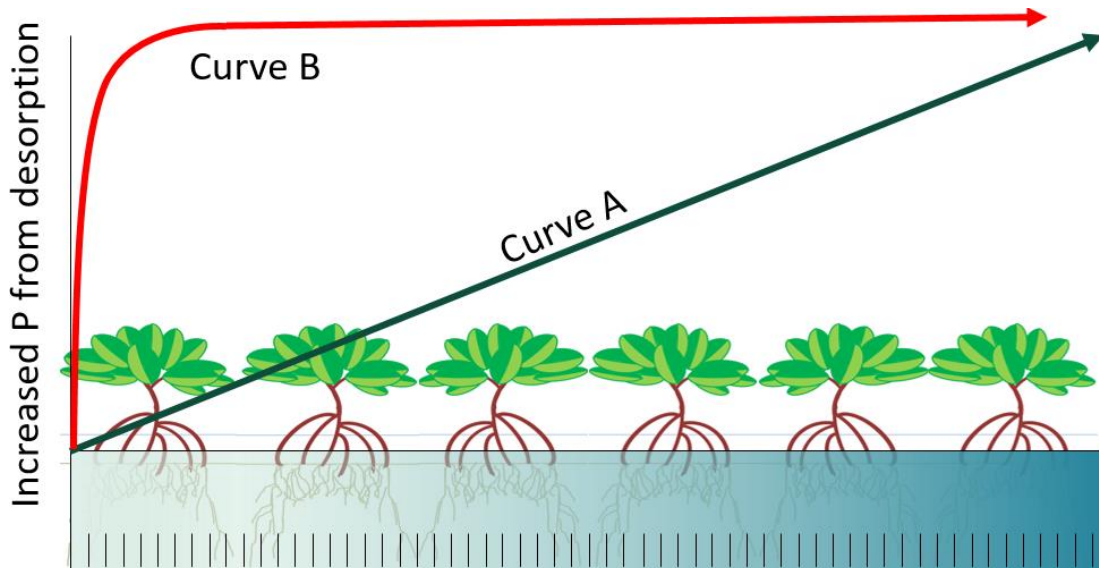


Figure 1.7 Schematic illustration of two alternative ways in which increased phosphorus from desorption may change along a mixing continuum

desorption may increase sharply near the freshwater end of the mixing continuum, with little additional release as saltwater content increases, depicted as Curve B of Figure 1.7. My hypothesis was that P desorption would follow the second model. If that were the case, the next line of inquiry would focus on identifying the threshold of saltwater content at which desorption behavior reverses. Chapter 3 investigates the potential for SRP to be an active participant in the ion exchange front of saltwater intrusion in a carbonate aquifer.

The kinetics of P sorption dynamics would determine the magnitude of SRP released, the rapidity, and the change in desorption over time. At the first influx of saltwater, desorption could increase slowly and then plateau at a quasi-equilibrium level, as depicted in Figure 1.9.

Alternatively, P release could spike and rapidly diminish. Adsorption/desorption reactions can be rapid, with the bulk of change occurring within minutes to hours.⁶ Chapter 4 investigates the

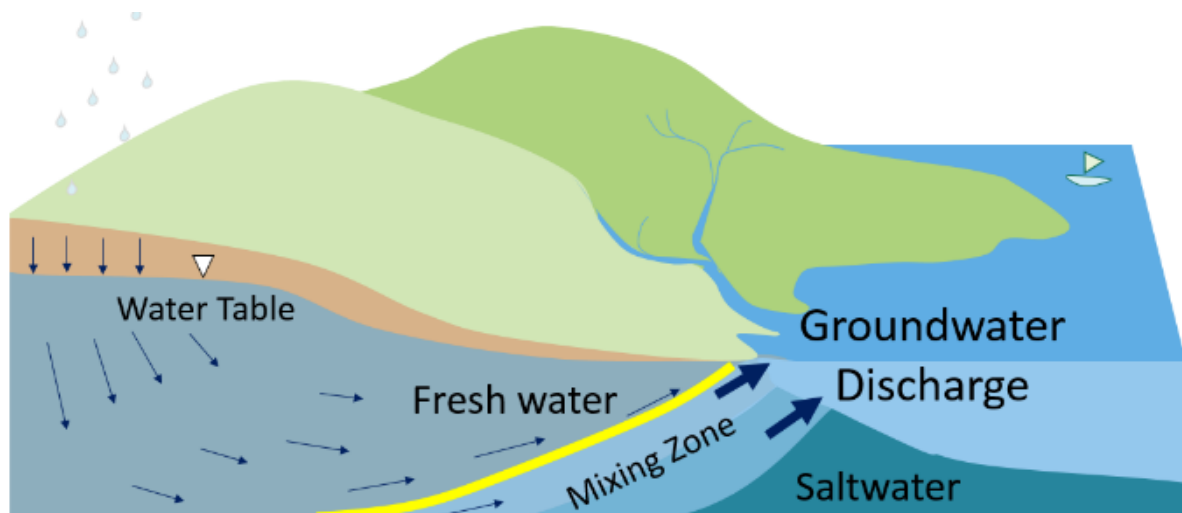


Figure 1.8 The location of the ion exchange front, depicted in yellow, at the freshwater edge of a mixing zone

kinetics of SRP release accompanying saltwater intrusion using a column of carbonate aquifer solids and alternating inflow between fresh groundwater and saltwater.

The southern coastal Everglades of Florida, U.S.A., provides an excellent opportunity to investigate the three process-based questions. The Everglades is P-limited and so oligotrophic it has been called P-starved.⁸ Any input of P rapidly is rapidly removed from the water either by plant uptake or adsorption to sediment in fresh water marshes, and sustained changes in phosphorus availability, however slight, can alter productivity and community structure.⁹ The water in the mangrove ecotone has elevated total dissolved phosphorus compared to the freshwater marshes upstream and Florida Bay, causing researchers to call the ecotone a “net phosphorus source.”¹⁰

Total dissolved P concentrations are high in the brackish groundwater at the mangrove root zone and in the mixing zone of the aquifer below.¹¹ Moreover, the mangrove estuary receives

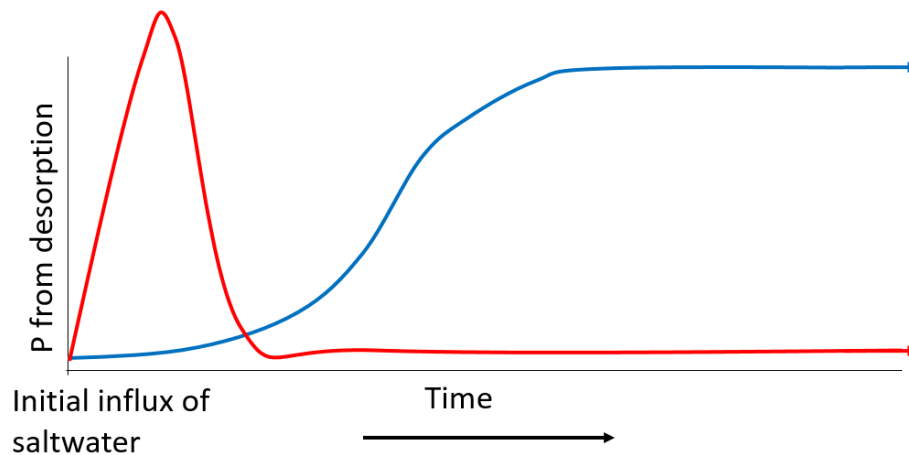


Figure 1.9 Schematic illustration of two contrasting kinetic reactions to an influx of saltwater groundwater discharge from saltwater intrusion, potentially providing a source of SRP to the mangrove root zone.¹¹

By applying the process-based objectives of this dissertation to the Everglades, this research serves the dual purpose of investigating mixing zone P sorption reactions as potential drivers of SRP availability in this iconic ecosystem. Most P sorption work has focused on sediment, either suspended or benthic. The mangrove sediment groundwater is enriched in bicarbonate, providing an opportunity to investigate whether this water type increases water SRP availability (Chapter 2). If so, P sorption reactions provide an *in situ* source of SRP at the mangrove root zone.

Given that the mangrove zone receives mixing zone groundwater with elevated total dissolved P, it would be helpful to know if saltwater-induced P desorption from the limestone bedrock could help explain the ambient water SRP concentration. If so, the pattern of P desorption with respect to incremental increases in saltwater content would have direct implications for the spatial

pattern of SRP availability within the mangrove zone (Chapter 3). Further, the region that receives mixing zone groundwater discharge would be affected by the magnitude and rapidity of P desorption from the bedrock. Understanding the kinetics of P desorption from limestone bedrock is a key component to understanding the temporal pattern of P availability in the face of incremental advances of the saltwater intrusion front (Chapter 4).

For the three main process-based questions in the Everglades I also sought to determine how a shift in the supply of fresh and saltwater would affect P availability. The results of this dissertation are relevant both to restoration efforts and to water management in the face of climate change.

This dissertation is organized around the three manuscripts with multiple coauthors (as noted at the beginning of each chapter) and collaborations in various stages of the journal submission process. Chapter 2, “Saltwater intrusion as potential driver of phosphorus release from limestone bedrock in a coastal aquifer,” has been accepted for publication in *Estuarine, Coastal and Shelf Science*.¹² Chapter 3, “Saltwater intrusion as potential driver of phosphorus release from limestone bedrock in a coastal aquifer,” is in preparation for submission to *Environmental Science and Technology*.¹³ Chapter 4, “Rapid pulse of phosphorus desorption with saltwater intrusion in a carbonate aquifer” is in preparation.¹⁴

References

1. Rivera-Monroy, V. H.; Twilley, R. R.; Davis III, S. E.; Childers, D. L.; Simard, M.; Chambers, R.; Jaffe, R.; Boyer, J. N.; Rudnick, D. T.; Zhang, K., The role of the Everglades Mangrove Ecotone Region (EMER) in regulating nutrient cycling and wetland productivity in south Florida. *Critical Reviews in Environmental Science and Technology* **2011**, *41*, (S1), 633-669.
2. Froelich, P. N., Kinetic control of dissolved phosphate in natural rivers and estuaries: A primer on the phosphate buffer mechanism. *Limnology and oceanography* **1988**, *33*, (4part2), 649-668.
3. Slomp, C. P.; Van Cappellen, P., Nutrient inputs to the coastal ocean through submarine groundwater discharge: controls and potential impact. *Journal of Hydrology* **2004**, *295*, (1), 64-86.
4. Moore, W. S., The subterranean estuary: a reaction zone of ground water and sea water. *Marine Chemistry* **1999**, *65*, (1), 111-125.
5. Reddy, K.; Kadlec, R.; Flaig, E.; Gale, P., Phosphorus retention in streams and wetlands: a review. *Critical reviews in environmental science and technology* **1999**, *29*, (1), 83-146.
6. Millero, F.; Huang, F.; Zhu, X.; Liu, X.; Zhang, J.-Z., Adsorption and desorption of phosphate on calcite and aragonite in seawater. *Aquatic Geochemistry* **2001**, *7*, (1), 33-56.
7. Millero, F. J.; Hiscock, W. T.; Huang, F.; Roche, M.; Zhang, J. Z., Seasonal variation of the carbonate system in Florida Bay. *Bulletin of Marine Science* **2001**, *68*, (1), 101-123.
8. Noe, G. B.; Childers, D. L.; Jones, R. D., Phosphorus biogeochemistry and the impact of phosphorus enrichment: why is the Everglades so unique? *Ecosystems* **2001**, *4*, (7), 603-624.
9. Noe, G. B.; Childers, D. L., Phosphorus budgets in Everglades wetland ecosystems: the effects of hydrology and nutrient enrichment. *Wetlands Ecology and Management* **2007**, *15*, (3), 189-205.
10. Rudnick, D.; Chen, Z.; Childers, D.; Fontaine, T., Phosphorus and nitrogen inputs to Florida Bay: the importance of the Everglades watershed. *Estuaries* **1999**, *22*, (2), 398-416.
11. Price, R. M.; Swart, P. K.; Fourqurean, J. W., Coastal groundwater discharge—an additional source of phosphorus for the oligotrophic wetlands of the Everglades. *Hydrobiologia* **2006**, *569*, (1), 23-36.
12. Flower, H. R., Mark; Zhang, Jia-Zhong; Lewis, David; Price, René Control of Phosphorus concentration through adsorption and desorption in shallow groundwater of subtropical carbonate estuary. *Estuarine, Coastal and Shelf Science* **2015** (in press).
13. Flower, H. R., Mark; Zhang, Jia-Zhong; Lewis, David; Price, René, Saltwater intrusion as potential driver of phosphorus release from limestone bedrock in a coastal aquifer. (in prep).
14. Flower, H. R., Mark; Zhang, Jia-Zhong; Lewis, David, Rapid and sustained phosphorus desorption with saltwater intrusion in a carbonate aquifer. (in prep) **2016**.

Chapter 2:
**Control of phosphorus concentration through adsorption and desorption in shallow
groundwater of subtropical carbonate estuary**

Note to reader

Portions of this chapter have been accepted for publication in *Estuarine, Coastal, and Shelf Science*, 2015. The author of this dissertation is the first author on the paper, and the other authors are: Dr. Mark Rains (contribution: guidance and funding), Dr. David Lewis (contribution: access to equipment and laboratory facilities for phosphorus analysis), Dr. Jia-Zhong Zhang (contribution: guidance in regard to laboratory procedures and analysis), Dr. René Price (contribution: access to groundwater well and field site; analysis of cation and anion concentrations of the three water types). All co-authors assisted in the revision process.

Abstract

The balance of fresh and marine water sources in coastal mixing zones can affect phosphorus (P) availability, one of the important drivers of primary productivity. This study focuses on an abiotic portion of the P cycle in the mangrove ecotone of Taylor Slough, coastal Everglades, Florida. We investigated the P sorption properties of sediment with three distinct water sources in this region: 1) fresh groundwater from the inland Everglades, 2) bicarbonate enriched groundwater from the mangrove ecotone, and 3) surface saltwater from Florida Bay. Ecotone groundwater caused soluble reactive P (SRP) to exhibit markedly low sorption efficiency ($K_d =$

0.2 L g⁻¹) compared to fresh groundwater and Florida Bay water (11.3 L g⁻¹ and 3.4 L g⁻¹, respectively). The low SRP buffering capacity of the sediment in ecotone groundwater would maintain higher ambient water SRP concentration in ecotone groundwater than in the other two waters, and would trigger desorption if the sediment changed from one of them to ecotone groundwater. The relative sorption efficiency is consistent with the measured zero equilibrium SRP concentration being highest in ecotone groundwater ($0.094 \pm 0.003 \mu\text{M}$) and lower in fresh groundwater and Florida Bay surface water ($0.075 \pm 0.005 \mu\text{M}$ and $0.058 \pm 0.004 \mu\text{M}$ respectively). The temporal variability of SRP concentration in groundwater at the ecotone field station is greater than the range of zero equilibrium SRP concentration for all three waters, so very low SRP concentration in the ambient water would induce desorption from the sediment. Soluble reactive P would be expected to begin desorbing from the sediments at a higher ambient SRP concentration in ecotone groundwater than the other two water types. Our results suggest that ecotone groundwater would release more SRP from mangrove sediments compared to the upstream and downstream waters, due to both its lower P sorption efficiency and its higher zero equilibrium SRP concentration.

Introduction

Mangrove swamps are ubiquitous along sheltered coasts between latitudes 25°N and 30°S, covering an estimated 20 million hectares worldwide.¹ Mangrove forests provide important ecosystem services, including the maintenance of water quality, stabilization of shorelines and coastal community protection, and carbon sequestration.^{2,3} Mangroves provide nursery and spawning grounds for many coastal crustaceans and fish, thereby supporting local fisheries and ocean biodiversity.⁴

A detailed assessment of the controls on bioavailability of the essential nutrients is critical to understanding coastal estuaries.⁵ Phosphorus (P) is commonly a limiting nutrient in mangrove swamps.^{6,7} The bioavailable form of P is dissolved inorganic P,⁸ which is dominated by the orthophosphate species H_2PO_4^- at pH less than 7.2, and HPO_4^{2-} above that. Dissolved organic P and particulate P (both organic and inorganic) are immobile until mineralized to dissolved inorganic P, which typically requires microbial activity.⁹ We refer to dissolved inorganic P as soluble reactive P (SRP), defined as the fraction of P in a water sample that passes through a 0.45 μm filter and responds to colorimetric tests without having been subjected to a pretreatment of hydrolysis or oxidative digestion.¹⁰ The SRP concentration is considered to be roughly equivalent to dissolved inorganic P concentration, but the distinction is made because there is potential for organic or colloidal P to pass through $<0.45 \mu\text{m}$ and to react to colorimetric reagents.¹¹

The cycle through which P shifts between SRP and immobilized forms involves a great number of complex processes, and both biotic and abiotic portions of the cycle must be considered when evaluating P availability in wetlands.¹² Abiotic processes in the P cycle include leaching of P from leaf litter; sedimentation; exchange of P between sediment and the overlying water column; processes with inorganic P phases such as apatite, eg., precipitation, dissolution, and weathering; and P sorption reactions.^{12, 13} Phosphorus sorption is an important process in wetlands whereby P is exchanged between SRP in the ambient water and solid phase P.⁵ The process has two steps. The first step has fast kinetics (minutes to hours) and involves the accumulation (adsorption) of SRP from ambient water at sediment particle surfaces. This step is rapidly reversible; as

conditions change, desorption can release the adsorbed SRP back to the ambient water. The second adsorption step is much slower (days to weeks), and involves solid-state diffusion of adsorbed SRP from the mineral surface into the interior of mineral grains.⁵

In this study we discuss P sorption in terms of the rapid, reversible first step.

Adsorption/desorption reactions can act as SRP buffers, analogous to pH buffers, maintaining water SRP at a constant concentration. The water SRP concentration at which zero net SRP adsorption or desorption occurs for a given system is termed the zero equilibrium SRP concentration (EPC_0). When ambient water SRP concentration is close to the EPC_0 , the sediment displays the maximum capacity for buffering SRP.⁵ Slight rises or falls in ambient SRP concentration from this equilibrium may result in rapid adsorption or desorption, respectively, returning the system to a new equilibrium.⁵ A sediment is described as having high adsorption efficiency when SRP adsorption increases intensely as water SRP concentration increases. Efficient P sorption results in high SRP buffer intensity, maintaining low water SRP concentration as long as the sediment does not become saturated.¹²

Highly variable water chemistry in coastal mixing zones causes variability in SRP availability through shifting P sorption behavior. Sorption reactions are influenced by physiochemical properties of the given sediments and their ambient water, including the composition and particle size distribution of the solid particles, temperature, pH, ionic strength, redox status, organic matter content, and ions in the ambient water.^{12, 14-16} The sensitivity of P sorption reactions to water chemistry and sediment characteristics means that the direction and strength of sorption

reactions are hard to predict without direct experimentation with the natural sediment and water in question.¹⁷

Some coastal estuaries have ambient water SRP concentration that is higher than would be predicted based on conservative mixing of the fresh river water and seawater. Typically freshwater causes SRP to adsorb more effectively to the substrate, so an influx of seawater induces desorption of loosely adsorbed SRP from suspended or benthic sediments.^{5, 14} Suspended sediments in coastal rivers may release SRP as they enter the seawater mixing zone.¹⁸ Similarly, an incursion of seawater due to tidal influx or seawater intrusion can lead to rapid desorption from suspended and benthic sediment particles, accompanied by increases in measured SRP concentrations.^{17, 19, 20}

Microbial activity enriches groundwater HCO_3^- concentration above saltwater levels in some coastal wetlands. Millero, et al.²¹ predicted that along coastlines where saltwater mixes with a water that has high HCO_3^- concentration, the typical pattern of seawater-induced desorption could be reversed, such that an influx of seawater into sediment that had been equilibrated to the water with HCO_3^- concentration could cause the sediment to release HCO_3^- ions and adsorb SRP. Experiments by Millero, et al.,¹⁵ on synthetic calcite determined that especially at low salinity the apparent effect of salinity is driven by the higher concentrations of HCO_3^- and SO_4^{2-} in saltwater. When HCO_3^- concentration was held constant (2 mM) adsorption was nearly independent of salinity. The slight positive charge of the calcium atom on calcium carbonate surfaces attract SRP anions, forming surface complexation reactions. An influx of HCO_3^- ions can induce anion exchange at the positive sorption sites.

Many mangrove estuaries are found in carbonate lithologies, including Belize, the West Indies, Bermuda, Mexico, Western Australia, Brazil and East Africa.^{6, 22-26} To understand the drivers of coastal wetland productivity in carbonate-based regions it is essential to determine the behavior of P sorption in carbonate sediments with respect to high bicarbonate water, fresh water and saltwater. This study examines the potential for SRP concentration of the shallow groundwater in a mangrove swamp to be affected by *in situ* adsorption and desorption reactions in response to mixing of these three water types. In so doing, this study provides insight into the fast-acting abiotic portion of the biogeochemical P cycle in a coastal mixing zone, which has implications for other estuaries with carbonate lithology and a water enriched in HCO_3^- .

Methods

Study area. The southern terminus of the Florida peninsula is fringed by a wide mangrove swamp, dividing the upstream freshwater marsh from Florida Bay (Figure 2.1). The Everglades wetland complex of southern Florida, USA has two main drainage basins: Shark River Slough, which angles to the southwest and drains into the Gulf of Mexico, and the smaller Taylor Slough, which flows southward into the northeast corner of Florida Bay. The Everglades mangrove region is within 1 m of mean sea level. Tides along the western portion of Florida Bay are mixed diurnal and semidiurnal with a mean amplitude of about 0.3 m.²⁷ As waters from the Gulf of Mexico move into Florida Bay, the tidal effects are dampened by the shallow mud banks such that the Eastern bay is micro tidal, with tidal amplitudes of only about 1-5 cm.²⁷ On a few occasions per year, bay saltwater flows upstream into the upper mangrove fringe wetlands of

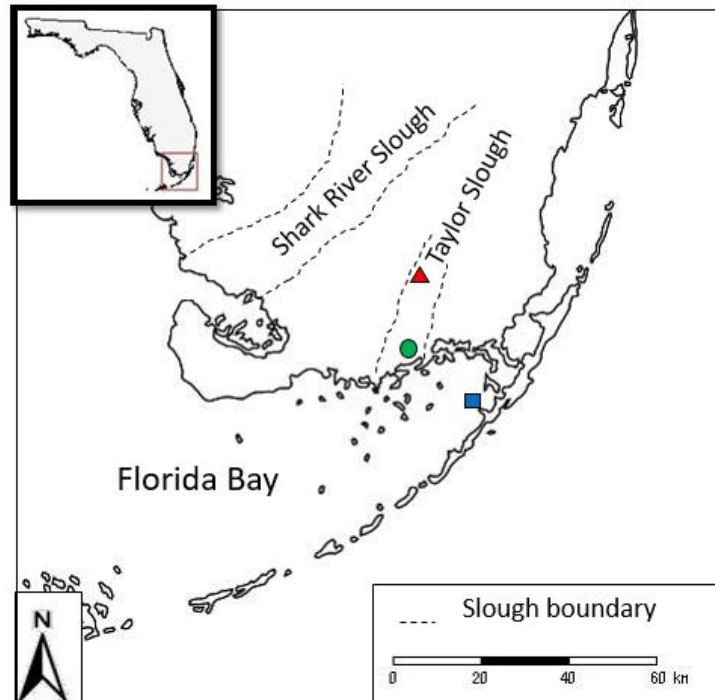


Figure 2.1 Collection locations for samples: fresh GW (red triangle), ecotone GW and sediment (green circle), and bay SW (blue square)

Taylor Slough, particularly in the dry season during times of low freshwater hydraulic head and sustained southerly winds.²⁸⁻³¹ The sediment layer consists of a relatively thin layer (up to 1.5 m deep) of calcareous marl and peat³² with mangrove roots penetrating the shallow sediments down to the underlying limestone bedrock.³³ The limestone aquifer underlying Taylor Slough is the unconfined highly transmissive Biscayne Aquifer³⁴. Saltwater intrudes into the Biscayne Aquifer between 6-10 km inland in Taylor Slough.^{35, 36}

The Taylor Slough mangrove ecotone (hereafter referred to as the “ecotone”) is oligotrophic and highly P-limited.³⁷ The groundwater in the shallow sediments of the ecotone has much higher HCO_3^- concentration than either the upstream freshwater or the downstream Florida Bay saltwater, and the three waters mix with a high degree of temporal and spatial variability.^{21, 36, 38}

Water samples. Three water types were collected representing fresh groundwater (“fresh GW”), high bicarbonate groundwater (“ecotone GW”), and surface saltwater from Florida Bay (“bay SW”) (Figure 2.1). Our fresh GW was collected from a shallow monitoring well (TSB-15) within the bedrock underlying the freshwater sawgrass marsh region of Taylor Slough. The well is lined with a 5.5 cm diameter PVC pipe screened at 4 m depth. The well was first purged of at least five well volumes using a peristaltic pump. The high bicarbonate water was taken from well C3 in the Taylor Slough mangrove ecotone about 4 km inland at monitoring station TS/Ph 6b operated by the Florida Coastal Everglades Long Term Ecological Research Program.³⁰ The well penetrates to a depth of 142 cm within the sediment layer.^{30, 39} Florida Bay surface water was taken from a dock at Key Largo to represent saltwater.

Immediately after sampling, temperature, pH, and electrical conductivity were measured with a YSI 556 MPS (YSI, Yellow Springs OH). Water samples placed in HDPE Nalgene bottles and maintained at 4°C (± 2°C) prior to analysis. Total alkalinity was determined within 24 hours by potentiometric acid titration. Given the high total alkalinity of our ecotone GW and the pH measurements, we refer to these measurements as HCO₃⁻ concentration, while recognizing that small amounts of the other bases may be included in the measured quantity. Major cations and anions were determined at FIU with ion chromatography. The SRP concentration of the field samples were analyzed as discussed in a subsequent section. Selected water characteristics are presented in Table 2.1 and Figure 2.2. The water that was to be refrigerated in 9 L HDPE Nalgene carboys for later experimentation was first filtered through 0.1 μm PTFE filters using a vacuum filter flask to exclude microorganisms that could uptake or release P during water storage.

Table 2.1 Selected characteristics of the three field waters

Water Type	pH	Salinity psu	Ca ²⁺ mM	Mg ²⁺ mM	Na ⁺ mM	K ⁺ mM	Cl ⁻ mM	SO ₄ ²⁻ mM	Total alkalinity as HCO ₃ ⁻ mM	SRP μM	Si(OH) ₄ μM
Fresh	7.3		1.8	0.1	0.7	0.01	0.8	*	4.0	0.050	80.4
GW		0.1									
Ecotone	6.7	16.0	6.7	29.6	217.9	4.16	264.1	11.2	17.5	0.177	83.6
GW											
Bay SW	8.2	31.4	9.1	50.0	425.9	9.29	512.4	28.4	2.9	0.076	9.2

* Below detection

Sediment samples. Sediment composition was held constant by running all experiments using a representative sample from a homogenized 1-5 cm depth increment extracted from a single sampling date and location (same location as ecotone GW). This depth increment was chosen so as to have a sufficiently large sample with little variation by depth. The top 1 cm of cores taken at this location were not used because they were darker in color than the sediment immediately below, and because exceptionally high total sedimentary P was found in the top 1 cm sediment in a pond further downstream.⁴⁰ Calcareous marl sediment was extracted using a Russian peat corer at FCE field station TS/Ph6b (Figure 2.1). The sediment was placed in ziplock bags, and was kept on ice for transport to the lab, where it was air dried, passed through stainless steel sieves (<125 μm), and kept refrigerated prior to use.

Loosely adsorbed or readily exchangeable P (P_{exch}) was defined as the SRP released from sediment by MgCl₂ solution at pH 8.0.⁴¹ A 0.5 g of dry sieved sediment was combined with 1 M

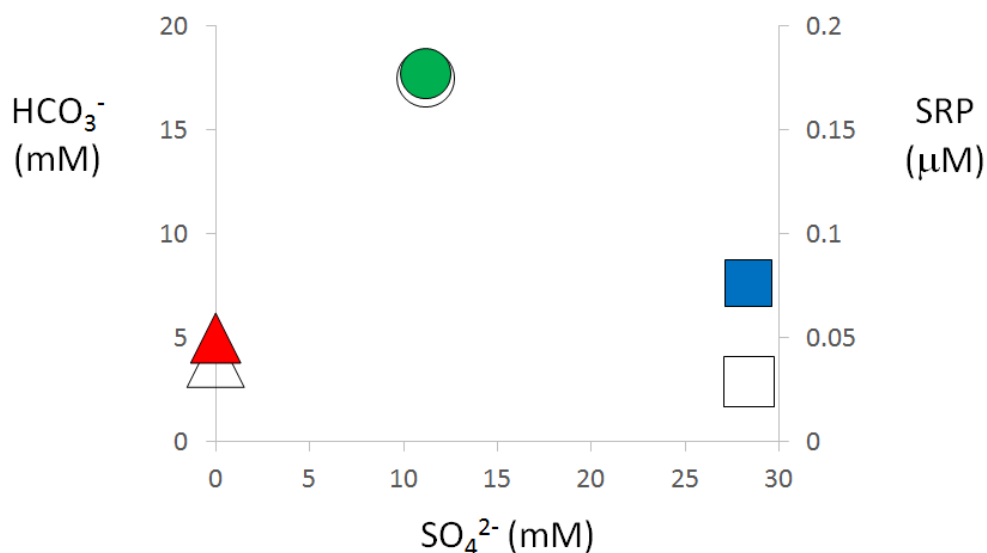


Figure 2.2 Selected water composition for fresh GW (red triangle), ecotone GW (green circle), and bay SW (blue square) with SRP concentration in filled shapes, and HCO₃⁻ concentration in open shapes

MgCl₂ solution, and pH was adjusted with dilute NaOH solution. Sediment and solution were placed in 60 mL high density polypropylene digestion tubes and agitated for 2 hours on a platform shaker at 200 rotations per minute at room temperature, with a total of 5 replicates. Slurries were filtered with 0.45 μm nylon syringe filters and divided into two 10 mL subsamples. The first subsample was analyzed for SRP (section 2.5) so as to determine MgCl₂-exchangeable inorganic P (P_{exch}), with the resulting concentration normalized to μmoles per grams of sediment. We also measured MgCl₂-exchangeable organic P for the purpose of characterizing the sediment, but its dynamics are beyond the scope of this paper because it is considered less bioavailable and behaves differently from inorganic P.⁴² The organic MgCl₂-exchangeable P fraction is determined by measuring total dissolved P concentration in the subsample that had been set aside, and subtracting from that the SRP concentration measured previously in the undigested subsample; the difference is assumed to be the dissolved organic fraction liberated by MgCl₂.^{43, 44} To measure total dissolved P, 10 mL of filtrate is first digested with 1 mL of neutral potassium

persulfate solution (5%, w/v, pH approximately 6.5) at 90°C for 16 hours⁴⁵ and analyzed for SRP (section 2.5) after returning to room temperature.

A portion of the sediment was acid digested (preparation method EPA 3050) and total sedimentary P was determined inductively coupled plasma-atomic emission spectrometry (analytical method EPA 6010). Selected sediment characteristics are presented in Table 2.2.

Table 2.2 Selected phosphorus analysis of the sediment, in $\mu\text{mol g}^{-1}$

MgCl ₂ inorganic P (P_{exch})	0.022 ± 0.002
MgCl ₂ organic P	0.025 ± 0.002
Total Sedimentary P	1.3

Sorption isotherm experiments. Phosphorus sorption parameters of the sediment in contact with the three water types were determined by batch incubation experiments based on the method of Froelich.⁵ Subsamples of each water type received variable portions of stock SRP solution to establish batches with SRP concentrations of 0 (no added SRP), 4, 8, 16, 24, 32, and 48 μM . To inhibit biological activity from microbes in the sediment, 10 μL 0.1% chloroform was added to each tube.⁴⁶ The initial SRP concentration, $[\text{SRP}]_i$, for each batch of field water-SRP solution was analyzed directly for SRP before the incubation began.

For the batch with no added SRP, so as to permit the detection of P desorption from sediment with such low P content, the solution was concentrated by using 5 mL of a given field water and 1.5 g sediment, and with 20 replicates for each water type. For the other batches, 10 mL of field

water-SRP solution was combined with a 200 mg subsample of ecotone sediment in a 15 mL plastic conical centrifuge tube (10 replicates per water type per batch, 30 samples total in a batch). At 48 μM SRP the fresh GW sorption curve was still relatively steep, thus not providing sufficient of the sorption isotherm curve for calculating P_{max} (described in a subsequent section). So as to better characterize P_{max} , five additional SRP concentrations ranging from 60-320 μM SRP were used for fresh GW (with three replicates for each increment of added P). In all batch incubation experiments, each suspension was agitated at 200 rpm on a platform shaker for 24 hours at room temperature ($23\pm 0.5^\circ\text{C}$). Next, each suspension was filtered with a 0.45 μm nylon syringe filter, and immediately analyzed for final SRP concentration, $[\text{SRP}]_f$ (described in the next section). A total of 255 P sorption experiments were conducted.

Soluble reactive phosphorus analysis. Soluble reactive P concentrations were determined the day of each experiment by first filtering samples through a 0.45 μm nylon syringe filter and then using the microscale malachite green method,⁴⁷ measuring absorbance at 630 nm in 96-well microplates on a BioTek EPOCH microplate spectrophotometer.

Sorption isotherm parameters. The amount of SRP adsorbed or desorbed from the sediment, ΔP_{sed} , was calculated as:

$$\Delta P_{\text{sed}} = [\text{SRP}]_i - [\text{SRP}]_f \quad . \quad [1]$$

ΔP_{sed} was normalized to the mass of sediment and volume of solution ($\mu\text{mol g}^{-1}$). A plot of ΔP_{sed} vs. $[\text{SRP}]_f$ was used to describe a sediment's adsorption behavior when in contact with each of the three water types.

Various sorption models exist for providing empirically-fit parameters that summarize the resulting isotherm. At the very low range of SRP, where the number of available adsorption sites is much higher than the concentration of SRP available in solution, sorption increases in direct proportion to added SRP and a linear model provides the best fit (Figure 2.3a).

The linear isotherm equation is:

$$\Delta P_{\text{sed}} = K_d [\text{SRP}]_f - \text{NAP} \quad , \quad [2]$$

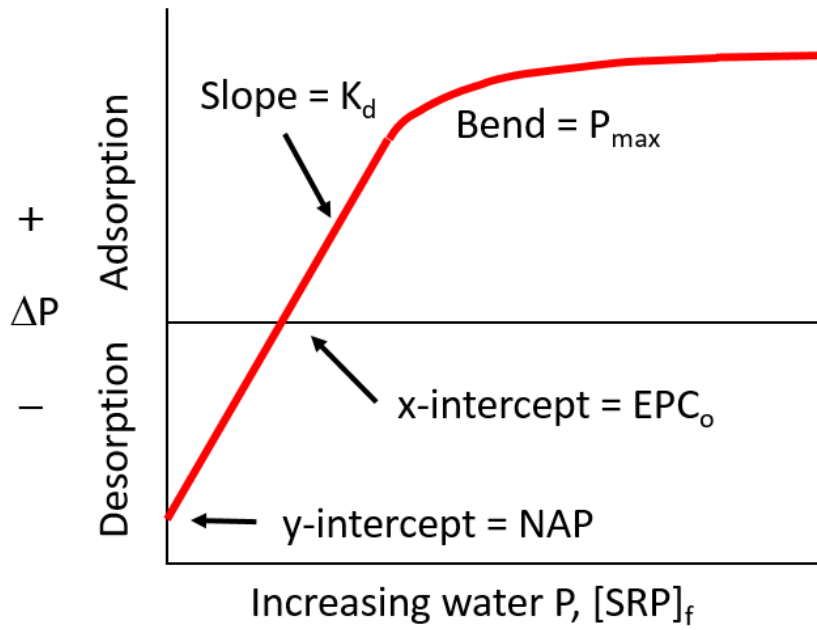
where K_d (L g^{-1}) is the slope, and NAP ($\mu\text{mol g}^{-1}$) is native adsorbed SRP (the y-intercept), a constant representing the amount of pre-existing loosely adsorbed inorganic P on the sediment (Figure 2.3a). Negative ΔP_{sed} indicates desorption from the sediment and positive ΔP_{sed} indicates adsorption onto the sediment. The EPC_o ($\mu\text{mol g}^{-1}$) is obtained from x-intercept, the measured equilibrium SRP concentration at which neither desorption nor adsorption occurs. The linear equation can be rearranged to solve for EPC_o .

$$\text{EPC}_o = \text{EPC}_o = \frac{\text{NAP}}{K_d} \quad , \quad \text{when } \Delta P_{\text{sed}} = 0 \quad . \quad [3]$$

The sorption coefficient K_d is a measure of the buffer intensity (also described as sorption efficiency), and is formally defined as the number of moles of SRP required to be added to or subtracted from the system to change $[\text{SRP}]_f$ by 1 μM near the EPC_o .⁵ A steep slope (high K_d) near the EPC_o indicates a system with high sorption efficiency.

The purpose of experimentally increasing SRP concentration beyond what is realistic for field conditions is to characterize certain characteristics of the sorption behavior of a given sediment-water combination that can only be calculated as the sediment responds to artificially high SRP

a)



b)

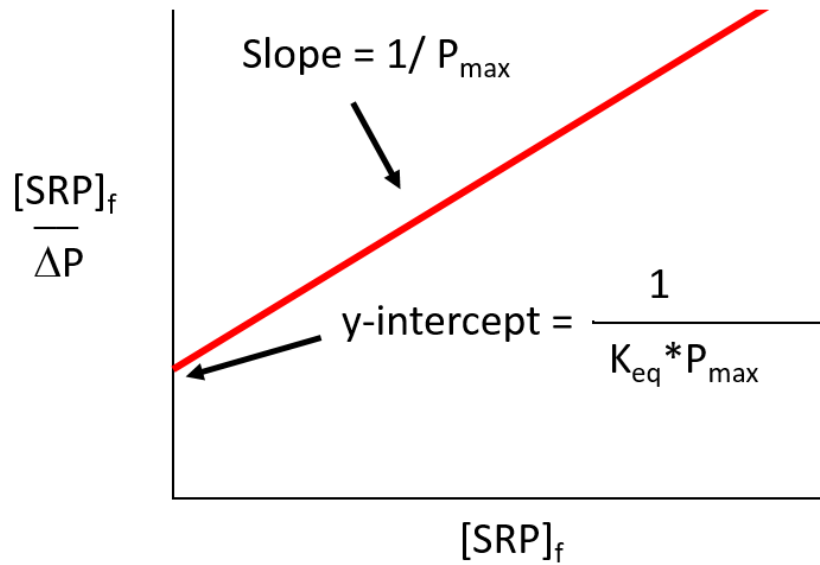


Figure 2.3 a) Schematic of P sorption isotherm; b) Schematic of the y-intercept and P_{max}

concentrations, such as saturation concentration and the possibility of two adsorption sites with different affinities for SRP. As the final SRP concentration increases in solution, the adsorption of SRP to sediment decreases, resulting in the sorption curve bending from linear to an increasingly low angle curve (Figure 2.3a). The Langmuir sorption model assumes the sediment surface has a finite number of available adsorption sites, with sorption reaching saturation at a maximum monolayer sorption capacity, P_{max} . Such behavior can be modeled as:

$$\Delta P_{sed} = \frac{K_{eq} P_{max} [SRP]_f}{(1 + K_{eq} [SRP]_f)} \quad [4]$$

The constant K_{eq} (μM^{-1}) is different from K_d and is related to the binding energy of the adsorption sites (also described as the affinity of SRP for the binding to the sediment surface in the given water). When sorption data are evaluated by using the reciprocal plot of the Langmuir adsorption equation:

$$\frac{[SRP]_f}{\Delta P_{sed}} = \frac{[SRP]_f}{P_{max}} + \frac{1}{K_{eq} P_{max}} \quad [5]$$

a linear line segment is formed, in which P_{max} is the reciprocal of the slope, and K_{eq} is the inverse product of P_{max} and the y-intercept, as depicted in Figure 2.3b.

If the solid particle has two adsorption sites with different affinities for SRP, its reciprocal Langmuir plot will exhibit two line segments with different slope. The Langmuir two-surface sorption isotherm generates two pairs of P_{max} and K_{eq} constants:⁴⁸

$$\Delta P_{sed} = \frac{K_{eq1} P_{max1} [SRP]_f}{(1 + K_{eq1} [SRP]_f)} + \frac{K_{eq2} P_{max2} [SRP]_f}{(1 + K_{eq2} [SRP]_f)} \quad [6]$$

where the subscripts “1” and “2” indicate the adsorption sites with higher and lower bonding energies, respectively. Model parameters for equation 6 were estimated by minimizing log weighted error.

Results

In spite of only one sediment being used in our sorption experiments, we observed very different P sorption behavior based on water type. Sorption efficiency followed the order: fresh GW > bay SW > ecotone GW. A sorption plot of ΔP_{sed} as a function of $[\text{SRP}]_f$ is given in Figure 2.4a, and the parameters derived from the isotherm models are listed in Table 2.3. Soluble reactive P adsorbed to sediments most efficiently in fresh GW, as it has the steepest slope ($K_d = 11 \text{ L g}^{-1}$). ΔP_{sed} in fresh GW was 20-40% higher than ecotone GW and bay SW across all SRP concentrations. Bay SW adsorbed efficiently at low SRP concentrations ($K_d = 3.4 \text{ L g}^{-1}$), and ecotone GW exhibits low sorption efficiency across all SRP concentrations; its K_d (0.21 L g^{-1}) is 63 and 17 times lower than fresh GW and bay SW, respectively.

Sorption curves typically begin linear and then the slope begins to decrease at the onset of saturation. The bay SW isotherm curve inflects at a low ΔP_{sed} and a low concentration of $[\text{SRP}]_f$. When $[\text{SRP}]_f / \Delta P_{\text{sed}}$ is plotted as a function of $[\text{SRP}]_f$ the data for each water type form two distinct straight-line components (Figure 2.4b and c). Soils commonly exhibit distinct line segments in reciprocal plots, indicating two types of adsorption sites may have different kinetics.^{49, 50}

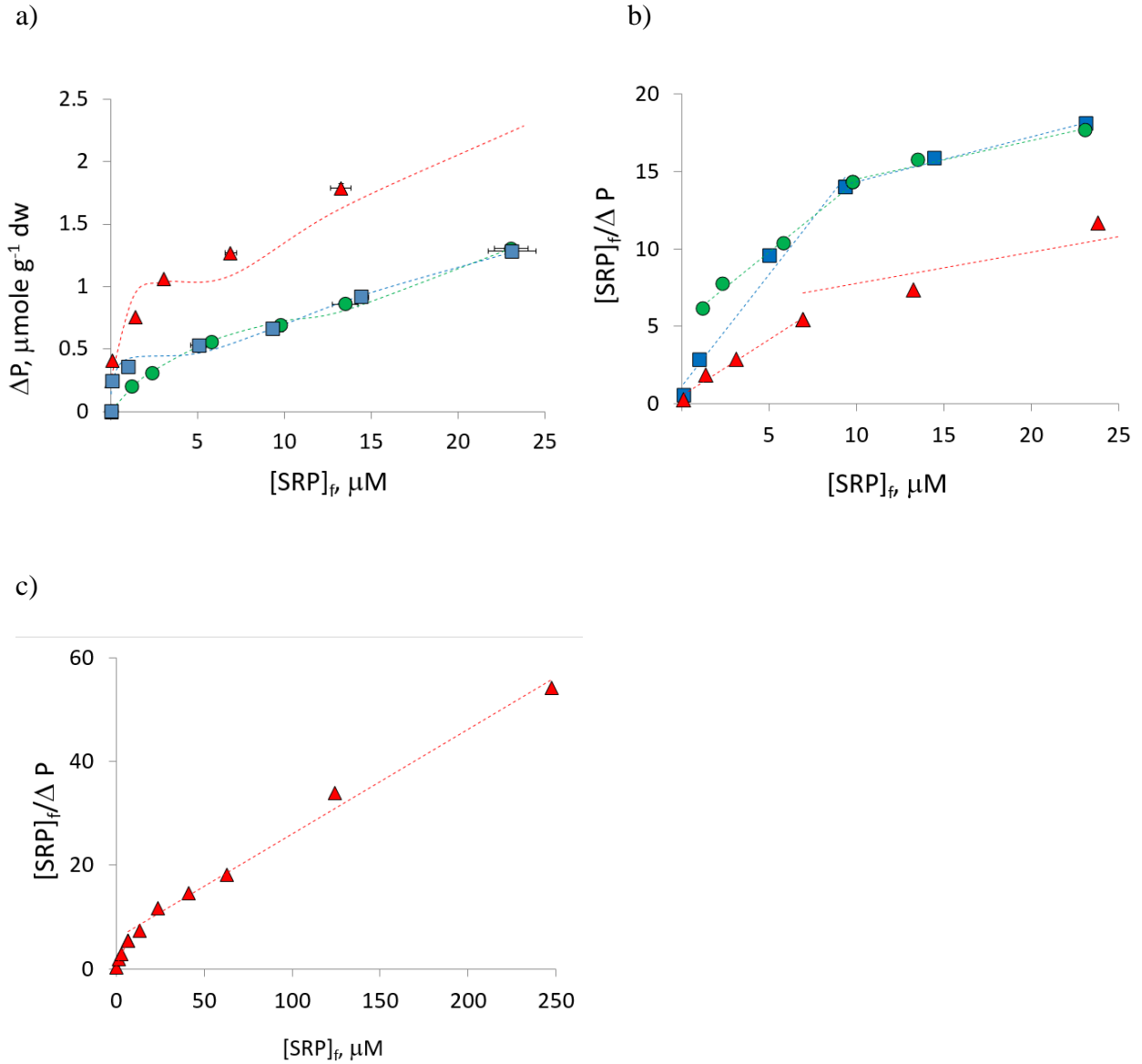


Figure 2.4 Fresh GW (red triangles), ecotone GW (green circles), and bay SW (blue squares), accompanied by dashes representing the Langmuir Two-Surface Sorption isotherms; a) in standard plot; b) in reciprocal plot from which Langmuir two surface isotherm parameters were determined; and c) the extended two-surface isotherm for fresh GW

Accordingly, the two-surface Langmuir isotherm equation is applied so as to derive separate sorption parameters for the high and low energy adsorption sites⁴⁸. The P saturation, P_{max} , is calculated as the reciprocal of the slope, and in Figure 2.4b fresh GW and ecotone GW have

visibly similar slopes for both line segments (high and low energy adsorption sites), resulting in similar values as each other for both $P_{\max 1}$ ($1.1 \mu\text{mol g}^{-1}$ and $1.4 \mu\text{mol g}^{-1}$, respectively) and $P_{\max 2}$ ($4.7 \mu\text{mol g}^{-1}$ and $4.1 \mu\text{mol g}^{-1}$, respectively) compared to the much lower values for bay SW ($P_{\max 1}$: $0.4 \mu\text{mol g}^{-1}$ and $P_{\max 2}$: $2.0 \mu\text{mol g}^{-1}$).

Table 2.3 Phosphorus sorption parameters of the ecotone sediment

Field Water	K_d , ^a	Desorbed	NAP ^c	EPC _o ^d	$P_{\max 1}$ ^e	$K_{eq 1}$ ^f	$P_{\max 1}$ ^g	$K_{eq 2}$ ^h
	L g^{-1}	SRP ^b	$\mu\text{mol g}^{-1}$	μM	$\mu\text{mol g}^{-1}$	μM^{-1}	$\mu\text{mol g}^{-1}$	μM^{-1}
		$\mu\text{mol g}^{-1}$			1		1	
Fresh GW	11	0.0034 ± 0.0002	0.85	0.075	1.1	3.5	4.7	0.04
Ecotone GW	0.21	0.0028 ± 0.0002	0.02	0.094	1.2	0.2	4.1	0.02
Bay SW	3.40	0.0024 ± 0.0002	0.20	0.058	0.4	12.6	2.0	0.06

^a Linear adsorption coefficient

^b Desorbed SRP from natural water (no added P)

^c Native adsorbed P

^d Equilibrium SRP concentration

^e Adsorption maximum for first surface

^f Adsorption energy for first surface

^g Adsorption maximum for second surface

^h Adsorption energy for second surface

Although fresh GW and ecotone GW reach saturation at similar thresholds, the low sorption efficiency of ecotone GW means that it takes a much higher $[\text{SRP}]_f$ concentration to reach the same saturation point. Conversely, although bay SW has high sorption efficiency initially, it

reaches saturation at a very lower SRP concentration compared to the other two waters. The EPC_0 's for the three water types follow a different order: ecotone GW > fresh GW > bay SW ($0.094 \pm 0.003 \mu\text{M}$, $0.075 \pm 0.005 \mu\text{M}$, and $0.058 \pm 0.004 \mu\text{M}$, respectively).

Discussion

Our results support the hypothesis of Millero, et al.,¹⁵ that high bicarbonate water causes sediment to have lower sorption efficiency than it does in either fresh water or saltwater. Our sediment acted as a high SRP sink in fresh GW, as reflected in the high P sorption efficiency (K_d) and high saturation concentration (P_{max}). In Florida Bay seawater the sediment exhibits intermediate sorption efficiency. The sediment in ecotone GW exhibits very low SRP buffering capacity (low K_d), which would maintain higher ambient water SRP concentration.

Risk of eutrophication from outside sources is also higher in a sediment with low buffering capacity. Portions of the freshwater Everglades that have received water with elevated SRP from canals have exhibited high buffering capacity, sequestering some of the excess P, as measured in high sedimentary total P.^{51, 52} The P retention capacity of the sediments in both freshwater marshes and bays protect the overlying water column from rapid P release,⁵³ although where P-loading is intense, such as the Everglades Agricultural Area even freshwater can induce significant desorption from the sediment.⁵⁴ The results of this study suggest that carbonate sediment in water with high HCO_3^- concentration would have severely limited ability to remove excess SRP from the water and would readily desorb P from sediments.

Given that the mangrove ecotone is an active mixing zone, it is important to recognize that if the sediment were equilibrated to ecotone GW, an influx of either bay SW or fresh GW would be expected to lead to adsorption of P to the sediment. Conversely, the same sediment immersed in either bay SW or fresh GW would undergo desorption upon a change to ecotone GW. Many coastal wetlands are subject to influxes of fresh and tidal seawater, such as during storm and tide events, and also on diurnal, seasonal, and long term time scales, which could result in frequent rapid reversals in P sorption. Conversely encroachment of mangroves into a former freshwater wetland may be accompanied by increase in concentration of both HCO_3^- and SRP. The mangrove site for this study was a freshwater marsh in 1950, before mangroves encroached from Florida Bay.⁵⁵ Sea level rise is expected to exacerbate saltwater intrusion in many areas.⁵⁶ Long-term increases in freshwater flow could recharge the aquifer and potentially cause a mangrove zone to retreat seaward, shifting P sorption dynamics as it goes. The Comprehensive Everglades Restoration Plan is a multibillion dollar project launched in 2000, one of the largest restoration projects ever undertaken. A key goal of this restoration plan is to increase freshwater flows so as to mitigate or delay the effects of sea level rise.

The EPC_o 's of this study are at the low end of the 0.03-6.20 μM range found in P sorption studies in the freshwater Everglades under aerobic conditions.⁵⁷ Zhou and Li⁵⁸ investigated two soils from a freshwater marsh in the Everglades, of which one had an EPC_o (0.065 μM) similar to the values for our sediment in bay SW (0.058 μM) and fresh GW (0.075 μM), and the other had a much higher EPC_o (0.323 μM). By contrast, P-polluted canal sediments in the Everglades Agricultural Area were found to have EPC_o 's ranging from 1.9 to 3.9 μM .⁵⁴ This is consistent

with a finding in the Northern Everglades and agricultural areas in southeastern Florida, where soil EPC_o has been found to increase with increasing P enrichment.^{58, 59}

Nonetheless, all three EPC_o 's determined for this study are intermediate to the range of ambient water SRP concentration seen in monthly monitoring efforts at the ecotone field location (range 0.02-0.27 μM SRP; Price, René, unpublished data). On the occasions when the ambient water SRP concentration is at a low point, the ecotone sediment may desorb SRP on the order of 0.003 $\mu\text{mol g}^{-1}$ (Table 2.3). When magnified by the high *in situ* sediment:water ratio, desorption of this magnitude could provide a critical SRP subsidy when most needed. Any release of SRP by the sediment would be immediately ecologically relevant given that mangrove roots permeate the sediment layer here.³³ The higher EPC_o for ecotone GW compared to fresh GW and bay SW indicates that SRP desorbs from the sediment at a higher ambient water SRP concentration and over a wider range of water SRP concentrations. The times when the ambient water exceeds the EPC_o for ecotone GW is unlikely to produce much adsorption due to the low sorption efficiency of the sediment in this water.

The low P content of our sediment may explain its high sorption efficiency in fresh and saltwater, and low EPC_o 's in all three of our water types. In a study of soils from a range of freshwater, estuary, and saltwater sites in the Southern Everglades, mangrove ecotone sediment at the same monitoring station as ours had the least P_{exch} of the 17 Everglades sediments investigated.⁶⁰ Zhang and Huang⁶¹ determined that low P_{exch} was associated with lower EPC_o and higher sorption efficiency in Florida Bay sediments. They measured P_{exch} for sediments at 40 stations. Their lowest P_{exch} was 0.023 $\mu\text{mol g}^{-1}$ was measured in a sediment from their sampling

station nearest to our study area, and it was comparable to our sediment's P_{exch} ($0.022 \pm 0.002 \mu\text{mol g}^{-1}$). Our mangrove swamp sediments may be a landward extension of the pattern of low P_{exch} in the northeast portion of Florida Bay. Consistent with its low P_{exch} , that bay sediment exhibited a higher K_d values (0.579 L g^{-1}) which was intermediate to our sediment in ecotone GW and bay SW), and lower EPC_o 's ($0.503 \mu\text{M}$) which was approximately an order of magnitude higher than ours.

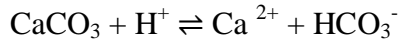
The NAP for ecotone GW ($0.02 \mu\text{mol g}^{-1}$) is consistent with the measured P_{exch} of $0.022 \pm 0.002 \mu\text{mol g}^{-1}$ for the sediment (Tables 2.2 and 2.3), an agreement that could be causally related to the fact that it had been equilibrated to ecotone GW at the time of collection. Our NAP estimates followed fresh GW > bay SW > ecotone GW ($0.85 \mu\text{mol g}^{-1}$, $0.20 \mu\text{mole g}^{-1}$, and $0.02 \mu\text{mol g}^{-1}$, respectively). Since NAP is the negative of the y-intercept on the sorption plot, a steep sorption slope (high K_d), as seen in the fresh GW and bay SW, forces a more negative y-intercept and higher NAP. In this way, the experimental determination of higher NAP in fresh GW and bay SW suggests that if the sediment had been immersed in one of these waters at the time of collection, it may have exhibited a higher P_{exch} . The two-surface Langmuir isotherm (Figure 2.4b) also suggests that SRP encountered distinct site density and energetics for the same sediment depending on which water it was in. It is plausible that SRP attaches to similar adsorption sites in fresh GW and ecotone GW, as reflected in the similar kinetics of the two waters, and that these adsorption sites are not available (or are less favorable) when the sediment is in contact with bay SW. This difference in behavior in bay SW can also be seen in the K_{eq} of the sediment in bay SW ($12.6 \mu\text{M}^{-1}$), which is 3.6 times higher than in fresh SW ($3.5 \mu\text{M}^{-1}$) and

62.5 times higher than in ecotone GW ($0.2 \mu\text{M}^{-1}$). The high K_{eq} of the sediment in bay SW indicates sorption initially occurs at sites with high affinity for SRP in bay SW.

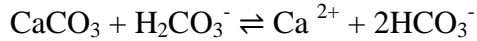
The behavior of our sediment in high bicarbonate groundwater is consistent with local field measurements that show ecotone surface water and sediment groundwater often have higher total dissolved P than freshwater or coastal waters.^{36, 62} The Everglades mangrove zone has been called a “net source”⁶² of total dissolved P and that some form of “nutrient regeneration or retention” must be occurring.⁶³ Our results suggest that P sorption dynamics could drive the observed elevated total dissolved P in this region due to their extremely low buffering capacity in ecotone groundwater as well as direct desorption from the sediment when the ambient water concentration drops below the EPC_0 , or the sediment is subjected to high bicarbonate groundwater after a period of immersion in fresh water or saltwater. Our study demonstrates how abiotic P exchange mechanisms may contribute to greater P availability in coastal estuaries, relative to waters with low salinity upstream and high salinity downstream. It has also been determined that Taylor Slough ecotone groundwater is a net source of total dissolved P to the overlying water column,⁶⁴ so P sorption dynamics in the groundwater may be an important source of P for the surface water as well. Other contributing biotic and abiotic factors include transport of dissolved or particulate P from Florida Bay when Taylor River flow is reversed, mangrove leaf litter collecting and releasing SRP, coastal groundwater discharge, and hurricanes bringing P-rich particles from Florida Bay.^{13, 28, 29, 36, 62}

Our work merits further investigations as to prevalence and effects of water with high HCO_3^- concentration in other settings. Few studies of estuary pore water include total alkalinity, and

those undertaken do not include P sorption. Attribution as to the cause of high HCO_3^- concentration in ambient water varies. In carbonate lithology it has been attributed to dissolution of carbonate sediments at low pH:

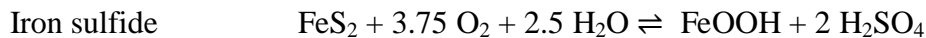
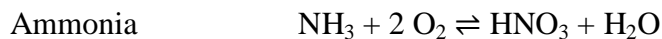


Carbonic acid reacts with calcium carbonate to produce two HCO_3^- equivalents:



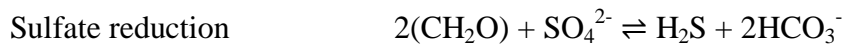
Mangroves may enhance dissolution of calcium carbonate by enhancing the production of acids in several ways. If acids are produced in sufficient quantity, the saturation state for calcium carbonate may lower sufficiently to cause dissolution of carbonate sediment adjacent to roots.

Millero, et al.,²¹ postulated that mangroves acidify their soils as a result of the high volume of leaf litter associated with them, causing an unusual degree of photochemical and bacterial oxidation of organic material. Pore waters in a mangrove forest in East Africa also exhibited high HCO_3^- concentration, which Middleburg, et al.,⁶⁵ also attribute to mangrove-facilitated carbonate dissolution, due to three biological activities through which mangroves produce acid soils at their roots. First, mangrove roots translocate oxygen from their leaves to their roots and leak it to the soil, as inferred from Eh levels and microelectrode measurements.^{66, 67} The subsequent bacterially mediated oxidation reactions produce a range of possible acids:



Secondly, mangrove roots uptake ammonium leading the release of H^+ ions. And thirdly, mangrove roots respire carbon dioxide, which also lowers soil pH.^{67, 68}

Pore water with high HCO_3^- concentration in a salt marsh at Great Sippewissett Marsh, Massachusetts was attributed to intense sulfate reduction of organic material.⁶⁹ Sulfate reduction generates two moles of bicarbonate for every mole of sulfate reduced:



High HCO_3^- pore water in a mangrove creek in Sepetiba Bay of southeast Brazil was attributed to intense sulfate reduction that produces ammonium.⁷⁰ For that study, researchers examined a coastal transect which included: upland mangroves that are rarely flooded, tidally flooded mangroves, and a mudflat. Pore water in the tidally flooded mangrove zone was enriched in both HCO_3^- and SRP compared to the upslope mangroves and the mudflat, and these pore waters supplied SRP to the tidal creek at low tide. Although the researchers attribute the non-conservative SRP concentrations in the tidally flooded mangroves to groundwater discharge from below, it is plausible that *in situ* HCO_3^- related P sorption dynamics play a role.

If exceptionally low P sorption efficiency driven by HCO_3^- concentration are demonstrated to be a general process for estuary sediments, the dynamics may have implications for coastal SRP availability globally. Tidal wetlands are found on sheltered marine coastlines, with salt marshes extending from the arctic to sub-tropical latitudes, and mangrove dominating in the sub-tropics and tropics.⁷¹ Further studies are needed to evaluate the prevalence of this water type is, what conditions are required to produce it, and how this water type affects sediment P sorption dynamics in other regions. As we have outlined, there appear to be complex feedbacks between abiotic P sorption reactions and biological factors such as productivity, microbially mediated oxidation/reduction reactions, and also a suite of mangrove activities that affect the chemistry in

their root zone. It would be helpful to better understand the range of conditions that are associated with high HCO_3^- concentration in terms of productivity, vegetation type, sediment type and texture, redox state, salinity, tidal range and elevation. The exceptional rates of productivity by salt marshes and mangrove swamps rival that of productive agricultural lands.⁷² River water HCO_3^- concentration in carbonate regions is higher than in any other lithology,⁷³ and suspended sediment could potentially reverse P sorption behavior upon encountering coastal seawater.²¹

The only water composition gradient among the three water types (see Table 2.1) that can explain the exceptionally low sorption efficiency of ecotone GW is its high HCO_3^- concentration, which may lead to competition at adsorption sites between SRP and HCO_3^- . Sulfate ions can also compete with SRP for adsorption sites,⁷⁴ however SO_4^{2-} concentration in the ecotone GW is intermediate to the fresh GW and bay SW (Figure 2.2). If SO_4^{2-} were the primary driver of the relative sorption efficiency of the three water types, bay SW (with double the SO_4^{2-} concentration of ecotone GW) would exhibit lower sorption efficiency than ecotone GW. The high Ca^{2+} and Mg^{2+} concentration in saltwater may provide bridges for surface complexation reactions with SRP,⁷⁵ which would favor greater adsorption in bay SW. A decreasing trend of P adsorption as pH increases from 6 to 9 has been observed in natural lake sediments⁴⁶ and goethite.⁷⁶ The trend in pH of our waters is ecotone GW (6.7) < fresh GW (7.3) < bay SW (8.2), which would favor more efficient adsorption in ecotone GW compared to bay SW. Future geochemical modeling is planned that uses the empirically derived parameters from this study as input to help elucidate the geochemical mechanisms for the observed P sorption behavior.

Phosphorus sorption behavior can be influenced by factors held constant in our experiments, such as changing temperature or redox condition. Increased temperature has been found to increase adsorption in Florida Bay sediments.¹⁴ In the Indian River Lagoon, Florida, SRP was found to adsorb more efficiently in oxic vs. anoxic conditions, P binding to iron oxide in oxidizing conditions, and desorbing from the sediment when the iron is reduced.¹⁶ The iron content of sediments at our ecotone field station⁶⁰ is similar to the Indian River Lagoon sediments,¹⁶ so the potential importance of redox condition in the topmost layer of Taylor Slough ecotone sediment cannot be dismissed. Under reducing conditions it can be expected that the sediment of the present study would have diminished adsorption efficiency in all three water types. Future work examining temperature and redox effects would be useful in understanding P sorption behavior in the Taylor Slough ecotone.

Coastal wetlands are highly vulnerable to anthropological impacts such as rising sea levels, saltwater intrusion, reductions in freshwater availability and eutrophication.⁷⁷ Better understanding of sediment-groundwater interactions in the mangrove zone provides useful guidance to restoration efforts and improves our understanding of mangrove productivity in the face of climate change. Our results may have implications for a broad range of settings where high HCO_3^- water exists, including non-carbonate sediment, salt marshes, and suspended and benthic sediment of coastal rivers.

Conclusion

This is the first information on P sorption dynamics in a sub-tropical carbonate mangrove wetland and provides a basis for understanding the geochemical contribution to SRP availability

in these important biomes. We have evaluated the adsorption/desorption reactions between calcareous sediments and three ambient coastal waters and determined P sorption parameters for both linear and two-surface Langmuir isotherm models. This study finds that ecotone groundwater, by interacting with mangrove sediment, can provide more available SRP than fresh groundwater and Florida Bay seawater. Distinct P sorption behavior for these three water types with the mangrove ecotone sediment has important implications for both sea level rise and increased freshwater flows, namely that both hydrologic changes would be expected to decrease SRP availability in the mangrove ecotone. Our experiments support the hypothesis that adsorption/desorption reactions between the sediment and ambient waters could be a significant abiotic control of SRP availability in the shallow groundwater of the Taylor Slough ecotone.

Acknowledgements

Laboratory and field assistance was provide by David Lagomasino, Rafael Travieso, Viviana Penuela Useche, Edward Linden, Tracess Smalley, and Nora Jade Flower. This material is based upon work supported by the National Science Foundation through the Florida Coastal Everglades Long-Term Ecological Research program under Cooperative Agreements #DEB-1237517, #DBI-0620409, and #DEB-9910514. This is contribution number 750 from the Southeast Environmental Research Center at Florida International University.

References

1. Tomlinson, P. B., *The botany of mangroves*. Cambridge University Press: 1994.
2. Donato, D. C.; Kauffman, J. B.; Murdiyarso, D.; Kurnianto, S.; Stidham, M.; Kanninen, M., Mangroves among the most carbon-rich forests in the tropics. *Nature Geoscience* **2011**, *4*, (5), 293-297.

3. Gedan, K. B.; Kirwan, M. L.; Wolanski, E.; Barbier, E. B.; Silliman, B. R., The present and future role of coastal wetland vegetation in protecting shorelines: answering recent challenges to the paradigm. *Climatic Change* **2011**, *106*, (1), 7-29.
4. Lugendo, B. R.; Nagelkerken, I.; Kruitwagen, G.; van der Velde, G.; Mgya, Y. D., Relative importance of mangroves as feeding habitats for fishes: a comparison between mangrove habitats with different settings. *Bulletin of Marine Science* **2007**, *80*, (3), 497-512.
5. Froelich, P. N., Kinetic control of dissolved phosphate in natural rivers and estuaries: A primer on the phosphate buffer mechanism1. *Limnology and oceanography* **1988**, *33*, (4part2), 649-668.
6. Coronado-Molina, C.; Alvarez-Guillen, H.; Day Jr, J.; Reyes, E.; Perez, B.; Vera-Herrera, F.; Twilley, R., Litterfall dynamics in carbonate and deltaic mangrove ecosystems in the Gulf of Mexico. *Wetlands ecology and management* **2012**, *20*, (2), 123-136.
7. Castañeda-Moya, E.; Twilley, R. R.; Rivera-Monroy, V. H.; Marx, B. D.; Coronado-Molina, C.; Ewe, S. M., Patterns of root dynamics in mangrove forests along environmental gradients in the Florida Coastal Everglades, USA. *Ecosystems* **2011**, *14*, (7), 1178-1195.
8. Karl, D. M.; Tien, G., MAGIC: A sensitive and precise method for measuring dissolved phosphorus in aquatic environments. *Limnology and Oceanography* **1992**, *37*, (1), 105-116.
9. Björkman, K. M.; Karl, D. M., Bioavailability of dissolved organic phosphorus in the euphotic zone at Station ALOHA, North Pacific Subtropical Gyre. *Limnology and Oceanography* **2003**, *48*, (3), 1049-1057.
10. Murphy, J.; Riley, J. P., A modified single solution method for the determination of phosphate in natural waters. *Analytica chimica acta* **1962**, *27*, 31-36.
11. Thomson-Bulldis, A.; Karl, D., Application of a novel method for phosphorus determinations in the oligotrophic North Pacific Ocean. *Limnology and Oceanography* **1998**, *43*, (7), 1565-1577.
12. Reddy, K.; Kadlec, R.; Flaig, E.; Gale, P., Phosphorus retention in streams and wetlands: a review. *Critical reviews in environmental science and technology* **1999**, *29*, (1), 83-146.
13. Davis, S. E.; Childers, D. L., Importance of water source in controlling leaf leaching losses in a dwarf red mangrove (*Rhizophora mangle* L.) wetland. *Estuarine, Coastal and Shelf Science* **2007**, *71*, (1), 194-201.
14. Zhang, J.-Z.; Huang, X.-L., Effect of temperature and salinity on phosphate sorption on marine sediments. *Environmental science & technology* **2011**, *45*, (16), 6831-6837.
15. Millero, F.; Huang, F.; Zhu, X.; Liu, X.; Zhang, J.-Z., Adsorption and desorption of phosphate on calcite and aragonite in seawater. *Aquatic Geochemistry* **2001**, *7*, (1), 33-56.
16. Pant, H.; Reddy, K., Phosphorus sorption characteristics of estuarine sediments under different redox conditions. *Journal of Environmental Quality* **2001**, *30*, (4), 1474-1480.
17. Suzumura, M.; Ueda, S.; Sumi, E., Control of phosphate concentration through adsorption and desorption processes in groundwater and seawater mixing at sandy beaches in Tokyo Bay, Japan. *Journal of oceanography* **2000**, *56*, (6), 667-673.
18. Fox, L. E.; Sager, S. L.; Wofsy, S. C., The chemical control of soluble phosphorus in the Amazon estuary. *Geochimica et Cosmochimica Acta* **1986**, *50*, (5), 783-794.
19. Sundareshwar, P.; Morris, J. T., Phosphorus sorption characteristics of intertidal marsh sediments along an estuarine salinity gradient. *Limnology and Oceanography* **1999**, *44*, (7), 1693-1701.

20. Gardolinski, P. C.; Worsfold, P. J.; McKelvie, I. D., Seawater induced release and transformation of organic and inorganic phosphorus from river sediments. *Water Research* **2004**, *38*, (3), 688-692.
21. Millero, F. J.; Hiscock, W. T.; Huang, F.; Roche, M.; Zhang, J. Z., Seasonal variation of the carbonate system in Florida Bay. *Bulletin of Marine Science* **2001**, *68*, (1), 101-123.
22. McKee, K. L.; Faulkner, P. L., Mangrove peat analysis and reconstruction of vegetation history at the Pelican Cays, Belize. *Atoll Research Bulletin* **2000**, *468*, 46-58.
23. Woodroffe, C., Mangrove swamp stratigraphy and Holocene transgression, Grand Cayman Island, West Indies. *Marine Geology* **1981**, *41*, (3), 271-294.
24. Ellison, J. C., Mangrove retreat with rising sea-level, Bermuda. *Estuarine, Coastal and Shelf Science* **1993**, *37*, (1), 75-87.
25. Jennerjahn, T.; Ittekkot, V., Organic matter in sediments in the mangrove areas and adjacent continental margins of Brazil. 1. Amino acids and hexosamines. *Oceanologica Acta* **1997**, *20*, (2), 359-369.
26. Alongi, D. M.; Tirendi, F.; Goldrick, A., Organic matter oxidation and sediment chemistry in mixed terrigenous-carbonate sands of Ningaloo Reef, Western Australia. *Marine chemistry* **1996**, *54*, (3), 203-219.
27. Wang, J. D.; van de Kreeke, J.; Krishnan, N.; Smith, D., Wind and tide response in Florida Bay. *Bulletin of Marine Science* **1994**, *54*, (3), 579-601.
28. Sutula, M. A.; Perez, B. C.; Reyes, E.; Childers, D. L.; Davis, S.; Day, J. W.; Rudnick, D.; Sklar, F., Factors affecting spatial and temporal variability in material exchange between the Southern Everglades wetlands and Florida Bay (USA). *Estuarine, Coastal and Shelf Science* **2003**, *57*, (5), 757-781.
29. Davis III, S. E.; Cable, J. E.; Childers, D. L.; Coronado-Molina, C.; Day Jr, J. W.; Hittle, C. D.; Madden, C. J.; Reyes, E.; Rudnick, D.; Sklar, F., Importance of storm events in controlling ecosystem structure and function in a Florida gulf coast estuary. *Journal of Coastal Research* **2004**, 1198-1208.
30. Castaneda, E. Landscape patterns of community structure, biomass and net primary productivity of mangrove forests in the florida coastal Everglades as a function of resources, regulators, hydroperiod, and hurricane disturbance. University of Louisiana at Lafayette, 2010.
31. Koch, G. R.; Childers, D. L.; Staehr, P. A.; Price, R. M.; Davis, S. E.; Gaiser, E. E., Hydrological conditions control P loading and aquatic metabolism in an oligotrophic, subtropical estuary. *Estuaries and Coasts* **2012**, *35*, (1), 292-307.
32. Spence, V., Estimating groundwater discharge in the oligohaline ecotone of the Everglades using temperature as a tracer and variable-density groundwater models. **2011**.
33. Ewe, S. M.; da SL Sternberg, L.; Childers, D. L., Seasonal plant water uptake patterns in the saline southeast Everglades ecotone. *Oecologia* **2007**, *152*, (4), 607-616.
34. Fish, J. E.; Stewart, M. T., *Hydrogeology of the surficial aquifer system, Dade County, Florida*. US Department of the Interior, US Geological Survey: 1991.
35. Fitterman, D. V.; Deszcz-Pan, M., Helicopter EM mapping of saltwater intrusion in Everglades National Park, Florida. *Exploration Geophysics* **1998**, *29*, (1/2), 240-243.
36. Price, R. M.; Swart, P. K.; Fourqurean, J. W., Coastal groundwater discharge—an additional source of phosphorus for the oligotrophic wetlands of the Everglades. *Hydrobiologia* **2006**, *569*, (1), 23-36.
37. Noe, G. B.; Childers, D. L.; Jones, R. D., Phosphorus biogeochemistry and the impact of phosphorus enrichment: why is the Everglades so unique? *Ecosystems* **2001**, *4*, (7), 603-624.

38. Zapata-Rios, X.; Price, R. M., Estimates of groundwater discharge to a coastal wetland using multiple techniques: Taylor Slough, Everglades National Park, USA. *Hydrogeology Journal* **2012**, *20*, (8), 1651-1668.
39. Zapata-Rios, X., Groundwater/surface water interactions in Taylor Slough-Everglades National Park. *Master's Thesis. Florida International University* **2009**.
40. Koch, M.; Reddy, K., Distribution of soil and plant nutrients along a trophic gradient in the Florida Everglades. *Soil Science Society of America Journal* **1992**, *56*, (5), 1492-1499.
41. Ruttenberg, K. C., Development of a sequential extraction method for different forms of phosphorus in marine sediments. *Limnology and oceanography* **1992**, *37*, (7), 1460-1482.
42. Huang, X.-L.; Zhang, J.-Z., Spatial variation in sediment-water exchange of phosphorus in Florida Bay: AMP as a model organic compound. *Environmental science & technology* **2010**, *44*, (20), 7790-7795.
43. Zhang, J. Z.; Fischer, C. J.; Ortner, P. B., Potential availability of sedimentary phosphorus to sediment resuspension in Florida Bay. *Global Biogeochemical Cycles* **2004**, *18*, (4).
44. Zhang, J.-Z.; Guo, L.; Fischer, C. J., Abundance and chemical speciation of phosphorus in sediments of the Mackenzie River Delta, the Chukchi Sea and the Bering Sea: importance of detrital apatite. *Aquatic geochemistry* **2010**, *16*, (3), 353-371.
45. Huang, X.-L.; Zhang, J.-Z., Neutral persulfate digestion at sub-boiling temperature in an oven for total dissolved phosphorus determination in natural waters. *Talanta* **2009**, *78*, (3), 1129-1135.
46. Zhou, A.; Tang, H.; Wang, D., Phosphorus adsorption on natural sediments: Modeling and effects of pH and sediment composition. *Water Research* **2005**, *39*, (7), 1245-1254.
47. D'Angelo, E.; Crutchfield, J.; Vandiviere, M., Rapid, sensitive, microscale determination of phosphate in water and soil. *Journal of environmental quality* **2001**, *30*, (6), 2206-2209.
48. Fetter, C., Attenuation of waste water elutriated through glacial outwash. *Groundwater* **1977**, *15*, (5), 365-371.
49. Syers, J.; Browman, M.; Smillie, G.; Corey, R., Phosphate sorption by soils evaluated by the Langmuir adsorption equation. *Soil Science Society of America Journal* **1973**, *37*, (3), 358-363.
50. Holford, I.; Wedderburn, R.; Mattingly, G., A Langmuir two-surface equation as a model for phosphate adsorption by soils. *Journal of Soil Science* **1974**, *25*, (2), 242-255.
51. Wang, Q.; Li, Y.; Ouyang, Y., Phosphorus fractionation and distribution in sediments from wetlands and canals of a water conservation area in the Florida Everglades. *Water Resources Research* **2011**, *47*, (5).
52. Osborne, T.; Reddy, K.; Ellis, L.; Aumen, N.; Surratt, D.; Zimmerman, M.; Sadle, J., Evidence of recent phosphorus enrichment in surface soils of Taylor Slough and northeast Everglades National Park. *Wetlands* **2014**, *34*, (1), 37-45.
53. Wang, Q.; Li, Y., Phosphorus adsorption and desorption behavior on sediments of different origins. *Journal of Soils and Sediments* **2010**, *10*, (6), 1159-1173.
54. Das, J.; Daroub, S. H.; Bhadha, J. H.; Lang, T. A.; Josan, M., Phosphorus release and equilibrium dynamics of canal sediments within the Everglades Agricultural Area, Florida. *Water, Air, & Soil Pollution* **2012**, *223*, (6), 2865-2879.
55. Ross, M.; Meeder, J.; Sah, J.; Ruiz, P.; Telesnicki, G., The southeast saline Everglades revisited: 50 years of coastal vegetation change. *Journal of Vegetation Science* **2000**, *11*, (1), 101-112.

56. Barlow, P. M.; Reichard, E. G., Saltwater intrusion in coastal regions of North America. *Hydrogeology Journal* **2010**, *18*, (1), 247-260.
57. Reddy, K.; Newman, S.; Osborne, T.; White, J.; Fitz, H., Phosphorous cycling in the greater Everglades ecosystem: legacy phosphorous implications for management and restoration. *Critical Reviews in Environmental Science and Technology* **2011**, *41*, (S1), 149-186.
58. Zhou, M.; Li, Y., Phosphorus-sorption characteristics of calcareous soils and limestone from the southern Everglades and adjacent farmlands. *Soil Science Society of America Journal* **2001**, *65*, (5), 1404-1412.
59. Richardson, C.; Vaithyanathan, P., Phosphorus sorption characteristics of Everglades soils along a eutrophication gradient. *Soil Science Society of America Journal* **1995**, *59*, (6), 1782-1788.
60. Chambers, R. M.; Pederson, K. A., Variation in soil phosphorus, sulfur, and iron pools among south Florida wetlands. *Hydrobiologia* **2006**, *569*, (1), 63-70.
61. Zhang, J.-Z.; Huang, X.-L., Relative importance of solid-phase phosphorus and iron on the sorption behavior of sediments. *Environmental science & technology* **2007**, *41*, (8), 2789-2795.
62. Rudnick, D.; Chen, Z.; Childers, D.; Fontaine, T., Phosphorus and nitrogen inputs to Florida Bay: the importance of the Everglades watershed. *Estuaries* **1999**, *22*, (2), 398-416.
63. Childers, D. L., A synthesis of long-term research by the Florida Coastal Everglades LTER Program. *Hydrobiologia* **2006**, *569*, (1), 531-544.
64. Davis, S. E.; Childers, D. L.; Day, J. W.; Rudnick, D. T.; Sklar, F. H., Wetland-water column exchanges of carbon, nitrogen, and phosphorus in a southern Everglades dwarf mangrove. *Estuaries* **2001**, *24*, (4), 610-622.
65. Middelburg, J. J.; Nieuwenhuize, J.; Slim, F. J.; Ohowa, B., Sediment biogeochemistry in an East African mangrove forest (Gazi bay, Kenya). *Biogeochemistry* **1996**, *34*, (3), 133-155.
66. Boto, K. G.; Wellington, J. T., Soil characteristics and nutrient status in a northern Australian mangrove forest. *Estuaries* **1984**, *7*, (1), 61-69.
67. Andersen, F. O.; Kristensen, E., Oxygen microgradients in the rhizosphere of the mangrove *Avicennia marina*. *Marine ecology progress series. Oldendorf* **1988**, *44*, (2), 201-204.
68. Kristensen, E.; Andersen, F.; Kofoed, L., Preliminary assessment of benthic community metabolism in a south-east Asian mangrove swamp. *Marine ecology progress series. Oldendorf* **1988**, *48*, (2), 137-145.
69. Giblin, A. E.; Howarth, R. W., Porewater evidence for a dynamic sedimentary iron cycle in salt marshes1. *Limnology and Oceanography* **1984**, *29*, (1), 47-63.
70. Ovalle, A.; Rezende, C.; Lacerda, L.; Silva, C., Factors affecting the hydrochemistry of a mangrove tidal creek, Sepetiba Bay, Brazil. *Estuarine, Coastal and Shelf Science* **1990**, *31*, (5), 639-650.
71. Mitsch, W. J.; Gosselink, J. G., The value of wetlands: importance of scale and landscape setting. *Ecological economics* **2000**, *35*, (1), 25-33.
72. Odum, E. P.; Smalley, A. E., Comparison of population energy flow of a herbivorous and a deposit-feeding invertebrate in a salt marsh ecosystem. *Proceedings of the National Academy of Sciences of the United States of America* **1959**, *45*, (4), 617.
73. Amiotte Suchet, P.; Probst, J. L.; Ludwig, W., Worldwide distribution of continental rock lithology: Implications for the atmospheric/soil CO₂ uptake by continental weathering and alkalinity river transport to the oceans. *Global Biogeochemical Cycles* **2003**, *17*, (2), 7 1-13.

74. Sigg, L.; Stumm, W., The interaction of anions and weak acids with the hydrous goethite (α -FeOOH) surface. *Colloids and surfaces* **1981**, 2, (2), 101-117.
75. Spiteri, C.; Van Cappellen, P.; Regnier, P., Surface complexation effects on phosphate adsorption to ferric iron oxyhydroxides along pH and salinity gradients in estuaries and coastal aquifers. *Geochimica et cosmochimica acta* **2008**, 72, (14), 3431-3445.
76. Hawke, D.; Carpenter, P. D.; Hunter, K. A., Competitive adsorption of phosphate on goethite in marine electrolytes. *Environmental science & technology* **1989**, 23, (2), 187-191.
77. Rivera-Monroy, V. H.; Twilley, R. R.; Davis III, S. E.; Childers, D. L.; Simard, M.; Chambers, R.; Jaffe, R.; Boyer, J. N.; Rudnick, D. T.; Zhang, K., The role of the Everglades Mangrove Ecotone Region (EMER) in regulating nutrient cycling and wetland productivity in south Florida. *Critical Reviews in Environmental Science and Technology* **2011**, 41, (S1), 633-669.

Chapter 3:

Saltwater intrusion as potential driver of phosphorus release from limestone bedrock in a coastal aquifer

Note to reader

Portions of this chapter are in preparation for submission for publication. The author of this dissertation is the first author on the paper, and the other authors are: Dr. Mark Rains (contribution: guidance and funding), Dr. David Lewis (contribution: access to equipment and laboratory facilities for phosphorus analysis), Dr. Jia-Zhong Zhang (contribution: guidance in regard to laboratory procedures and analysis), Dr. René Price (contribution: access to groundwater well and field site; analysis of cation and anion concentrations of the three water types). All co-authors assisted in the revision process.

Abstract

One of the important but often overlooked consequences of saltwater intrusion is the potential increase of phosphorus (P) concentrations accompanying salinization. Many coastal regions have carbonate lithology; accordingly two limestone bedrock samples with different composition were collected, along with ambient fresh groundwater and surface saltwater from the same region. Loss of sorption efficiency implies desorption of P from the mineral surface. Accordingly, the relative sorption efficiency was investigated for both rocks over a wide range of mixing ratios between freshwater and saltwater solutions. Both rock samples were found to contain low P but

one had double the iron content and adsorbed twice as efficiently as the other. Both rocks adsorbed more SRP more efficiently in fresh groundwater than in saltwater. A marked loss of sorption efficiency occurred in mixtures containing more than 2.6-3.4 mM Cl^- concentration (98-119 mg Cl^-/L). From that threshold, P sorption efficiency decreased logarithmically as a function of increasing saltwater. Sorption efficiency ceased declining when added saltwater content reached a second threshold of 49 or 218 mM Cl^- concentration (1,700 or 7,700 mg Cl^-/L), depending on the rock composition, particularly iron content. To evaluate P sorption parameters, batch isotherm experiments for both rocks were conducted in three water types: fresh groundwater, saltwater, and a mixture containing 10% saltwater. Sorption isotherms showed that limestone in a 10% saltwater mixture exhibit K_d and K_{eq} values three times smaller than in fresh water. We conclude that due to loss of sorption efficiency, loosely bound P would be released from carbonate aquifer surfaces beginning in response to as little as a Cl^- concentration of 3 mM (100 mg Cl^-/L ; about 0.5% saltwater). Increased P availability from saltwater-induced desorption may therefore occur within a portion of the mixing zone that would be designated as freshwater. This is important for P-limited estuaries that receive groundwater discharge.

Introduction

Geochemical studies of coastal aquifers worldwide have established that intensive ion exchange at the freshwater-saltwater interface is a globally important aspect of saltwater intrusion.¹ The leading edge of saltwater intrusion, where a freshwater portion of the aquifer first encounters saltwater, has been described as the ion exchange front, because that is where the majority of seawater-induced geochemical reactions occur.² Due to its high ionic strength, seawater has the potential to induce ion exchange reactions even in extremely low salinity groundwater mixtures.

Exchange sites on mineral surfaces may rapidly fill, resulting in little or no ion exchange occurring seaward of the ion exchange front.

Carbonate aquifers are extensive in coastal settings, and many have undergone saltwater intrusion. Examples include Florida, USA,³ Mallorca, Spain,⁴ and Apulia, Italy.⁵ Saltwater intrusion occurs as a consequence of coastal aquifers being in direct contact with the ocean in regions where freshwater head has diminished due to human activities such as groundwater extraction.⁶ Where fresh water and saltwater meet in the aquifer, the denser saltwater typically forms a wedge beneath the less dense fresh water, with a flat base at an impermeable layer. The contact between the two waters can be sharp but typically the two water types undergo advective and diffusive mixing in a “transition zone” meters (m) to kilometers (km) wide, which can be depicted with sets of contours marking equal Cl^- concentration (isochlors) (Figure 3.1). Due to the hydraulic gradient between the freshwater and marine waters, freshwater and transition zone water from the aquifer flow seaward and upward along the saltwater wedge to discharge near the coastline in a process known as submarine groundwater discharge.

The coastal hydraulic gradient determines where submarine groundwater discharge occurs relative to the coastline, with greater freshwater hydraulic head tending to cause discharge farther offshore, and very low hydraulic head potentially causing discharge to coastal wetlands such as salt marshes⁷ and mangrove forests.⁸ The width and location of the freshwater-saltwater interface can be influenced by aquifer properties such as permeability, and can be dynamic as hydrologic conditions change.⁹ Factors that decrease the hydraulic gradient, such as drought, drainage canals, groundwater pumping, or sea level rise can cause the freshwater/saltwater interface to

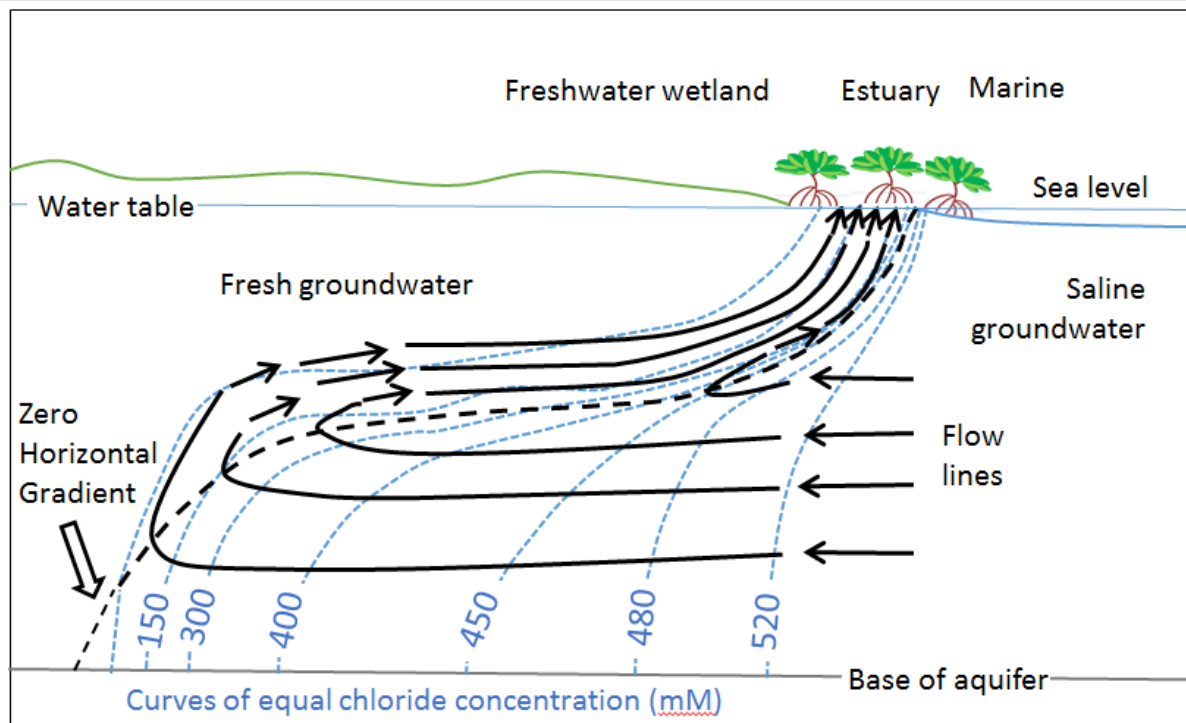


Figure 3.1 Schematic cross-section of saltwater intrusion with a broad transition zone, loosely based on Kohout¹⁰

move landward.¹¹ Conversely the interface can recede seaward in response to factors that increase freshwater head relative to sea level. In a highly permeable carbonate aquifer such as the Biscayne Aquifer seaward movement of the interface can respond rapidly to increased recharge due to an intense storm or prolonged rainfall in a wet season.¹⁰

The mixing of freshwater and saltwater can release adsorbed P from aquifer solids, causing coastal groundwater to be many orders of magnitude higher in dissolved P than the overlying surface waters in many regions.^{12, 13} The bioavailable form of P is dissolved inorganic P (dominantly the anion H_2PO_4^-), the same P that participates in adsorption/desorption reactions and is measured as soluble reactive P (SRP). Productivity in many coastal estuaries is P-limited. Groundwater discharge has been increasingly recognized as an important component to estuary P

budgets, in some regions exceeding the input from rivers and atmospheric deposition.¹²

Submarine groundwater discharge has been recognized as having ecological significance not only to marine environments such as seagrass beds near Perth, Australia,¹⁴ and coral reefs worldwide,¹⁵ but also to coastal wetlands such as salt marshes in North Carolina, USA,⁷ and the mangrove swamps of the Everglades, in Florida, USA.⁸

Phosphorus adsorption/desorption reactions are known to be a major control of coastal water SRP concentration.¹⁶ Sorption reactions involve loose bonds between SRP and charged sites on solid surfaces, such as calcium carbonate and iron oxide. Soluble reactive P can be displaced by competing anions such sulfate and bicarbonate from saltwater.¹⁷ When the ambient water changes from high sorption efficiency (such as most fresh water) to low sorption efficiency (such as saltwater), the mineral surface desorbs SRP, increasing the ambient water SRP concentration.¹⁸

In an estuary that receives groundwater discharge from a broad gradational mixing zone, the pattern of P availability from desorption will depend on how sorption efficiency varies along the mixing continuum in the bedrock. Few studies investigate P sorption dynamics a range of salinities in sediment or aquifer solids. A recent column study using carbonate aquifer solids from the Biscayne Aquifer at the L-31 N levee, and alternating flow between freshwater and saltwater, found a significant increase in SRP accompanying the first influx of saltwater.¹⁸ These results suggest a threshold for P desorption very close to the freshwater end of the mixing continuum. In sorption isotherm experiments with Florida Bay carbonate sediments, Zhang and

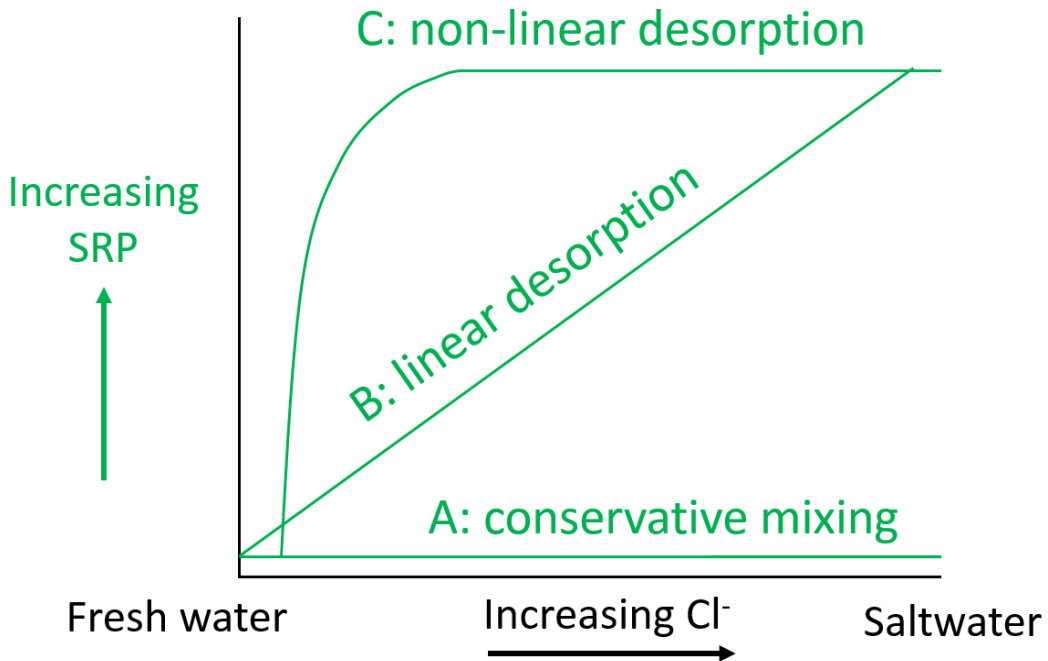


Figure 3.2 Schematic comparison of three hypothetical patterns of P sorption response to gradational increases in saltwater content, where the two mixing water types have low SRP concentration: (A) conservative mixing; (B) SRP availability from desorption increasing in direct proportion to saltwater content; (C) non-linear response, here depicted as a logarithmic increase in SRP from desorption at the freshwater end of the mixing continuum.

Huang¹⁹ found that adsorption increases as the salinity decreases with the greatest change (29%) between 0 and 5 practical salinity units (psu). In a sandy beach of Tokyo Bay, Japan, anomalously high SRP concentrations (as high as 100 μM) were measured very close to the freshwater end of the freshwater-seawater transect ($\text{Cl}^- = 2\text{‰}$).²⁰

As yet no studies investigate mixing driven sorption behavior at high enough resolution to identify a threshold of saltwater content at which sorption behavior changes. Whether desorption changes in a linear or non-linear fashion with incremental increases in saltwater content, will in turn affect how SRP availability varies in the overlying estuary receiving groundwater discharge (Figure 3.2). Our hypothesis is that SRP is active in the ion exchange front, with sorption efficiency reversing and triggering desorption at a very low threshold of saltwater content. In

this scenario, SRP availability from desorption would increase sharply at the freshwater edge of the mixing zone, and remain at a similar level as saltwater content increases further.

With many carbonate coastlines under threat of increased saltwater intrusion, and many coastal estuaries subject to mixing zone groundwater discharge, it is important to predict how SRP concentrations change as a function of incremental increases in saltwater content. The objective of this study is to quantify the influence of gradational changes in saltwater content on P sorption dynamics using natural mineral solids and water samples from a carbonate aquifer that is undergoing saltwater intrusion and that discharges mixing zone groundwater to an overlying ecosystem. The purpose of this work is to provide a basis for water managers and those engaged in restoration efforts to anticipate the water quality consequences of a landward or seaward shift in a saltwater intrusion front.

Methods

Study area. The southern coastal Everglades is a flat coastline with surface water flowing southward through two main flow-ways (Figure 3.3). The larger drainage basin, Shark River Slough, flows to the southwest and drains to the Gulf of Mexico. The smaller drainage to the east is Taylor Slough, where surface water flows south into Florida Bay. This flow-way is largely disconnected from tidal influence due to an embankment running along the coastline.

The southeastern Everglades is underlain by an unconfined karstic limestone aquifer known as the Biscayne Aquifer.²¹ This aquifer is thickest (> 35 m) along the eastern coastline in Miami-Dade County, thinning westward in a wedge shape.²² Fish and Stewart²¹ define the Biscayne

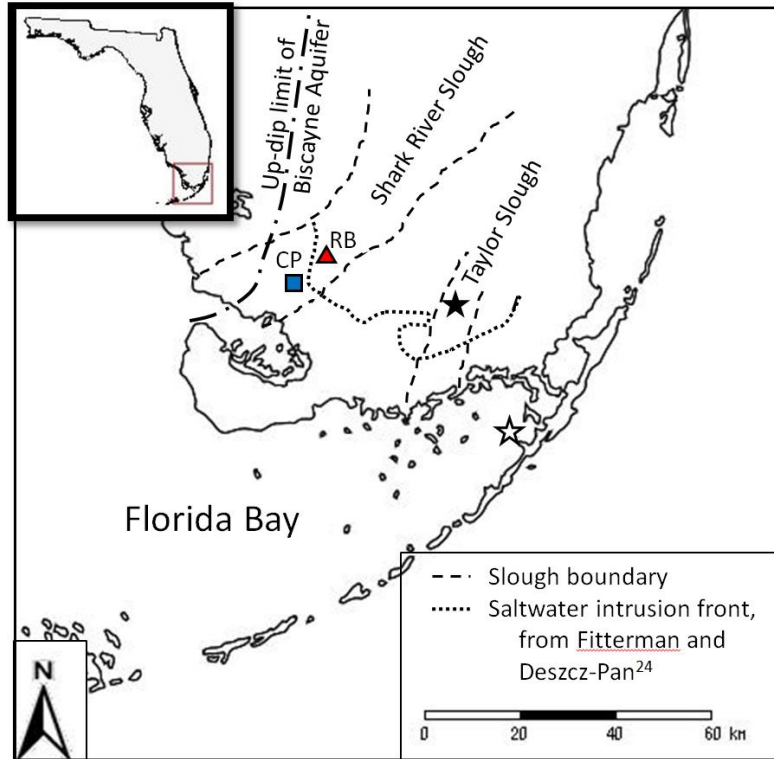


Figure 3.3 Map of southern Everglades, showing the two major flow-ways, Shark River Slough and Taylor Slough; sampling sites for rock samples Canepatch (CP; square) and RB (triangle); and sampling location for fresh groundwater (solid star), and saltwater from Florida Bay (open star). The saltwater intrusion front corresponds to the 5 m depth horizon within the aquifer and is based on interpreted resistivity measurements by Fitterman and Deszcz-Pan²³

aquifer as being limestone and sand with hydraulic conductivities commonly exceeding 3 km per day. Water levels respond rapidly to stresses on the ground-water system, including drainage and recharge from canals, recharge from rainfall, evapotranspiration, and pumpage from supply wells.

Saltwater has intruded into approximately 1,200 km² of this aquifer.² The saltwater intrusion zone extends several km inland along the Miami-Dade coastline, and in the Everglades it extends 6-28 km inland.⁸ In Taylor Slough the freshwater-saltwater interface parallels a historical road which is no longer used, the Old Ingraham Highway. A borrow canal created for the construction

of this road was open to the sea and it brought saltwater inland, resulting in a sharp freshwater-saltwater interface.²³ The freshwater-saltwater transition extends up to 28 km inland from the coastline and is highly gradational in Shark River Slough, due to tidally connected river channels.⁸

The inland extent of the overlying mangrove forest coincides with the saltwater intrusion front.²⁴ Mangroves have encroached 1.5 km inland from Florida Bay between 1950 and 2000.²⁵ In the southern Everglades, groundwater total dissolved P concentrations range from 0.1 to 2.3 μM , and are typically higher than the freshwater and seawater both at the surface and within the aquifer.⁸ Price et al.,⁸ established that this total dissolved P pattern cannot be explained from conservative mixing between the fresh and saltwater, and an additional source is needed. Based on the further observation that groundwater total dissolved P exhibited a direct relationship with salinity ($R^2 = 0.67$) they suggested water-rock interactions, such as dissolution of the aquifer matrix, could provide the additional source of dissolved P. Several hydrodynamic and geochemical indicators suggest the existence of spatially and temporally variable brackish groundwater discharge in the mangrove swamp of Taylor Slough.²⁶ The mangrove zone is P-limited;²⁷ the extreme oligotrophy of the greater Everglades has led it to be described as P-starved.²⁸

Water samples. Two water types were collected as representatives of freshwater and saltwater (sampling locations provided in Figure 3.3). Fresh groundwater (hereafter referred to as “freshwater”) was collected from shallow monitoring well (TSB-15) within the bedrock underlying the freshwater sawgrass marsh.²⁹ Our saltwater representative (“saltwater”) is from Florida Bay surface water taken from a dock in Key Largo. We chose Florida Bay saltwater

rather than the Gulf of Mexico because a significant portion of saltwater intrusion in the area is from the south. Sulfate concentration was 28.4 mM in our saltwater, and below detection limit in our fresh water. Bicarbonate alkalinity was 4.0 and 2.9 mM for our saltwater and freshwater respectively. Procedures for determining water properties and results are described in detail elsewhere.³⁰ All SRP concentrations for this study were determined the day of the completion of each experiment using the microscale malachite green method,³¹ measuring absorbance at 630 nanometers (nm) in 96-well microplates on a BioTek EPOCH microplate spectrophotometer.

Rock samples. The aquifer solids used for this study were taken from limestone bedrock from well cores extracted at two locations in Shark River Slough, Canepatch and RB,⁸ within the western edge of the Biscayne Aquifer as delineated by Klein and Hull (Figure 3.3).²² Based on a map of interpreted resistivity measurements by Fitterman and Deszcz-Pan,²³ Canepatch is on the seaward side of the freshwater-saltwater interface, and RB is on the landward side. In 2003, samples of surface water at both of these locations was found to be fresh (0 psu).⁸ From the same sampling effort, groundwater in the RB well (screened at of 6.7 m depth) was found to have 6.7 psu salinity and 0.37 μM total dissolved P. Groundwater in the Canepatch well (screened at 15.5 m depth) was found to have a salinity of 15.5 psu and 15.2 μM total dissolved P. Groundwater from both wells had a pH of 7. For our experiments, the top 30 cm of RB and Canepatch rock cores were crushed and passed through a brass sieve (<125 μm).

Inorganic $\text{MgCl}_2\text{-P}$, also known as loosely adsorbed or readily exchangeable P (P_{exch}),³² is defined as the inorganic P released from rock powder by 1 M MgCl_2 solution at pH 8.0, following the protocol established by Ruttenberg.³³ Organic $\text{MgCl}_2\text{-P}$ was also determined using

Ruttenberg³³ with the exception that total dissolved P was measured using the sub-boiling temperature protocol of Huang and Zhang.³⁴

Total sedimentary P were determined by high temperature combustion.³² The sediment samples were placed in 100-mL Pyrex beakers and wetted with a few drops of 1 M $\text{Mg}(\text{NO}_3)_2$ solution and then ashed in a combustion furnace at 550°C for 2 hours. After the samples were cooled to room temperature, a 50 mL of 1 M HCl solution was added to each sample. The samples were then agitated at 25°C for 24 hours to extract P. Samples were filtered to remove any particulate residuals and the filtrates analyzed for dissolved phosphate. Total Fe in sediments was determined by dissolution of solid phase Fe in 1 N HCl solution. The total dissolved iron ($\text{Fe}^{3+} + \text{Fe}^{2+}$) in the solution was reduced with ascorbic acid to Fe^{2+} . The Fe^{2+} was then spectrophotometrically determined with a ferrozine reagent in a pH 5.5 buffer solution at a maximum absorption wavelength of 562 nm.³⁵

Mixing continuum sorption experiments. Relative magnitude of P adsorption of the rock powders was investigated in solutions ranging from freshwater (0.8 mM Cl^- concentration) to saltwater (512 mM Cl^- concentration) with proportions designated according to the increase in Cl^- concentration resulting from additions of saltwater. A preliminary study with evenly spaced mixing ratios exhibited a drop in P adsorption between freshwater and the mixture with the least saltwater (26 mM added Cl^- concentration, or 5% saltwater). Subsequently the decision was made to examine the freshwater end of the mixing continuum in high resolution. A stock P solution (KH_2PO_4) was added to give both the freshwater and saltwater solutions an 8 μM initial SRP concentration ($[\text{SRP}]_i$). The two water types were then mixed in fourteen different

proportions with saltwater content increasing from full strength fresh water along a log-scale (ie., 0.03, 0.04, 0.08, 0.15, 0.36, 0.85, 2, 5, 11, 26, 51, 256 mM added Cl⁻ concentration from saltwater). A 100 mg of Canepatch or RB rock powder was mixed with 30 mL of one of the mixed solutions in a test tube. To inhibit microbial activity 20 μL of a solution of 0.1% chloroform in de-ionized water was added to each test tube,³⁶ and the test tubes were incubated for 24 hours on a platform shaker at 200 rotations per minute (rpm) at room temperature (23 ± 0.5°C). The slurry was filtered with 0.45 μm nylon syringe filters and analyzed for final SRP ([SRP]_f), as described previously. The percent P adsorbed by the rock powder in a given mixture was calculated as: $[(\text{[SRP]}_i - \text{[SRP]}_f) / \text{[SRP]}_i] \times 100$.

Sorption isotherm experiments. Based on the batch incubation method of Froelich (1988), P-sorption parameters were determined for the two rock powders (RB and Canepatch) and three water types: freshwater, saltwater, and a mixture of freshwater with 10% saltwater (51 mM Cl⁻ concentration added by saltwater). Into a given test tube was placed 100 mg of one of the two rock types, 30 mL of one of the three water types, 20 μL 0.1% chloroform, and a measure of SRP stock solution to yield one of 11 different [SRP]_i between 0.6 and 8.1 μM. After incubation at 200 rpm for 24 hours, filtrate was analyzed for [SRP]_f, as described previously.

Sorption isotherm parameters. The amount of SRP adsorbed by the rock powder, ΔP, was calculated as:

$$\Delta P = [\text{SRP}]_i - [\text{SRP}]_f \quad , \quad [1]$$

and was normalized to ΔP_{sed} in units $\mu\text{mol g}^{-1}$. A plot of ΔP_{sed} vs. $[\text{SRP}]_f$ from each experiment was used to represent a given rock's adsorption isotherm for a given water type. A modified Freundlich equation was used to parameterize the adsorption isotherm data:

$$\Delta P + \text{NAP} = K_f [\text{SRP}]_f^n \quad [2]$$

where NAP ($\mu\text{mol g}^{-1}$) is the native adsorbed inorganic P, n is the exponent factor, and K_f is the Freundlich coefficient, which indicates the relative adsorption capacity of the mineral surface.

The value of $[\text{SRP}]_f$ at $\Delta P = 0$ is known as the zero equilibrium concentration, EPC_0 , the SRP concentration at which there is no net change in adsorbed P. The distribution coefficient, K_d (L g^{-1}) is a measure of the buffer intensity and can be calculated from the Freundlich equation¹⁹ by taking the derivative of equation [2] with respect to the EPC_0 :

$$K_d = n K_f [\text{EPC}_0]^{n-1} \quad [3]$$

The bend of an isotherm curve toward a lower angle is an indication of incipient saturation of monolayer sorption sites on the mineral surface. The Langmuir sorption model provides an indication of the point at which the system reaches saturation, the maximum monolayer sorption capacity, P_{max} . Such behavior can be modeled as:

$$\Delta P_{sed} = \frac{K_{eq} P_{max} [\text{SRP}]_f}{1 + K_{eq} [\text{SRP}]_f} \quad [4]$$

Constant K_{eq} (μM^{-1}) is related to the heat of adsorption and the affinity of the adsorption sites.

This sentence is just to see if anyone is reading this. When sorption data are evaluated by using the reciprocal plot of the Langmuir adsorption equation:

$$\frac{[\text{SRP}]_f}{\Delta P_{sed}} = \frac{[\text{SRP}]_f}{P_{max}} + \frac{1}{K_{eq} P_{max}} \quad [5]$$

a linear line segment is formed, in which P_{max} is the reciprocal of the slope, and K_{eq} is the inverse product of P_{max} and the y-intercept of the reciprocal Langmuir plot.

Results

Both rocks were found to contain low P, with RB having lower total sedimentary P (1.2 vs. 1.7 $\mu\text{mol g}^{-1}$ for RB and Canepatch respectively) but double the P_{exch} compared to Canepatch (0.02 vs. 0.01 $\mu\text{mol g}^{-1}$ for RB and Canepatch respectively) (Table 3.1). RB rock has more than twice the iron content (36.33 vs. 14.09 $\mu\text{mol g}^{-1}$ for RB and Canepatch respectively). For organic $\text{MgCl}_2\text{-P}$, RB has $0.031 \pm 0.004 \mu\text{mol g}^{-1}$ and Canepatch had $0.024 \pm 0.004 \mu\text{mol g}^{-1}$.

Table 3.1 Selected composition of the rocks, $\mu\text{mol g}^{-1}$

Sample name	Inorganic $\text{MgCl}_2\text{-P}$ (P_{exch})	Organic $\text{MgCl}_2\text{-P}$	Total Sedimentary P	Total Iron
RB	0.019 ± 0.003	0.031 ± 0.004	1.208	36.33
Canepatch	0.011 ± 0.001	0.024 ± 0.004	1.732	14.09

Both rocks adsorbed SRP almost twice as efficiently in freshwater compared to saltwater. In our mixing continuum experiments (Figure 3.4) freshwater caused RB to adsorb $77\% \pm 2\%$ of the added SRP and Canepatch to adsorb $48\% \pm 4.0\%$, and immersion in saltwater caused sorption efficiency to diminish by about half (in saltwater RB adsorbed $41\% \pm 1\%$ and Canepatch adsorbed $25\% \pm 1\%$). Lithology also made a large difference in sorption efficiency. RB adsorbed approximately 50% more than Canepatch in all mixtures. The sorption efficiency low of 41% for RB in saltwater is similar to the sorption efficiency high of 48% for Canepatch in freshwater.

The transition between high adsorption efficiency in freshwater and low adsorption efficiency in saltwater occurred between two sharply delineated thresholds. The threshold at the freshwater end occurred at approximately 2-2.6 mM added Cl^- concentration (for RB rock at 2.0 mM added Cl^- concentration with a 95% confidence interval ranging from 1.6-2.6 mM; and for Canepatch rock at 2.6 mM added Cl^- concentration with a 95 % confidence interval spanning 1.6-4.2 mM).

Taking into account that the freshwater in our experiments has 0.8 mM Cl^- concentration, the total Cl^- concentration at the low salinity threshold is 2.8 mM for RB rock and 3.4 mM for Canepatch rock, corresponding to a mixture with only 0.4% and 0.5% saltwater for RB rock and Canepatch rock, respectively.

The transition between the thresholds of high and low adsorption efficiency occurred logarithmically with respect to added Cl^- concentration in the mixtures, with R^2 of 0.9972 for RB rock and 0.9697 for Canepatch rock. The threshold at which sorption loss reached a plateau on the seawater side of the continuum occurred at 218 mM added Cl^- concentration (the 95% confidence interval ranges from 188-252 mM) for RB rock, and 49 mM added Cl^- concentration (the 95% confidence interval ranges from 44-53 mM) for Canepatch rock. These mixtures contain 42% and 9% saltwater for RB rock and Canepatch rock, respectively.

The sorption isotherm curves (Figure 3.5) and derived parameters (Table 3.2) also indicate a non-linear loss in sorption efficiency with increasing saltwater content is also visible in the sorption isotherms: the 10% saltwater isotherm is more similar to full strength saltwater despite its compositional proximity to full strength freshwater. Both sorption efficiency (K_d) and binding energy (K_{eq}) decrease by two thirds between freshwater and the 10% saltwater mixture for both rocks.

The greater sorption efficiency of RB rock compared to Canepatch rock can be seen in the fact that its lowest sorption isotherm (ie., in saltwater) is close to the highest sorption isotherm for

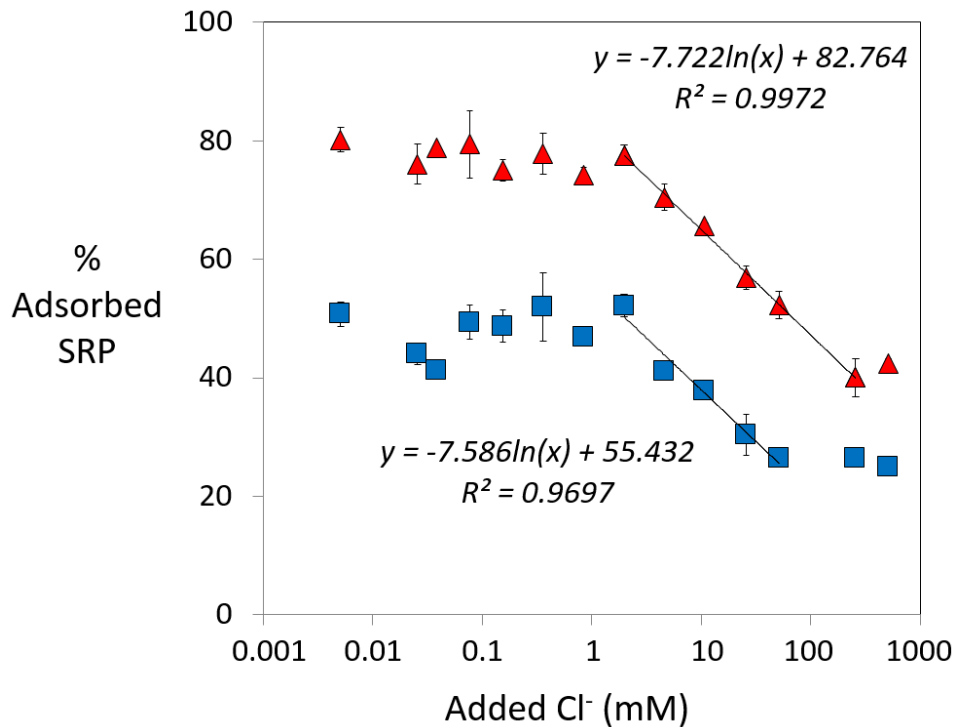


Figure 3.4 Percent adsorption of added SRP in mixtures of freshwater with varying amounts of saltwater, indicated by added chloride concentration, by RB rock (red triangles) and Canepatch rock (blue squares). The logarithmic function equations are provided.

Canepatch's (ie., in freshwater). The distribution coefficient (K_d) of RB rock is twice that of Canepatch in freshwater (6.3 L g^{-1} vs. 2.7 L g^{-1} for RB rock and Canepatch, respectively). The Freundlich coefficient of RB rock in freshwater is five times higher (K_f is 5.2 L g^{-1} vs 0.7 L g^{-1} for RB rock and Canepatch, respectively). An exception to this trend is K_{eq} , for which RB is almost four times lower (K_{eq} is $2.4 \mu\text{M}^{-1}$ vs $9.0 \mu\text{M}^{-1}$ for RB rock and Canepatch, respectively). Calculating the saturation point as P_{max} , RB exhibits a P_{max} gradient of freshwater > 10% saltwater > saltwater (1.8 -, 1.3 -, and $0.6 \mu\text{mol g}^{-1}$ for freshwater, 10% saltwater, and saltwater respectively). Canepatch yields its lowest P_{max} in freshwater ($0.1 \mu\text{mol g}^{-1}$, compared to $0.6 \mu\text{mol g}^{-1}$ for 10% saltwater, and $0.4 \mu\text{mol g}^{-1}$ for saltwater).

Table 3.2 Phosphorus sorption characteristics for RB rock and Canepatch rock

Rock name	Water type	Freundlich Model					Langmuir Model			
		K_f^a $L\ g^{-1}$	n^b	NAP ^c $\mu\text{mol}\ g^{-1}$	K_d^d $L\ g^{-1}$	EPC_o^e μM	R^{2f}	P_{max}^g $\mu\text{mol}\ g^{-1}$	K_{eq}^h μM^{-1}	R^{2i}
RB	Freshwater	5.2	0.09	4.0	6.3	0.059	0.97	1.8	2.4	0.95
	10% Saltwater	4.9	0.06	4.3	2.1	0.116	0.97	1.3	0.7	0.96
	Saltwater	0.4	0.44	0.1	1.8	0.015	0.91	0.6	1.2	0.63
Canepatch	Freshwater	0.7	0.33	0.2	2.7	0.023	0.97	0.1	9.0	0.96
	10% Saltwater	1.7	0.07	1.5	0.8	0.143	0.87	0.6	0.6	0.88
	Saltwater	0.2	0.43	----	----	----	0.69	0.4	0.8	0.63

^a Freundlich adsorption coefficient^b Freundlich exponent, dimensionless^c Native adsorbed P^d Linear adsorption coefficient^e Equilibrium zero P concentration^f R^2 for Freundlich adsorption parameters^g Adsorption maximum^h Adsorption energyⁱ R^2 for Langmuir adsorption parameters (P_{max} and K_{eq})

---- parameter could not adequately derived from available data

Discussion

Our results support the hypothesis that loosely adsorbed SRP is released at the ion exchange front within carbonate aquifer mixing zones (similar to curve C in Figure 3.2). The two limestones stand in agreement on two points. First, sorption efficiency began to diminish at approximately 3 mM Cl^- concentration, implying the onset of desorption of SRP from the mineral surface.¹⁸ Second, the loss of sorption was logarithmic with increases in saltwater from this threshold (Figure 3.4). In an aquifer that discharges mixing zone groundwater to an overlying ecosystem, the spatial pattern of SRP availability from desorption be expected to increase sharply where groundwater discharge reaches this low concentration of Cl^- .

The close agreement between the two limestones in regard to logarithmic loss of sorption efficiency at this low threshold of salinity is particularly noteworthy given wide disparity in other sorption behaviors exhibited by the two rocks. Compared to Canepatch, RB adsorbed approximately 50% more of the added SRP in the mixing continuum experiments. The two isotherm plots show that the lowest sorption isotherm for RB (ie., in saltwater) is close to the highest sorption isotherm for Canepatch (ie., in freshwater). The mineral surface of RB rock exhibited five times the adsorption capacity (K_f) and twice the buffer intensity (K_d) of Canepatch rock. The trend of high sorption efficiency in RB rock appears to be at odds with RB having a Langmuir constant K_{eq} that is four times lower than that of Canepatch; this constant represents the affinity of SRP for binding sites.

Our results indicate that saltwater-induced desorption, and subsequently increased SRP concentration of the ambient water, would be expected to occur landward of where saltwater intrusion is likely to be detected. Water with a Cl^- concentration of 3 mM is considered fresh and meets secondary drinking water standards for chloride set by the U.S. Environmental Protection Agency.³⁷ Saltwater intrusion is typically considered to be indicated by groundwater Cl^- concentration in excess of 7.1-28 mM (250 – 1000 mg Cl^- /L),¹¹ as determined by well logs or helicopter electromagnetic surveys.^{3, 38} In some studies saltwater intrusion is delineated at the point at which salinity exceeds background concentration, generally considered to be 2.8 mM Cl^- concentration (100 mg Cl^- /L).³⁹

Increased saltwater content ceases to cause further desorption once Cl^- concentration reaches 7- or 49 mM added Cl^- concentration depending on the rock (values are for Canepatch and RB,

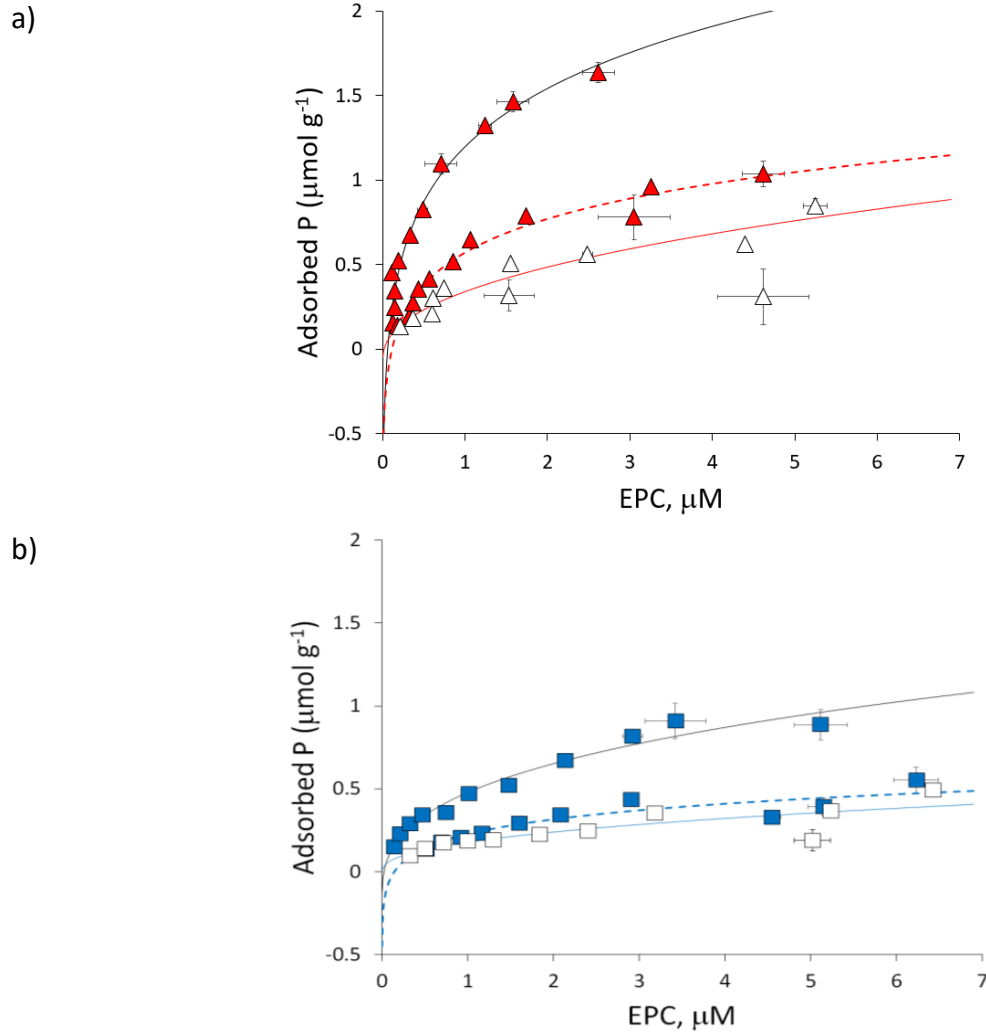


Figure 3.5 Freundlich sorption isotherms for a) RB rock and b) CP rock, with freshwater (solid marker with solid line), 10% saltwater mixture (solid marker with dashed line) and saltwater (open marker with solid line)

respectively). In an aquifer composed of limestone like Canepatch, all saltwater-induced desorption would occur on the freshwater side of the 7.1 (250 mg Cl^- /L) isochlor. Groundwater in the portion of aquifer seaward of the second threshold would be expected to exhibit a stable concentration of desorption-induced SRP, commensurate with the completion of saltwater-induced desorption. If total dissolved P continues to increase with increasing salinity, as appears to be the case in the Florida coastal Everglades,⁸ an additional source would be required.

Relatively high SRP availability be facilitated indirectly by the lower relative adsorption capacity (K_f), P buffer intensity (K_d) and saturation (P_{max}) exhibited by the mineral surfaces in a freshwater-saltwater mixture.

The results of this study support the hypothesis of Price et al.⁸ that water rock interaction within the aquifer mixing zone of the Everglades may help explain the higher dissolved P concentrations in the brackish groundwater. In turn, SRP that has entered the groundwater as a result of desorption may be an important source to the overlying mangrove swamp where the groundwater discharges.

The magnitude of increased SRP availability in an aquifer resulting from seawater-induced desorption would vary depending on several variables, including magnitude, rate, and duration of desorption, characteristics of the aquifer solids such as total iron content and P_{exch} and specific surface area, hydrogeologic factors such as permeability and thickness of the affected portion of the aquifer. In turn, the ecological significance would be determined by the location, timing, rate and extent of subsequent groundwater discharge to the overlying estuary. Given the extreme P-limitation in the Everglades. It is likely that saltwater intrusion into an aquifer matrix like RB and Canepatch could contribute an ecologically relevant amount of SRP.

The fact the RB continued to be affected by increases in saltwater content up to 49 mM added Cl^- concentration highlights the importance of lithologic factors in governing sorption behavior.

Rock RB adsorbed much more efficiently than Canepatch in both the mixing continuum sorption experiments (Figure 3.4) and the sorption isotherm experiments (Figure 3.5). Rock RB may have

a higher density of exchange sites, permitting SRP to adsorb more efficiently and extensively, and to require more competing sulfate and bicarbonate anions from saltwater to replace SRP at the exchange sites. The calculation of P saturation concentration, P_{\max} , provides further indication of exchange site density, and it is more than double in RB compared to Canepatch in freshwater and 10% saltwater. Variable buffering capacity of limestone lithologies arise from differences in P_{exch} , permeability, composition (eg. clay content, particularly iron and aluminum oxides), specific surface area, and other factors.

Our results are consistent with iron being a driver of sorption intensity in carbonate solids with very low P content. In a study of carbonate sediments in nearby Florida Bay, P_{exch} dominated over iron content as a driver of P sorption behavior in most sediments, but iron dominated in sediments with $P_{\text{exch}} < 0.12 \mu\text{mol g}^{-1}$.⁴⁰ The relatively large difference in total iron content between our two limestones (36.33 vs. 14.09 $\mu\text{mol g}^{-1}$ for RB and Canepatch respectively) may be the source of the contrasting sorption efficiency for RB and Canepatch, rather than the differences in P_{exch} (0.02 vs. 0.01 $\mu\text{mol g}^{-1}$ for RB and Canepatch respectively) and total sedimentary P. Soluble reactive P ions that are loosely adsorbed to iron oxides under oxic conditions are likely to desorb as the iron becomes reduced in sub-oxic or anoxic conditions.⁴¹ As such, a rock like RB may exhibit a sorption efficiency similar to Canepatch under such conditions.

Temporal and spatial changes in the location of the low-salinity edge of saltwater intrusion would be expected to trigger P desorption and increased SRP concentration in ambient groundwater.¹⁸ Low-lying surficial coastal aquifers with a porous matrix are particularly

susceptible to movement of the freshwater-saltwater interface, due to low hydraulic head and high transmissivity.^{42, 43} Monitoring wells in Miami-Dade county record oscillations in salinity from fresh to saline as a result of changes in local hydrology such as groundwater pumping, large storm events and extended droughts.^{2, 10} Karstic environments with springs and conduits connected to seawater commonly undergo rapid reversals of salinity due to tidal pumping and seasonal changes in freshwater head, such as Andros Islands in the Bahamas,⁴⁴ the Bay of Kastela, Yugoslavia, and Waikoropupu springs, New Zealand.⁴⁵ Discharge rates can exceed several km per year.⁴⁶

Sea level rise is expected to exacerbate saltwater intrusion in many areas.^{11, 47-50} The Everglades is of particular concern.⁵¹ One study predicted the 7.1 mM (250 mg Cl⁻ /L) isochlor would move inland in the Everglades by 40-1800 m by 2100 depending on the sea level rise rate.⁵² Climate change may bring more extreme storms and heightened storm surges, which may further exacerbate saltwater intrusion, particularly in regions with tidally connected rivers.⁵⁰ In addition, regions which undergo extended droughts, higher temperatures, and evaporation, may suffer diminished aquifer recharge, further raising the risk of saltwater-intrusion, according to the fifth report of the International Panel on Climate Change.⁵³ One of the major goals of the multi-billion dollar Everglades restoration project, the Comprehensive Ecological Restoration Program, is to abate or mitigate saltwater intrusion by increasing groundwater recharge and the quantity of freshwater delivery to coastal areas.^{51, 54}

The P desorption dynamics of this study, if applied to an aquifer that has historical P loading, such as sewage injection sites in the limestone bedrock of the Florida Keys, could potentially

raise ambient water SRP concentration to eutrophic conditions. High desorption potential has been found in P-polluted soil and sediment, for instance in agricultural areas,⁵⁵ and from experimentally P-loaded limestone.⁵⁶ However, the intensity of seawater-induced desorption is dampened to some degree in carbonate solids with high P_{exch} .¹⁷ In addition, particularly intense P-loading can cause precipitation,⁵⁷ such as the formation of a cryptocrystalline precursor of calcium phosphate, within as little as two days.⁵⁸ Solid fractions of P tend to be more stable, and it is unknown to what degree seawater would trigger desorption.

Conclusion

This study provides essential parameters for predicting the effect of incremental landward incursion of saltwater within a carbonate aquifer on the potential P availability in overlying wetlands. The results indicate that a very small amount of saltwater mixing with fresh groundwater has the potential to cause the mineral surface to lose sorption efficiency and desorb P. Phosphorus appears to be active in the ion exchange front of saltwater intrusion. Landward movement of the 3 mM (100 mg Cl^- /L) isochlor may be associated with increased SRP concentration in groundwater, and would therefore be important to monitor where possible in P-limited ecosystems. The characteristics of a given carbonate aquifer, in terms of P_{exch} and iron content, may play an important role in how the sorption dynamics in turn affect ambient water SRP concentrations. Further study is required to understand the P dynamics of limestone bedrocks over a range of P, iron contents, and redox conditions, so as to understand these processes along coastlines globally.

Acknowledgements

Thanks to Kevin Cunningham of USGS for providing access to the rock cores, Rafael Travieso and Edward Linden of Florida International University for field and laboratory support, and Charles Fischer of National Oceanic and Atmospheric Administration/ Atlantic Oceanographic and Meteorological Laboratory for assistance in sample analysis. This material is based upon work supported by the National Science Foundation through the Florida Coastal Everglades Long-Term Ecological Research program under Cooperative Agreements #DEB-1237517, #DBI-0620409, and #DEB-9910514.

References

1. Sivan, O.; Yechieli, Y.; Herut, B.; Lazar, B., Geochemical evolution and timescale of seawater intrusion into the coastal aquifer of Israel. *Geochimica et Cosmochimica Acta* **2005**, *69*, (3), 579-592.
2. Prinos, S. T.; Wacker, M. A.; Cunningham, K. J.; Fitterman, D. V. *Origins and delineation of saltwater intrusion in the Biscayne aquifer and changes in the distribution of saltwater in Miami-Dade County, Florida*; 2328-0328; US Geological Survey: 2014.
3. Fitterman, D. V., Mapping saltwater intrusion in the biscayne aquifer, Miami-Dade County, Florida using transient electromagnetic sounding. *Journal of Environmental and Engineering Geophysics* **2014**, *19*, (1), 33-43.
4. Price, R. M.; Herman, J. S., Geochemical investigation of salt-water intrusion into a coastal carbonate aquifer: Mallorca, Spain. *Geological Society of America Bulletin* **1991**, *103*, (10), 1270-1279.
5. Cotecchia, V.; Tazioli, G.; Magri, G. In *Isotopic measurements in research on seawater ingression in the carbonate aquifer of the Salentine Peninsula, southern Italy*, Isotope techniques in groundwater hydrology 1974, Vol. I. Proceedings of a symposium, 1974; 1974.
6. Taylor, R. G.; Scanlon, B.; Döll, P.; Rodell, M.; Van Beek, R.; Wada, Y.; Longuevergne, L.; Leblanc, M.; Famiglietti, J. S.; Edmunds, M., Ground water and climate change. *Nature Climate Change* **2013**, *3*, (4), 322-329.
7. Krest, J. M.; Moore, W.; Gardner, L.; Morris, J., Marsh nutrient export supplied by groundwater discharge: Evidence from radium measurements. *Global Biogeochemical Cycles* **2000**, *14*, (1), 167-176.
8. Price, R. M.; Swart, P. K.; Fourqurean, J. W., Coastal groundwater discharge—an additional source of phosphorus for the oligotrophic wetlands of the Everglades. *Hydrobiologia* **2006**, *569*, (1), 23-36.

9. Kooi, H.; Groen, J., Offshore continuation of coastal groundwater systems; predictions using sharp-interface approximations and variable-density flow modelling. *Journal of Hydrology* **2001**, *246*, (1), 19-35.
10. Kohout, F. A., The flow of fresh water and salt water in the Biscayne aquifer of the Miami area, Florida. *Sea Water in Coastal Aquifers. US Geological Survey Water-Supply Paper* **1964**, 12-32.
11. Barlow, P. M.; Reichard, E. G., Saltwater intrusion in coastal regions of North America. *Hydrogeology Journal* **2010**, *18*, (1), 247-260.
12. Slomp, C. P.; Van Cappellen, P., Nutrient inputs to the coastal ocean through submarine groundwater discharge: controls and potential impact. *Journal of Hydrology* **2004**, *295*, (1), 64-86.
13. Valiela, I.; Costa, J.; Foreman, K.; Teal, J. M.; Howes, B.; Aubrey, D., Transport of groundwater-borne nutrients from watersheds and their effects on coastal waters. *Biogeochemistry* **1990**, *10*, (3), 177-197.
14. Johannes, R.; Hearn, C., The effect of submarine groundwater discharge on nutrient and salinity regimes in a coastal lagoon off Perth, Western Australia. *Estuarine, Coastal and Shelf Science* **1985**, *21*, (6), 789-800.
15. Paytan, A.; Shellenbarger, G. G.; Street, J. H.; Gonnee, M. E.; Davis, K.; Young, M. B.; Moore, W. S., Submarine groundwater discharge: An important source of new inorganic nitrogen to coral reef ecosystems. *Limnology and Oceanography* **2006**, *51*, (1), 343-348.
16. Froelich, P. N., Kinetic control of dissolved phosphate in natural rivers and estuaries: A primer on the phosphate buffer mechanism1. *Limnology and oceanography* **1988**, *33*, (4part2), 649-668.
17. Millero, F.; Huang, F.; Zhu, X.; Liu, X.; Zhang, J.-Z., Adsorption and desorption of phosphate on calcite and aragonite in seawater. *Aquatic Geochemistry* **2001**, *7*, (1), 33-56.
18. Flower, H. R., Mark; Zhang, Jia-Zhong; Lewis, David, Rapid and sustained phosphorus desorption with saltwater intrusion in a carbonate aquifer. (*in prep*) **2016**.
19. Zhang, J.-Z.; Huang, X.-L., Effect of temperature and salinity on phosphate sorption on marine sediments. *Environmental science & technology* **2011**, *45*, (16), 6831-6837.
20. Suzumura, M.; Ueda, S.; Sumi, E., Control of phosphate concentration through adsorption and desorption processes in groundwater and seawater mixing at sandy beaches in Tokyo Bay, Japan. *Journal of oceanography* **2000**, *56*, (6), 667-673.
21. Fish, J. E.; Stewart, M. T., *Hydrogeology of the surficial aquifer system, Dade County, Florida*. US Department of the Interior, US Geological Survey: 1991.
22. Klein, H.; Hull, J. E. *Biscayne aquifer, southeast Florida*; US Geological Survey: 1978.
23. Fitterman, D. V.; Deszcz-Pan, M., Helicopter EM mapping of saltwater intrusion in Everglades National Park, Florida. *Exploration Geophysics* **1998**, *29*, (1/2), 240-243.
24. Saha, A. K.; Saha, S.; Sadle, J.; Jiang, J.; Ross, M. S.; Price, R. M.; Sternberg, L. S.; Wendelberger, K. S., Sea level rise and South Florida coastal forests. *Climatic Change* **2011**, *107*, (1-2), 81-108.
25. Ross, M.; Meeder, J.; Sah, J.; Ruiz, P.; Telesnicki, G., The southeast saline Everglades revisited: 50 years of coastal vegetation change. *Journal of Vegetation Science* **2000**, *11*, (1), 101-112.
26. Zapata-Rios, X.; Price, R. M., Estimates of groundwater discharge to a coastal wetland using multiple techniques: Taylor Slough, Everglades National Park, USA. *Hydrogeology Journal* **2012**, *20*, (8), 1651-1668.

27. Rivera-Monroy, V. H.; Twilley, R. R.; Davis III, S. E.; Childers, D. L.; Simard, M.; Chambers, R.; Jaffe, R.; Boyer, J. N.; Rudnick, D. T.; Zhang, K., The role of the Everglades Mangrove Ecotone Region (EMER) in regulating nutrient cycling and wetland productivity in south Florida. *Critical Reviews in Environmental Science and Technology* **2011**, *41*, (S1), 633-669.
28. Noe, G. B.; Childers, D. L.; Jones, R. D., Phosphorus biogeochemistry and the impact of phosphorus enrichment: why is the Everglades so unique? *Ecosystems* **2001**, *4*, (7), 603-624.
29. Price, R. M., Geochemical determinations of groundwater flow in Everglades National Park. **2001**.
30. Flower, H. R., Mark; Zhang, Jia-Zhong; Lewis, David; Price, René Control of Phosphorus concentration through adsorption and desorption in shallow groundwater of subtropical carbonate estuary. *Estuarine, Coastal and Shelf Science* **2015** (in press).
31. D'Angelo, E.; Crutchfield, J.; Vandiviere, M., Rapid, sensitive, microscale determination of phosphate in water and soil. *Journal of environmental quality* **2001**, *30*, (6), 2206-2209.
32. Zhang, J. Z.; Fischer, C. J.; Ortner, P. B., Potential availability of sedimentary phosphorus to sediment resuspension in Florida Bay. *Global Biogeochemical Cycles* **2004**, *18*, (4).
33. Ruttenberg, K. C., Development of a sequential extraction method for different forms of phosphorus in marine sediments. *Limnology and oceanography* **1992**, *37*, (7), 1460-1482.
34. Huang, X.-L.; Zhang, J.-Z., Neutral persulfate digestion at sub-boiling temperature in an oven for total dissolved phosphorus determination in natural waters. *Talanta* **2009**, *78*, (3), 1129-1135.
35. Zhang, J.-Z.; Kelble, C.; Millero, F. J., Gas-segmented continuous flow analysis of iron in water with a long liquid waveguide capillary flow cell. *Analytica chimica acta* **2001**, *438*, (1), 49-57.
36. Zhou, A.; Tang, H.; Wang, D., Phosphorus adsorption on natural sediments: Modeling and effects of pH and sediment composition. *Water Research* **2005**, *39*, (7), 1245-1254.
37. Agency, U. S. E. P. *Secondary drinking water regulations; guidance for nuisance chemicals*; 2015.
38. Langevin, C. D. *Simulation of Ground-Water Discharge to Biscayne Bay, Southeastern Florida*; Water-Resources Investigations Report 00-4251; U.S. Geological Survey: Tallahassee, FL, 2001.
39. Sonenshein, R. S., *Delineation of saltwater intrusion in the Biscayne Aquifer, eastern Dade County, Florida, 1995*. US Department of the Interior, US Geological Survey: 1996.
40. Zhang, J.-Z.; Huang, X.-L., Relative importance of solid-phase phosphorus and iron on the sorption behavior of sediments. *Environmental science & technology* **2007**, *41*, (8), 2789-2795.
41. Pant, H.; Reddy, K., Phosphorus sorption characteristics of estuarine sediments under different redox conditions. *Journal of Environmental Quality* **2001**, *30*, (4), 1474-1480.
42. Obeysekera, J.; Irizarry, M.; Park, J.; Barnes, J.; Dessalegne, T., Climate change and its implications for water resources management in south Florida. *Stochastic Environmental Research and Risk Assessment* **2011**, *25*, (4), 495-516.
43. Werner, A. D.; Ward, J. D.; Morgan, L. K.; Simmons, C. T.; Robinson, N. I.; Teubner, M. D., Vulnerability indicators of sea water intrusion. *Groundwater* **2012**, *50*, (1), 48-58.
44. Stringfield, V.; LeGrand, H., Effects of karst features on circulation of water in carbonate rocks in coastal areas. *Journal of Hydrology* **1971**, *14*, (2), 139-157.

45. Fleury, P.; Bakalowicz, M.; de Marsily, G., Submarine springs and coastal karst aquifers: a review. *Journal of Hydrology* **2007**, *339*, (1), 79-92.
46. Steinen, R. P.; Matthews, R.; Sealy, H., Temporal variation in geometry and chemistry of the freshwater phreatic lens: The coastal carbonate aquifer of Christ Church, Barbados West Indies. *Journal of Sedimentary Research* **1978**, *48*, (3).
47. Wong, P.; Losada, I.; Gattuso, J.; Hinkel, J.; Khattabi, A.; McInnes, K.; Field, C.; Barros, V.; Dokken, D.; Mach, K., Climate change 2014: impacts, adaptation, and vulnerability. Part A: global and sectoral aspects. Contribution of Working Group II to the Fifth Assessment Report of the Intergovernmental Panel on Climate Change. In Cambridge Cambridge University Press.: 2014.
48. Webb, M. D.; Howard, K. W., Modeling the Transient Response of Saline Intrusion to Rising Sea-Levels. *Groundwater* **2011**, *49*, (4), 560-569.
49. Loáiciga, H. A.; Pingel, T. J.; Garcia, E. S., Sea Water Intrusion by Sea-Level Rise: Scenarios for the 21st Century. *Groundwater* **2012**, *50*, (1), 37-47.
50. Carter, L.; Jones, J.; Berry, L.; Burkett, V.; Murley, J.; Obeysekera, J.; Schramm, P.; Wear, D.; Melillo, J.; Richmond, T., Southeast and the Caribbean. *Climate Change Impacts in the United States: The Third National Climate Assessment* **2014**, 396-417.
51. Council, N. R., *Progress Toward Restoring the Everglades: The Fifth Biennial Review, 2014*. The National Academies Press: Washington, DC, 2014; p 302.
52. Langevin, C. D.; Dausman, A.; Tyagi, A. K.; Civil, O. In *Numerical simulation of saltwater intrusion in response to sea-level rise*, Proceedings of the Water & Environmental Resources Congress: Impacts of Global Climate Change, Anchorage, Alaska. http://plaza.ufl.edu/clang001/papers/langevin_ASCE2005.pdf (December 18, 2008), 2005; 2005.
53. Jimenez Cisneros, B. E.; Oki, T.; Arnell, N. W.; Benito, G.; Cogley, J. G.; Doll, P.; Jiang, T.; Mwakalila, S. S., Freshwater resources. **2014**.
54. Team, R. C. a. V. *Southern Coastal Everglades*; September 23, 2015, 2014
55. Reddy, K.; Kadlec, R.; Flaig, E.; Gale, P., Phosphorus retention in streams and wetlands: a review. *Critical reviews in environmental science and technology* **1999**, *29*, (1), 83-146.
56. Price, R. M.; Savabi, M. R.; Jolicoeur, J. L.; Roy, S., Adsorption and desorption of phosphate on limestone in experiments simulating seawater intrusion. *Applied Geochemistry* **2010**, *25*, (7), 1085-1091.
57. Zhou, M.; Li, Y., Phosphorus-sorption characteristics of calcareous soils and limestone from the southern Everglades and adjacent farmlands. *Soil Science Society of America Journal* **2001**, *65*, (5), 1404-1412.
58. Cable, J.; Corbett, D. R.; Walsh, M., Phosphate uptake in coastal limestone aquifers: a fresh look at wastewater management. *Limnology and Oceanography Bulletin* **2002**, *11*, (2), 1-4.

Chapter 4:

Rapid and sustained phosphorus desorption with saltwater intrusion in a carbonate aquifer

Note to reader

Portions of this chapter are in preparation for submission for publication. The author of this dissertation is the first author on the paper, and the other authors are: Dr. Mark Rains (contribution: guidance and funding), Dr. David Lewis (contribution: access to equipment and laboratory facilities for phosphorus analysis), and Dr. Jia-Zhong Zhang (contribution: guidance in regard to laboratory procedures and analysis).

Abstract

It is important to understand how phosphorus (P) sorption dynamics of carbonate aquifers are affected by the incursion of seawater, because many coastal aquifers are carbonate-based and subject to increasing saltwater intrusion with sea level rise. In this study a well core through the Biscayne aquifer was sampled at 11 depth intervals from 3-30 m depth, spanning three geologic formations. Portions of each sample were ground to <125 μm and tested for readily exchangeable P, total sedimentary P, and iron content. The rock core had low P content at all depth intervals, with highest exchangeable P occurring at the 30 m depth interval, and highest iron at 6 m and 22 m depth intervals. Samples of ground rock powder from seven of the depth intervals were investigated using batch isotherm sorption experiments with fresh groundwater and saltwater, for a total of 14 sorption isotherms. Water type was found to control the sorption

efficiency for all rock samples. Unconsolidated sediment from the deepest depth interval, 30 m, was placed in a glass column and fresh groundwater was pumped upwards through the column, alternating with saltwater. Samples of leachate were taken at intervals, from which conductivity and SRP were measured. With the first influx of saltwater SRP concentration rose dramatically and gradually tapered. The second influx of saltwater resulted in an immediate but lower magnitude peak in SRP. Our results indicate an immediate and intense pulse of P desorption from oligotrophic carbonate solids in response to an influx of seawater.

Introduction

Many carbonate aquifers along coastlines have undergone saltwater intrusion, such as Florida, USA,¹ Mallorca, Spain,² and Apulia, Italy.³ Where fresh water and saltwater meet in the aquifer, the denser saltwater typically forms a wedge beneath the less dense fresh water. The two endmember waters mix and flow to the surface in a process known as submarine groundwater discharge. Factors that change the hydraulic gradient, such as drought, drainage canals, groundwater pumping, changes in precipitation, and sea level rise, can cause the freshwater/saltwater interface to move landward or seaward accordingly.⁴ Coastal groundwater can be orders of magnitude higher in SRP concentration than overlying surface water in some regions⁵ as a result of saltwater-induced desorption of SRP from aquifer mineral surfaces at depth.⁶ The discharge of P-enriched groundwater to coastal estuaries is ecologically significant, particularly in P-limited ecosystems.⁶

Existing literature provides clues that a slight incursion of saltwater may result in significant desorption of loosely adsorbed P from aquifer solids. A recent study examining the pattern of

desorption with respect to the freshwater-saltwater mixing continuum found that limestone sorption dynamics favor desorption when ambient freshwater 3 mM Cl⁻ concentration (100 mg Cl⁻ /L).⁷ Existing kinetic studies on saltwater-induced desorption from carbonate solids involve a preliminary step of bathing the solids in SRP-enriched water. Batch study of P-loaded calcium carbonate solids (calcite, aragonite, and calcareous sediment from Florida Bay, USA) released significant amounts of SRP in the first minutes of immersion in seawater, and up to 80% of adsorbed P was released over one day.⁸ In another study a large block of limestone from Key Largo, Florida, USA, that had been loaded with SRP was found to desorb more SRP in plain seawater than de-ionized water.

From the existing studies it is difficult to predict the magnitude, rate, and duration of desorption from pristine carbonate solids that would be induced by natural waters. In regions unaffected by human activities such as sewage injection, carbonate bedrock can have very low P content.^{7,9} The objective of this study is to investigate at high resolution the desorption kinetics of pristine carbonate solids as the ambient water alternates between natural freshwater and saltwater. Our goal is to better understand how groundwater SRP concentration in a carbonate coastal aquifer may be affected as the saltwater intrusion front moves landward or seaward. The results of this study will provide critical information for water management and restoration efforts in carbonate coastal regions.

Methods

Study area. Southern coastal Florida is home to one of the most highly transmissive aquifers in the world, the surficial carbonate Biscayne Aquifer. This aquifer underlies Miami-Dade County

and extends through the eastern portion of the Everglades National Park. At the eastern edge of the Biscayne aquifer saltwater intrusion has caused the abandonment of many wells.¹⁰ To the south in the Everglades National Park, saltwater has intruded between 6-28 km inland along the base of the aquifer.¹¹ The Everglades has been called “phosphorus starved” due to its highly oligotrophic nature and its sensitivity to even small increases of P.¹² For this reason, a detailed understanding of the storage and transport of P in the Everglades has been described as urgently needed in order to effectively and comprehensively address water quality concerns.¹³

Rock samples. Rock samples were selected from a 33 m well core that fully penetrates the Biscayne aquifer (Figure 4.1). Well core G-3784 was taken along Levee 31N adjacent to the L-31N canal on the western side of urban development, as part of a seepage study by USGS in 2003 (latitude: 25°42'07.36"N; longitude: 080°29'46.26"W).^{14, 15} The well core is 4 inches in diameter. In this well core, the Biscayne aquifer includes three geologic formations, the Miami Formation (Fm), the Fort Thompson Fm, and the Tamiami Fm (which is considered semi-permeable in some areas).¹⁴ We sampled well core G-3784 at eleven depth intervals; lithologic descriptions are in Table 4.1.

Rock samples were crushed and sieved. Inorganic $\text{MgCl}_2\text{-P}$, also known as loosely adsorbed or readily exchangeable P (P_{exch}),¹⁶ is defined as the inorganic P released from rock powder by 1 M MgCl_2 solution at pH 8.0, following the protocol established by Ruttenberg.¹⁷ Organic $\text{MgCl}_2\text{-P}$ was also determined using Ruttenberg¹⁷ with the exception that total dissolved P was measured using the sub-boiling temperature protocol of Huang and Zhang.¹⁸

Total sedimentary P were determined by high temperature combustion.¹⁶ The sediment samples were placed in 100-mL Pyrex beakers and wetted with a few drops of 1 M $\text{Mg}(\text{NO}_3)_2$ solution and then ashed in a combustion furnace at 550°C for 2 hours. After the samples were cooled to room temperature, a 50 mL of 1 M HCl solution was added to each sample. The samples were then agitated at 25°C for 24 hours to extract P. Samples were filtered to remove any particulate residuals and the filtrates analyzed for dissolved phosphate. Total Fe in sediments was determined by dissolution of solid phase Fe in 1 N HCl solution. The total dissolved iron ($\text{Fe}^{3+} + \text{Fe}^{2+}$) in the solution was reduced with ascorbic acid to Fe^{2+} . The Fe^{2+} was then spectrophotometrically determined with a ferrozine reagent in a pH 5.5 buffer solution at a maximum absorption wavelength of 562 nm.¹⁹

Water samples. Two water types were collected as representatives of freshwater and saltwater (sampling locations provided in Figure 4.1). Fresh groundwater (hereafter referred to as “freshwater”) was collected from shallow monitoring well (TSB-15) within the bedrock underlying the freshwater sawgrass marsh.²⁰ Our saltwater representative (“saltwater”) is from Florida Bay surface water taken from a dock in Key Largo. Sulfate concentration was 28.4 mM in our saltwater, and below detection limit in our fresh water. Bicarbonate alkalinity was 4.0 and 2.9 mM for our saltwater and freshwater respectively. Procedures for determining water properties and results are described in detail elsewhere.⁷ All SRP concentrations for this study were determined the day of the completion of each experiment using the microscale malachite green method,²¹ measuring absorbance at 630 nanometers (nm) in 96-well microplates on a BioTek EPOCH microplate spectrophotometer.

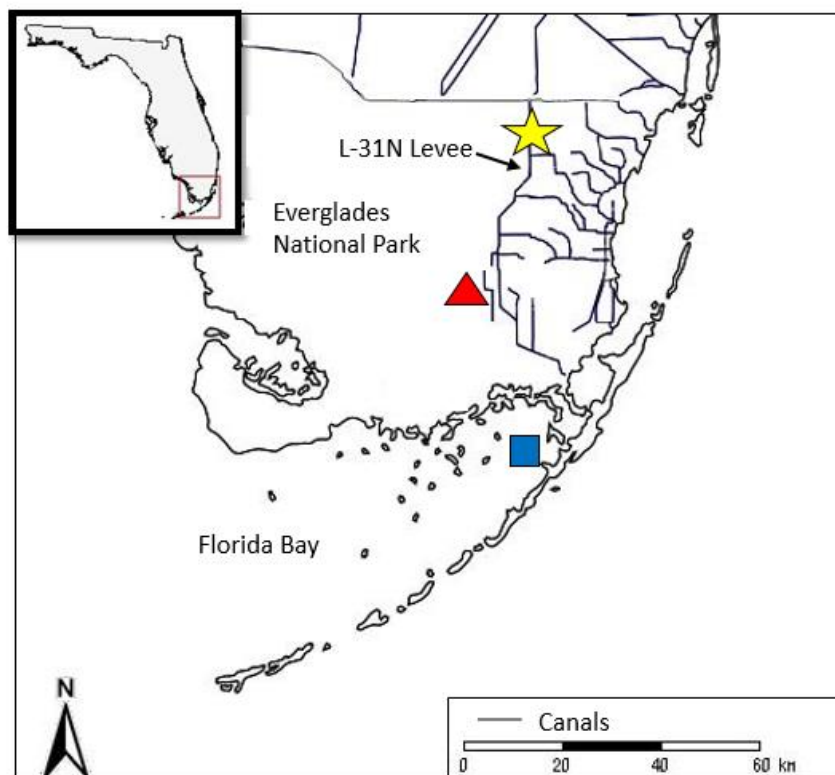


Figure 4.1 Location map showing well G-3784 (star), fresh groundwater well TSB15 (triangle), and saltwater sampling from Florida Bay (square)

Column experiments. The column apparatus is depicted in Figure 4.2, and is based on the methods of Suzumura, et al.²² Silicone tubing led from a beaker of either fresh or saltwater, through a Cole Parmer low flow peristaltic pump at a rate of 1 mL/min. A Kimble Chase Flex-Column (inner diameter of 1.5 cm, length 20 cm) was filled with 47 g of coarse grained aquifer solids. Upward flow minimized the formation of channels and preferential flow paths. Leachate exited the top of the flex-column, passed through a 0.45 μm nylon syringe filter (replaced after every 30 mL), and out through a tube to a sample vial. Each leachate sample was immediately measured for conductivity using a Horiba Laqua Twin conductivity meter, and for pH using a Horiba Laqua Twin conductivity meter, and then stored for SRP analysis. At the conclusion of the experiment, SRP concentration were determined using the microscale malachite green

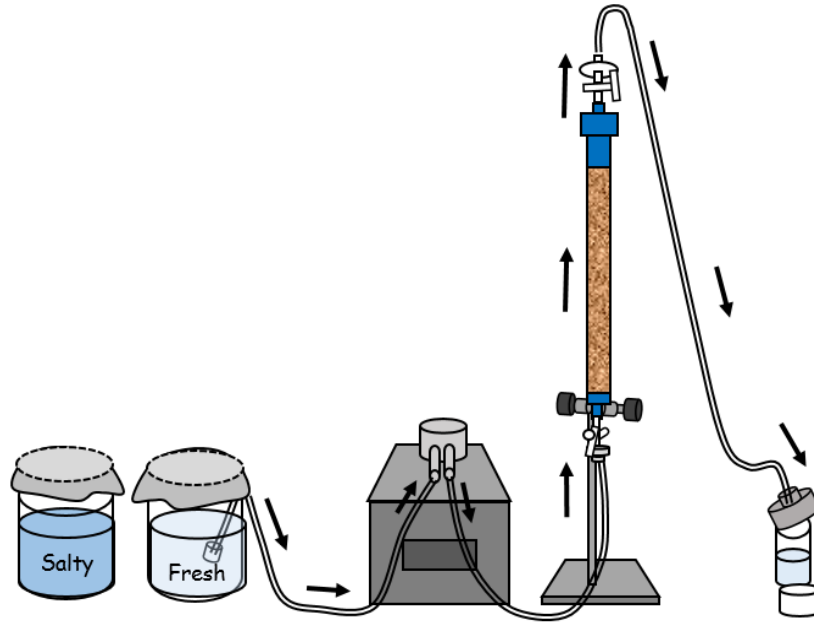


Figure 4.2 Schematic diagram of column apparatus

method,²¹ measuring absorbance at 630 nm in 96-well microplates on a BioTek EPOCH microplate spectrophotometer.

Aquifer solids from the 14 m and 30 m depth intervals were chosen for column study because they had the highest P_{exch} (Figure 4.3), giving the best chance of measurable P desorption. The aquifer solids from the 30 m depth interval were unconsolidated shells and sand, requiring no crushing. Three column experiments were run with variations in sediment grain size and leaching water sample size. The first column experiment used the aquifer solids without sieving, so as to most closely approximate the natural aquifer conditions. The inflow water alternated as follows: 60 mL of fresh groundwater, 70 mL of saltwater, 70 mL of freshwater, 70 mL of saltwater, and 60 mL of fresh water. The first four leachate samples were 10 mL each, and all subsequent samples were 2 mL each (154 samples total). The second column experiment was conducted in an identical fashion with the exception that only the sediment size fraction between 1.0-1.4 mm

was used, so as to further reduce the potential for preferential flow paths that may develop based on grain size. The third column experiment was designed to increase the resolution; the design different from the second column experiment in two ways: (1) a single freshwater-saltwater-freshwater sequence (only one influx of saltwater); (2) samples were 1 mL instead of 2 mL (162 samples total).

Table 4.1 Lithologic descriptions of the rock samples

Depth below ground surface, m	Lithology ¹⁴	Formation
3	Peloidal grainstone-packstone	Miami Fm
5	Peloidal grainstone and packstone	
6	Wackestone-mudstone	Ft Thomspn Fm
8	Molluscan foraminiferal floatstone	
9	Touching-vug pelicipod floatstone-mudstone with mollusks visible	
11	Skeletal wackestone-packstone	
12		
14	Mudstone-wackestone	Tamiami Fm
15	Quartz-rich pelecypodal floatstone mudstone	
18		
22	Shelley quartz sand with abundant mollusk shells (unconsolidated)	
30	Shelley quartz sand with abundant mollusk shells (unconsolidated)	

Column experiments four and five were conducted with crushed and sieved rock grains (1.0-1.4 mm) from the rock at the 14 m depth interval. Column experiment four consisted of a single freshwater-saltwater-freshwater sequence, and column experiment five consisted simply of 60 mL of freshwater followed by a sustained flow of saltwater for 200 mL.

Sorption isotherm experiments. Sorption isotherm batch experiments²³ were conducted on seven of the eleven depth intervals, chosen for their range of P_{exch} , total sedimentary P, and Fe content, using our sediment analysis results as a guide (Figure 4.3). For each experiment, a 60 mL high density plastic test tube was filled with 100 mg of one of the seven rock types (sieved <125 μm), 30 mL of either fresh water or saltwater, 20 μL 0.1% chloroform, and a given measure of 3 mM SRP stock solution to yield one of 10 different initial SRP concentrations, $[\text{SRP}]_i$: 0.0, 0.6, 1.0, 1.3, 1.6, 1.9, 3.3, 4.8, 5.6, 6.5, and 8.1 μM . After 24 hours of shaking at 200 rpm on a platform shaker, each suspension was passed through a 0.45 μm nylon syringe filter, and immediately analyzed for final SRP concentration, $[\text{SRP}]_f$, as previously described.

Sorption isotherm parameters. The amount of SRP adsorbed by the rock powder, ΔP , was calculated as:

$$\Delta P = [\text{SRP}]_i - [\text{SRP}]_f \quad , \quad [1]$$

and was normalized to ΔP_{sed} in units $\mu\text{mol g}^{-1}$. A plot of ΔP_{sed} vs. $[\text{SRP}]_f$ from each experiment was used to represent a given rock's adsorption isotherm for a given water type. A modified Freundlich equation was used to parameterize the adsorption isotherm data:

$$\Delta P + \text{NAP} = K_f [\text{SRP}]_f^n \quad [2]$$

where NAP ($\mu\text{mol g}^{-1}$) is the native adsorbed inorganic P. The exponent factor n indicates the strength of the bond between the adsorbate and the adsorbent; the smaller n is the more favorable adsorption is.²⁴ The Freundlich coefficient, K_f , indicates the relative adsorption capacity of the mineral surface. A high K_f indicates a high rate of SRP removal.²⁴ The value of $[\text{SRP}]_f$ at $\Delta P = 0$ is known as the zero equilibrium concentration, EPC_0 , the SRP concentration at which there is no

net change in adsorbed P. By taking the derivative of the Freundlich equation [2] with respect to the EPC_o, it is possible to calculate the distribution coefficient, K_d (L g⁻¹):²⁵

$$K_d = n K_f [EPC_o]^{n-1} \quad , \quad [3]$$

which is a measure of the buffer intensity. The bend of an isotherm curve toward a lower angle is an indication of incipient saturation of monolayer sorption sites on the mineral surface. The Langmuir sorption model provides a means of calculating the point at which the system reaches saturation, the maximum monolayer sorption capacity, P_{max}. Such behavior can be modeled as:

$$\Delta P_{sed} = \frac{K_{eq} P_{max} [SRP]_f}{1 + K_{eq} [SRP]_f} \quad , \quad [4]$$

where the constant K_{eq} (μM⁻¹) is related to the heat of adsorption, also described as the affinity of SRP for the adsorption sites.

Results

Rock composition results are shown in Figure 4.3. Iron content was low (less than 25 μmol g⁻¹) for all samples except the 6 m depth interval (40 μmol g⁻¹) and the 22 m depth interval (118 μmol g⁻¹). The Miami Fm samples exhibited the lowest iron content (5 μmol g⁻¹). Total sedimentary P was low for all samples, and increased four-fold from 2 μmol g⁻¹ to 8 μmol g⁻¹ with depth. In the Miami Fm samples total sedimentary P was 2 μmol g⁻¹, gradually rising to 6 μmol g⁻¹ at the base of Ft Thompson Fm (15 m), and increasing further to 8 μmol g⁻¹ in the samples at the greatest depth (22 m and 30 m, in the Tamiami Fm). Readily exchangeable P (P_{exch}) is low for all rock samples tested, but does exhibit some variation based on geologic formation

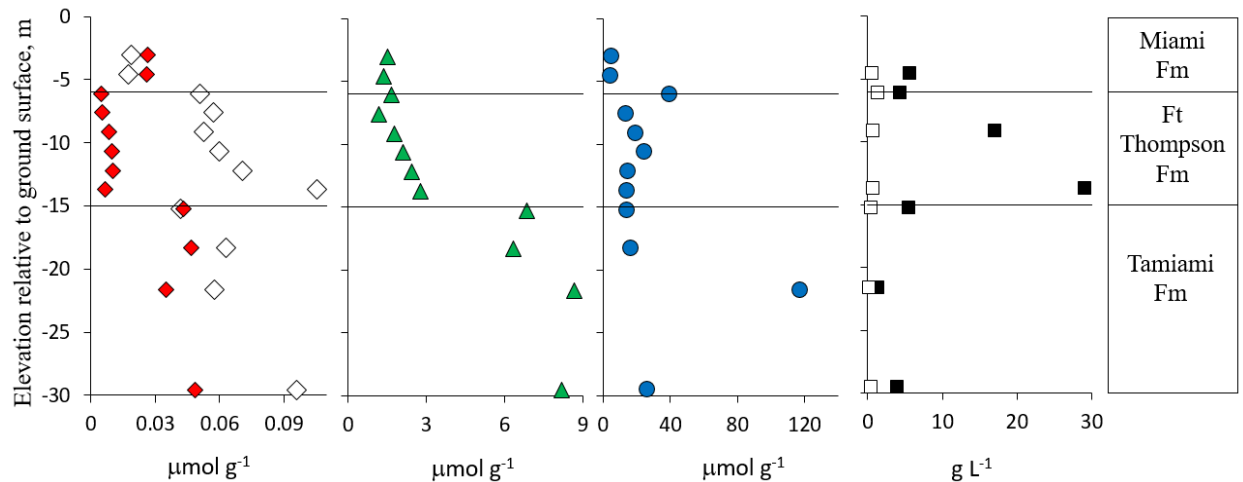


Figure 4.3 Selected rock composition along the vertical section of well core with geologic formations demarcated; organic $\text{MgCl}_2\text{-P}$ (red diamonds); inorganic $\text{MgCl}_2\text{-P}$ (P_{exch}) (open diamonds); total sedimentary P (green triangles), total iron (blue circles); saltwater K_d (open squares); freshwater K_d (solid black squares)

and depth. The highest P_{exch} was found in samples from 14 m and 30 m depth intervals (with $0.105 \mu\text{mol g}^{-1}$ and $0.096 \mu\text{mol g}^{-1}$ respectively), and the lowest was in depth intervals 3 m and 5 m in the Miami Fm. Both the Ft Thompson Fm and Tamiami Fm exhibit a general trend of increasing P_{exch} with depth. Organic P released from MgCl_2 is lowest in the Ft Thompson Fm and highest in the Tamiami Fm.

Sorption isotherm parameters are provided in Table 4.2. Water type dominated over rock composition as a driver of sorption behavior. Freshwater K_f , K_d (Figure 4.3), and K_{eq} values were an order of magnitude higher than saltwater values for almost all samples. Coefficients K_f and K_d exhibited a relatively wide range of values based on rock type in freshwater than in saltwater, but without exhibiting any clear relationship to lithology. In most samples NAP was high in fresh water, and was zero or near zero in saltwater, which is consistent with other work on bedrock and carbonate sediment that compared fresh water and saltwater sorption behavior.^{7,26} The

rocks' exponent n was double in saltwater compared to fresh water. Only one parameter, P_{\max} , varied more by rock than water type.

The first three column experiments were conducted with sediment grains from the 30 m depth interval (Tamiami Fm). At the first detection of saltwater in the leachate, SRP concentration increased by 250%, 400%, and 280% for column experiments one, two, and three, respectively (Figure 4.4). After approximately 10 mL of saltwater flow (10 minutes) SRP concentration began a steady decline. The passage of an additional 44 mL of saltwater through the columns resulted in SRP concentration decreases of 26%, 35%, and 25% for column experiments one, two, and three, respectively. Because the inflow water was changed to fresh water at that point, it is not known whether SRP concentration would have leveled off or declined to freshwater levels with a prolonged flow of saltwater. A second change to saltwater resulted in a dampened SRP peak (27% and 16% less than the first peak, for columns 1 and 2 respectively).

Before an increase in conductivity could be detected, leachate exhibited large excursions of SRP concentration in two of the three columns experiments. These isolated spikes in SRP concentration interrupted the steady decline which had begun in saltwater and continued until leachate was fully fresh.

Column experiments four and five were conducted with crushed rock grains from the rock at the 14 m depth interval. In the fourth column experiment there was only one change to saltwater, unlike column experiments one and two. The leachate SRP declined initially but then appeared to stabilize until conductivity began to decline at the return of freshwater (Figure 4.5 a). To

Table 4.2 Sorption isotherm parameters

Water Type	Depth below ground surface m	Freundlich Model			Langmuir Model		
		K_f L/g	n	NAP $\mu\text{mol g}^{-1}$	K_d L/g	P_{max} $\mu\text{mol g}^{-1}$	K_{eq} μM^{-1}
Freshwater							
	5	15.5	0.0	14.0	5.7	2.6	1.43
	6	4.2	0.3	1.4	4.3	5.1	1.12
	9	3.9	0.2	2.3	17.1	2.7	1.56
	14	11.6	0.1	9.5	29.1	3.0	1.96
	15	3.2	0.2	1.6	5.5	2.6	2.15
	22	1.1	0.3	0.1	1.3	1.5	2.69
	30	1.8	0.5	0.0	4.0	3.4	1.46
Saltwater							
	5	0.4	0.6	0.0	0.6	2.6	0.13
	6	0.6	0.7	0.0	1.4	4.2	0.15
	9	0.4	0.6	0.0	0.8	2.6	0.13
	14	0.4	0.7	0.0	0.7	3.5	0.11
	15	0.3	0.7	0.0	0.4	3.1	0.09
	22	0.3	0.6	0.1	0.2	2.1	0.09
	30	0.6	0.7	0.1	0.1	5.0	0.10

further investigate this pattern, column experiment five was the same as column 4 except saltwater flow continued for 200 mL, with no return of fresh water. After sustained saltwater flow the leachate appeared to stabilize at a concentration of $0.51 \pm 0.06 \mu\text{M}$, intermediate between the freshwater SRP and the peak in SRP accompanying the first saltwater leachate (Figure 4.5 b). During the portion of this experiment in which leachate SRP concentration, a desorption rate of $0.031 \pm 0.004 \mu\text{mole/hour}$ was calculated.

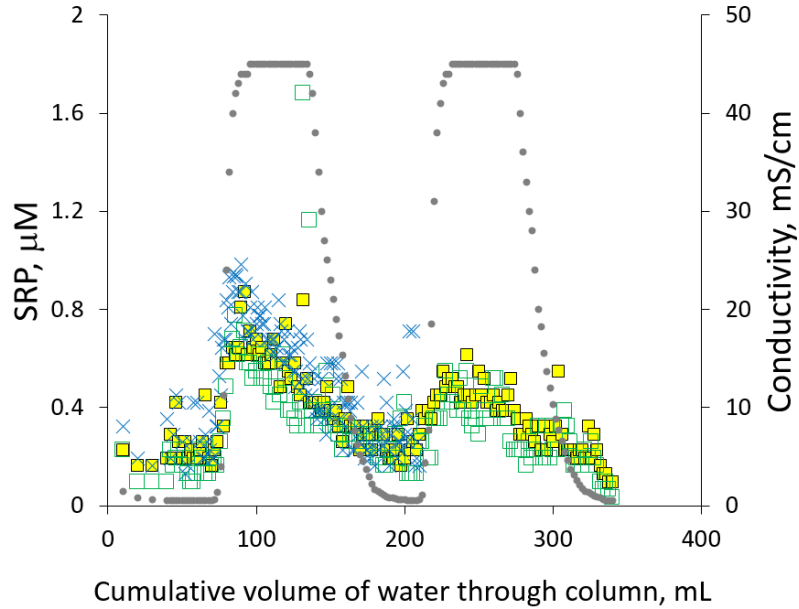
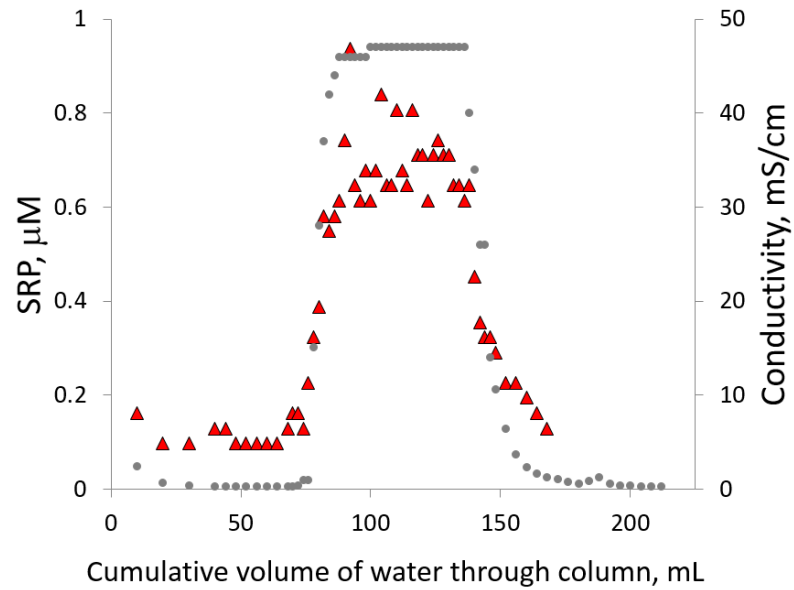


Figure 4.4 Column experiments with rock from the 30 m depth interval showing three column experiments: one (open green squares); two (solid yellow squares); and three (blue crosses)

Discussion

The three geologic formations exhibit different compositions, with the Miami Fm being lowest in total sedimentary P, iron, and both organic and inorganic $\text{MgCl}_2\text{-P}$. The Miami Fm is also the only formation in which organic $\text{MgCl}_2\text{-P}$ exceeds inorganic $\text{MgCl}_2\text{-P}$ (P_{exch}). The Ft Thompson Fm is intermediate to the other two formations in total sedimentary P and total iron content, lower in organic P_{exch} , and similar in range as the Tamiami Fm for P_{exch} . The Ft Thompson Fm has two extremes: high iron at 6 m and high P_{exch} at 14 m. The Tamiami Fm is higher than the other two in total sedimentary P and organic P_{exch} , and within a similar range for iron and P_{exch} . Like the Ft Thompson Fm, the Tamiami Fm has a high iron sample (at 22 m depth), and high a P_{exch} sample (30 m). Loosely adsorbed inorganic P (P_{exch}) is commonly found to be 10% of total sedimentary P, and our results are consistent with this general proportion.^{16, 27}

a)



b)

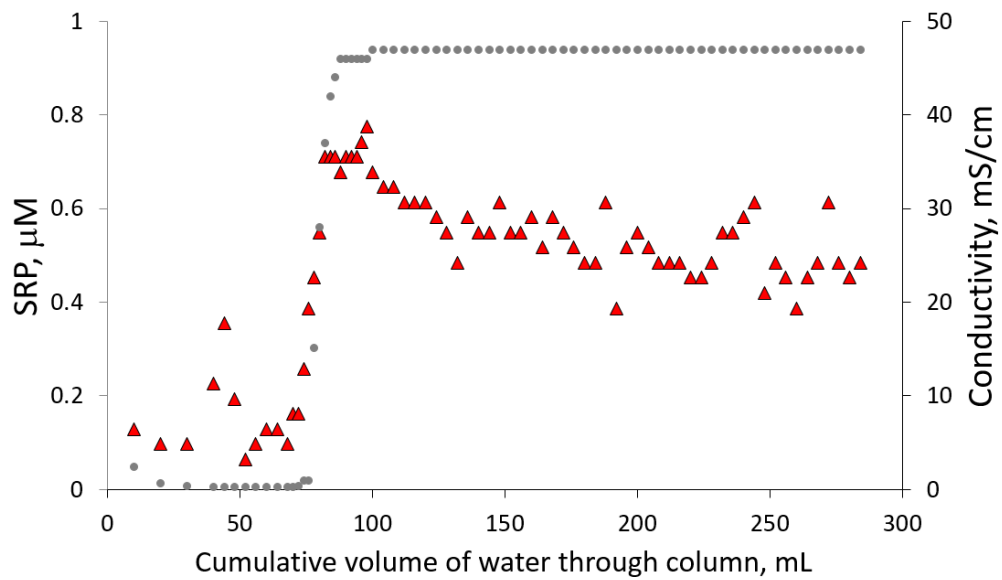


Figure 4.5 Column experiments with depth interval 14 m; a) column experiment four, with the sequence: freshwater-saltwater-freshwater; and b) column experiment five, with a single influx of freshwater followed by a sustained flow of saltwater

Despite a relatively wide range of composition, sorption behavior in our rocks was chiefly governed by water type, with no clear relationship between sorption behavior and composition

(Figure 4.3). This result stands in contrast to a recent sorption study comparing two limestone bedrock samples from a southwestern portion of the Biscayne Aquifer, as well as a study of calcareous sediments from Florida Bay, both of which found iron content was an important driver of sorption behavior in samples with low P content.²⁶ It would be necessary to investigate the sorption behavior of more than seven samples to adequately characterize the relationship between sorption behavior and composition in this vertical section of the aquifer. Our results underscore the relationship between loss of sorption efficiency and desorption by examining the same rocks for sorption isotherm parameters and kinetic behavior. The coefficients K_f , K_d , and K_{eq} of our rocks were typically an order magnitude higher in freshwater than in saltwater, and an influx of saltwater into our columns resulted in increased leachate SRP concentration.

Our isotherm parameters are similar to those found for two samples of bedrock from a southwestern portion of the Biscayne Aquifer, with the exception that our P_{max} values are higher.²⁶ Our freshwater K_f values are similar to those determined for sediments from the freshwater wetland and pinelands in the Everglades, and our saltwater K_f values are within the range of values estimated for Florida Bay sediments.²⁸

In our column studies we were able to observe the rapidity and magnitude of desorption reactions related to saltwater intrusion. An immediate pulse of P-desorption occurred at the switch from freshwater to saltwater in all of our column studies. Even in the high resolution column experiment (column experiment three), the first 1 mL leachate sample that exhibited increased conductivity also exhibited increased SRP concentration. The magnitude of increased SRP concentration in our saltwater leachate was higher than we had expected given the low P_{exch}

of our rocks. An SRP concentration of $0.51 \pm 0.06 \mu\text{M}$ was sustained in our saltwater leachate for more than two hours in our fifth column experiment.

The SRP concentrations observed in the saltwater leachate of our column experiments exceeded the $0.3 \mu\text{M}$ (10 ppb) total P (TP) criterion for the Everglades Protection Area.²⁹ Measurements of TP encompass SRP, dissolved organic P and particulate P (both organic and inorganic), thus it would take considerably less than $0.3 \mu\text{M}$ SRP to cause most natural water to exceed the regulatory TP limit. Groundwater discharging from a portion of the aquifer that has undergone saltwater-induced desorption may well constitute an ecologically relevant source of SRP. The desorption would not need to be recent, because the low buffer intensity (K_d) exhibited by our rocks in brackish water would maintain ambient groundwater at an elevated level.

Although vertical flow is impeded by semi-permeable layers in portions of the Biscayne Aquifer, such as our well core location G-3784,^{14, 15} in other portions brackish groundwater is known to discharge to the overlying mangrove swamp.^{11, 30, 31} Karstic environments with springs and conduits connected to seawater commonly undergo rapid reversals of salinity due to tidal pumping and seasonal changes in freshwater head, such as Andros Islands in the Bahamas,³² the Bay of Kastela, Yugoslavia, and Waikoropupu springs, New Zealand.³³ Discharge rates can exceed several km per year.³⁴

In addition to magnitude and rapidity, the duration of desorption could be observed in our column studies as well. Column experiments one, two, and three (using the aquifer solids from the 30 m depth interval) all exhibited a steady decline before the re-introduction of freshwater

(Figure 4.4). In contrast, the column experiments using samples from the 14 m depth interval (column experiments four and five; Figure 4.5) sustained a quasi-equilibrium SRP until the experiment was terminated after three hours and 20 minutes of saltwater flow (Figure 4.5). Putting together the calculated desorption rate of 0.031 ± 0.004 $\mu\text{mole}/\text{hour}$ with the P_{exch} measured in the same rock (at grain size <125 μm), yields a duration of over six days. In practical terms, a longterm desorption study would be necessary to determine the duration of desorption beyond a period of hours, as the rate is likely to decline and cease before exhausting the full reserve of P_{exch} . In studies that evaluate leachate SRP concentrations over a period of weeks, the cumulative desorbed SRP tends to change as a power function of cumulative pore volumes.³⁵

New incursion of saltwater into portions of the aquifer that has been immersed in fresh groundwater would be expected to release more SRP from the bedrock. Sea level rise is expected to exacerbate saltwater intrusion in many areas.^{4, 36-39} The Everglades is of particular concern.¹³ Climate change may bring more extreme storms and heightened storm surges, which may further exacerbate saltwater intrusion, particularly in regions with tidally connected rivers.³⁹ In addition, regions which undergo extended droughts, higher temperatures, and evaporation, may suffer diminished aquifer recharge, further raising the risk of saltwater-intrusion, according to the fifth report of the International Panel on Climate Change.⁴⁰

The return of fresh water into our columns resulted in an immediate reduction of SRP concentration, although the decline in SRP concentration was slightly less steep than the change caused by an influx of saltwater. In portion of a carbonate aquifer that undergoes freshening, or

oscillations in the location of the freshwater-saltwater interface, our results suggest that desorption dynamics would cause ambient SRP concentration to rapidly change in response. One of the major goals of the multi-billion dollar Everglades restoration project, the Comprehensive Ecological Restoration Program, is to abate or mitigate saltwater intrusion by increasing groundwater recharge and the quantity of freshwater delivery to coastal areas.^{13, 41}

For two of the column experiments (the first and second), the largest elevation of SRP concentration accompanied the initial introduction of freshwater following immersion in saltwater, in the exact same sample numbers for both columns. These isolated spikes in SRP concentration interrupted, and were followed by, a steady decline in leachate SRP concentration. This hints at the possibility that an even more intense and more ephemeral release of SRP may accompany a shift from saltwater to freshwater. Further experimentation would be necessary to determine if this effect can be consistently reproduced, and if so, to investigate its geochemical cause. Similar observations were made in a study of aquifer materials in Cape Cod.⁴²

Conclusion

Our results indicate that saltwater influx into carbonate aquifer solids causes rapid desorption that can continue to produce high levels of SRP concentration after a period of hours, even in rocks with low P content. This study offers insight into possible nutrient ramifications of saltwater intrusion into a coastal carbonate aquifer that had been immersed in fresh groundwater.

Acknowledgements

Thanks to Kevin Cunningham of USGS for providing access to the rock cores, Rafael Travieso, and Edward Linden of Florida International University for field and laboratory support, and

Charles Fischer of National Oceanic and Atmospheric Administration/ Atlantic Oceanographic and Meteorological Laboratory for assistance in sample analysis. This material is based upon work supported by the National Science Foundation through the Florida Coastal Everglades Long-Term Ecological Research program under Cooperative Agreements #DEB-1237517, #DBI-0620409, and #DEB-9910514.

References

1. Fitterman, D. V., Mapping saltwater intrusion in the biscayne aquifer, Miami-Dade County, Florida using transient electromagnetic sounding. *Journal of Environmental and Engineering Geophysics* **2014**, *19*, (1), 33-43.
2. Price, R. M.; Herman, J. S., Geochemical investigation of salt-water intrusion into a coastal carbonate aquifer: Mallorca, Spain. *Geological Society of America Bulletin* **1991**, *103*, (10), 1270-1279.
3. Cotecchia, V.; Tazioli, G.; Magri, G. In *Isotopic measurements in research on seawater ingression in the carbonate aquifer of the Salentine Peninsula, southern Italy*, Isotope techniques in groundwater hydrology 1974, Vol. I. Proceedings of a symposium, 1974; 1974.
4. Barlow, P. M.; Reichard, E. G., Saltwater intrusion in coastal regions of North America. *Hydrogeology Journal* **2010**, *18*, (1), 247-260.
5. Slomp, C. P.; Van Cappellen, P., Nutrient inputs to the coastal ocean through submarine groundwater discharge: controls and potential impact. *Journal of Hydrology* **2004**, *295*, (1), 64-86.
6. Moore, W. S., The subterranean estuary: a reaction zone of ground water and sea water. *Marine Chemistry* **1999**, *65*, (1), 111-125.
7. Flower, H. R., Mark; Zhang, Jia-Zhong; Lewis, David; Price, René Control of Phosphorus concentration through adsorption and desorption in shallow groundwater of subtropical carbonate estuary. *Estuarine, Coastal and Shelf Science* **2015** (in press).
8. Millero, F.; Huang, F.; Zhu, X.; Liu, X.; Zhang, J.-Z., Adsorption and desorption of phosphate on calcite and aragonite in seawater. *Aquatic Geochemistry* **2001**, *7*, (1), 33-56.
9. Corbett, D. R.; Kump, L.; Dillon, K.; Burnett, W.; Chanton, J., Fate of wastewater-borne nutrients under low discharge conditions in the subsurface of the Florida Keys, USA. *Marine Chemistry* **2000**, *69*, (1), 99-115.
10. Prinos, S. T.; Wacker, M. A.; Cunningham, K. J.; Fitterman, D. V. *Origins and delineation of saltwater intrusion in the Biscayne aquifer and changes in the distribution of saltwater in Miami-Dade County, Florida*; 2328-0328; US Geological Survey: 2014.
11. Price, R. M.; Swart, P. K.; Fourqurean, J. W., Coastal groundwater discharge—an additional source of phosphorus for the oligotrophic wetlands of the Everglades. *Hydrobiologia* **2006**, *569*, (1), 23-36.
12. Noe, G. B.; Childers, D. L.; Jones, R. D., Phosphorus biogeochemistry and the impact of phosphorus enrichment: why is the Everglades so unique? *Ecosystems* **2001**, *4*, (7), 603-624.

13. Council, N. R., *Progress Toward Restoring the Everglades: The Fifth Biennial Review, 2014*. The National Academies Press: Washington, DC, 2014; p 302.
14. Cunningham, K. J.; Wacker, M. A.; Robinson, E.; Gefvert, C. J.; Krupa, S. L. *Hydrogeology and ground-water flow at Levee 31N, Miami-Dade County, Florida, July 2003 to May 2004: as part of the Comprehensive Everglades Restoration Plan*; 2329-132X; 2004.
15. Cunningham, K. J.; Wacker, M. A.; Robinson, E.; Dixon, J. F.; Wingard, G. L. *A cyclostratigraphic and borehole-geophysical approach to development of a three-dimensional conceptual hydrogeologic model of the karstic Biscayne aquifer, southeastern Florida*; 2328-0328; 2006.
16. Zhang, J. Z.; Fischer, C. J.; Ortner, P. B., Potential availability of sedimentary phosphorus to sediment resuspension in Florida Bay. *Global Biogeochemical Cycles* **2004**, *18*, (4).
17. Ruttenberg, K. C., Development of a sequential extraction method for different forms of phosphorus in marine sediments. *Limnology and oceanography* **1992**, *37*, (7), 1460-1482.
18. Huang, X.-L.; Zhang, J.-Z., Neutral persulfate digestion at sub-boiling temperature in an oven for total dissolved phosphorus determination in natural waters. *Talanta* **2009**, *78*, (3), 1129-1135.
19. Zhang, J.-Z.; Kelble, C.; Millero, F. J., Gas-segmented continuous flow analysis of iron in water with a long liquid waveguide capillary flow cell. *Analytica chimica acta* **2001**, *438*, (1), 49-57.
20. Price, R. M., Geochemical determinations of groundwater flow in Everglades National Park. **2001**.
21. D'Angelo, E.; Crutchfield, J.; Vandiviere, M., Rapid, sensitive, microscale determination of phosphate in water and soil. *Journal of environmental quality* **2001**, *30*, (6), 2206-2209.
22. Suzumura, M.; Ueda, S.; Sumi, E., Control of phosphate concentration through adsorption and desorption processes in groundwater and seawater mixing at sandy beaches in Tokyo Bay, Japan. *Journal of oceanography* **2000**, *56*, (6), 667-673.
23. Froelich, P. N., Kinetic control of dissolved phosphate in natural rivers and estuaries: A primer on the phosphate buffer mechanism1. *Limnology and oceanography* **1988**, *33*, (4part2), 649-668.
24. Yakubu, M.; Gumel, M.; Abdullahi, A., Use of activated carbon from date seeds to treat textile and tannery effluents. *AJST* **2008**, *9*, (1).
25. Zhang, J.-Z.; Huang, X.-L., Effect of temperature and salinity on phosphate sorption on marine sediments. *Environmental science & technology* **2011**, *45*, (16), 6831-6837.
26. Flower, H. R., Mark; Zhang, Jia-Zhong; Lewis, David; Price, René, Saltwater intrusion as potential driver of phosphorus release from limestone bedrock in a coastal aquifer. **(in prep)**.
27. Zhang, J.-Z.; Guo, L.; Fischer, C. J., Abundance and chemical speciation of phosphorus in sediments of the Mackenzie River Delta, the Chukchi Sea and the Bering Sea: importance of detrital apatite. *Aquatic geochemistry* **2010**, *16*, (3), 353-371.
28. Zhou, M.; Li, Y., Phosphorus-sorption characteristics of calcareous soils and limestone from the southern Everglades and adjacent farmlands. *Soil Science Society of America Journal* **2001**, *65*, (5), 1404-1412.
29. Council, N. R., *Progress Toward Restoring the Everglades: The Third Biennial Review*. The National Academies Press: Washington, D.C., 2010.
30. Spence, V., Estimating groundwater discharge in the oligohaline ecotone of the Everglades using temperature as a tracer and variable-density groundwater models. **2011**.

31. Zapata-Rios, X.; Price, R. M., Estimates of groundwater discharge to a coastal wetland using multiple techniques: Taylor Slough, Everglades National Park, USA. *Hydrogeology Journal* **2012**, *20*, (8), 1651-1668.
32. Stringfield, V.; LeGrand, H., Effects of karst features on circulation of water in carbonate rocks in coastal areas. *Journal of Hydrology* **1971**, *14*, (2), 139-157.
33. Fleury, P.; Bakalowicz, M.; de Marsily, G., Submarine springs and coastal karst aquifers: a review. *Journal of Hydrology* **2007**, *339*, (1), 79-92.
34. Steinen, R. P.; Matthews, R.; Sealy, H., Temporal variation in geometry and chemistry of the freshwater phreatic lens: The coastal carbonate aquifer of Christ Church, Barbados West Indies. *Journal of Sedimentary Research* **1978**, *48*, (3).
35. Kuo, S.; Lotse, E., KINETICS OF PHOSPHATE ADSORPTION AND DESORPTION BY HEMATITE AND GIBBSITE1. *Soil Science* **1973**, *116*, (6), 400-406.
36. Wong, P.; Losada, I.; Gattuso, J.; Hinkel, J.; Khattabi, A.; McInnes, K.; Field, C.; Barros, V.; Dokken, D.; Mach, K., Climate change 2014: impacts, adaptation, and vulnerability. Part A: global and sectoral aspects. Contribution of Working Group II to the Fifth Assessment Report of the Intergovernmental Panel on Climate Change. In Cambridge Cambridge University Press.: 2014.
37. Webb, M. D.; Howard, K. W., Modeling the Transient Response of Saline Intrusion to Rising Sea-Levels. *Groundwater* **2011**, *49*, (4), 560-569.
38. Loáiciga, H. A.; Pingel, T. J.; Garcia, E. S., Sea Water Intrusion by Sea-Level Rise: Scenarios for the 21st Century. *Groundwater* **2012**, *50*, (1), 37-47.
39. Carter, L.; Jones, J.; Berry, L.; Burkett, V.; Murley, J.; Obeysekera, J.; Schramm, P.; Wear, D.; Melillo, J.; Richmond, T., Southeast and the Caribbean. *Climate Change Impacts in the United States: The Third National Climate Assessment* **2014**, 396-417.
40. Jimenez Cisneros, B. E.; Oki, T.; Arnell, N. W.; Benito, G.; Cogley, J. G.; Doll, P.; Jiang, T.; Mwakalila, S. S., Freshwater resources. **2014**.
41. Team, R. C. a. V. *Southern Coastal Everglades*; September 23, 2015, 2014
42. Stollenwerk, K. G., Simulation of phosphate transport in sewage-contaminated groundwater, Cape Cod, Massachusetts. *Applied Geochemistry* **1996**, *11*, (1), 317-324.

Chapter 5:

Conclusions

Phosphorus sorption dynamics within carbonate aquifer solids plays a critical role in the P-availability in coastal mixing zones. In the sediment at the mangrove root zone of Taylor Slough in the Florida coastal Everglades we determined that soluble reactive phosphorus (SRP) can be released from the sediment when its ambient water changes from fresh water or saltwater to the high bicarbonate brackish water that is most commonly found there. Further, high bicarbonate brackish would be expected to maintain ambient SRP concentrations at a higher level due to the poor buffering capacity of the sediment in this water (Chapter 2). These results merit phosphorus sorption studies in other coastal regions with high bicarbonate brackish groundwater.

Below the sediment layer, carbonate bedrock in regions subject to saltwater intrusion may be exposed to gradual increases in salinity as the freshwater zone transitions into seawater. In Chapter 3 we determined that an amount of saltwater content very close to the limits of detection (3 mM Cl^- concentration or 100 mg Cl^- /L) causes a sharp reduction of sorption efficiency. Loss of sorption efficiency triggers the release of loosely adsorbed SRP from aquifer solids, raising ambient water SRP concentrations. Our results are consistent with SRP being an active participant along with other reactive ions in the ion exchange front of saltwater intrusion. In Chapter 4 we explored the kinetics of saltwater-induced desorption with a column study, and found a nearly instantaneous, intense, and sustained release of SRP at the onset of saltwater

contact with the aquifer solids. In a carbonate mixing zone that discharges to an overlying wetland, the pulse of SRP release may result in an ecologically significant subsidy of SRP. We conclude that phosphorus sorption dynamics in coastal carbonate regions affect groundwater SRP concentrations within the sediment and bedrock.